

DEVELOPMENT AND PRODUCTION OF IMMEDIATE RELEASE ORAL SOLID  
DOSAGE PRODUCTS VIA COMPRESSION AND INJECTION MOLDING

by

Caitlin Cato Wood

(Under the Direction of Jason Locklin)

ABSTRACT

Material science is the study of structural and chemical features that give rise to bulk material properties. Understanding the fundamental structure-function relationship of materials enables the intentional manipulation of a material to achieve desirable traits for developing useful products. One such application is the development of immediate release pharmaceutical oral solid dosage forms (tablets) for treating illnesses. Tablets must function in accordance with rigorous standards to ensure adequate performance and safety for patients. Tablets must be mechanically strong enough to withstand production processing but weak enough to disintegrate and release active pharmaceutical ingredient (API) in a reasonable amount of time. This is just one example of the tension between desirable tablet attributes that a formulator must consider and engineer for. Explored in this work is the relationship between particle morphology and critical quality attributes such as flowability, tabletability, disintegration, and friability for the purpose of more efficiently developing formulations. Using materials science and small-scale-material-sparing test methods, the timeline and amount of API needed to produce a successful tablet formulation were drastically reduced compared to current industry practices.

Additionally, a modified material-sparing granulation method was used to alter an API with an inherent tendency to segregate. The granulation work expanded on the more efficient formulation development approach, showing that even challenging APIs can be successfully formulated using minimal API and time. Lastly, an innovative technology for producing amorphous solid dispersion (ASD) tablets using injection molding was explored for the production of immediate release tablets. Injection molding is more efficient than the current production methods for ASD tablets. Furthermore, tablets produced via injection molding exhibited superior mechanical strength and content uniformity compared to tablets made via powder compression. This formulation development was also done using the rapid and material-sparing approach. Less than 10 g of API was needed to formulate and test tablets against industry standards. As these studies highlight, the implementation of materials science is a powerful tool for producing effective tablet formulations efficiently, which is beneficial for shortening the timeline for patients to gain access to life-saving drugs.

INDEX WORDS: Injection Molding, Amorphous Solid Dispersion, Formulation Development, Material-Sparing and Expedited Tablet Development, Immediate Release Tablets, Granulation,

DEVELOPMENT AND PRODUCTION OF IMMEDIATE RELEASE ORAL SOLID  
DOSAGE PRODUCTS VIA COMPRESSION AND INJECTION

by

CAITLIN CATO WOOD

B.S., University of Georgia, 2017

A Dissertation Submitted to the Graduate Faculty of The University of Georgia in Partial  
Fulfillment of the Requirements for the Degree

DOCTOR OF PHILOSOPHY

ATHENS, GEORGIA

2023

© 2023

CAITLIN CATO WOOD

All Rights Reserved

DEVELOPMENT AND PRODUCTION OF IMMEDIATE RELEASE ORAL SOLID  
DOSAGE PRODUCTS VIA COMPRESSION AND INJECTION MOLDING

by

CAITLIN CATO WOOD

Major Professor:	Jason Locklin
Committee:	Sammy Bell
	Branson Ritchie
	Michael Bartlett

Electronic Version Approved:

Ron Walcott  
Vice Provost for Graduate Education and Dean of the Graduate School  
The University of Georgia  
December 2023

## DEDICATION

### *Soli Deo Gloria- Glory to God alone*

This work was done as an act of worship for my beloved heavenly father, Yahweh Elohim, the creator of the universe and the savior of my soul. If there is any merit in this work, it is His alone. Without God's sustaining hand, I, and as a result, this work would not exist, so He alone is to be praised for this work. Thank you, Father, Son, and Holy Ghost, for saving a wretched sinner like me and for using graduate school to make me more like Jesus. I pray that my life and work will glorify you now and forever. Amen!

1. Romans 3:23, "For all have sinned, and come short of the glory of God."
2. Romans 6:23, "For the wages of sin is death; but the gift of God is eternal life through Jesus Christ our Lord."
3. Romans 5:8, "but God shows his love for us in that while we were still sinners, Christ died for us."
4. Romans 10:9, "because, if you confess with your mouth that Jesus is Lord and believe in your heart that God raised him from the dead, you will be saved."
5. Romans 5:1, "Therefore, since we have been justified by faith, we have peace with God through our Lord Jesus Christ."

## ACKNOWLEDGEMENTS

Thank you to my husband, Zachary, for all that you do. You are an excellent leader of our family, and I am so thankful to have you as a husband. You strive to love me like Christ loves the church. Christ gave His life to redeem and sanctify His bride, and I see and appreciate your desire and efforts to do likewise.

Thank you also to my family and friends. Your love and support helped to encourage me when grad school got hard. I am so thankful for the wonderful community of people near and far that made this journey smoother. I am especially grateful to Mary Eppling, Maddi (Mad dog) Smith, Sarah Jackson, Virginia Weber, Jessica Bramhall, Kush Patel, Jessica Drewke, Nohora Manovacia, Karson Durie, and Joe Grubbs III for your advice, pep talks, help in and out of the lab, prayers, and friendship. Thank you also to Josh Bledsoe, Michael Broich, Lawrence Ferguson, Adaeze Oskawe, Ethan Stinchcomb, Ryan Maynard, and all the other Locklin lab members, new and old, who made coming to work so much fun. I love you all, and I am thankful to have met you. I look forward to seeing what God has in store for you.

Thank you, Sammy, for introducing me to pharmaceuticals and your willingness to answer my endless questions about making drug products. You were patient and encouraging as I worked to establish this new area of research at the Locklin lab. I pray that your work will continue to help many patients to live happier and healthier lives. Keep up the good work, Sammy! Dr. Ritchie, thank you for all the fun projects and the peaches. You were a wonderful mentor, and I am thankful you agreed to be on my

committee. Dr. Locklin, thank you for the opportunity to work in your lab and for your time and energy in refining me as a scientist. I have grown much under your mentorship, and I wish you the best as you continue mentoring the next generation of researchers.



## TABLE OF CONTENTS

	Page
DEDICATION .....	iv
ACKNOWLEDGEMENTS .....	v
LIST OF TABLES.....	ix
LIST OF FIGURES .....	xi
CHAPTER	
1 Introduction and Literature Review .....	1
Pharmaceutical Market Analysis .....	1
Tablet Manufacturing Challenges .....	1
Powder and Tablet Material Properties for Quality-by-Design Applications .....	3
Innovative Drug Delivery Methods, Continuous Manufacturing, and Overcoming Solubility/Bioavailability Limitations .....	9
Manufacturing Amorphous Solid Dispersions.....	12
Objectives and Outlines of this Dissertation.....	13
2 5 grams in 2 weeks: Material Sparing Tablet Development of Direct Compression Formulations for Immediate Release Applications .....	25
Abstract.....	26
Introduction.....	26
Materials and Methods.....	28

Results and Discussion .....	34
Conclusion .....	51
References.....	54
3 Material Sparing Granulation for the Development of Immediate Release	
Tablet Compression Formulations .....	57
Abstract.....	58
Introduction.....	59
Materials and Methods.....	61
Results and Discussion .....	64
Conclusion .....	73
References.....	74
4 Development of Immediate Release Amorphous Solid Dispersion Formulation	
for Manufacturing Injection Molded Solid Dosage Products .....	77
Abstract.....	78
Introduction.....	78
Materials and Methods.....	81
Results and Discussion .....	88
Conclusion .....	107
References.....	110
5 Conclusions and Future Outlook .....	114
Conclusions and Future Work .....	115
Final Remarks .....	118

## LIST OF TABLES

	Page
Table 2.1: HPLC Methods for Each API .....	33
Table 2.2: BI-1 HPLC Method Mobile Phase Gradient .....	33
Table 2.3: BI-3 HPLC Method Mobile Phase Gradient .....	33
Table 2.4: Synopsis of API Particle Morphology .....	35
Table 2.5: Compression Behavior of API.....	42
Table 2.6: Powder Blend Formulations and Flowability Evaluation .....	44
Table 2.7: Friability and Disintegration Analysis of Tablets.....	48
Table 2.8: Content Uniformity and Segregation Analysis.....	49
Table 2.9: Quantification of Percent Degradation After Accelerated Stability Testing at 70°C/75% RH temp and humidity .....	50
Table 3.1: Intragranular Formulation .....	69
Table 3.2: Extragranular Formulation.....	70
Table 3.3: Friability and Disintegration Analysis of Tablets.....	71
Table 3.4: Content Uniformity of Granules, Unmodified BI-2 Formulation Tablets, and Granulated Formulation Tablets .....	71
Table 4.1: Extrusion parameters for Process 11 .....	84
Table 4.2: Moxidectin HPLC Method Mobile Phase Gradient .....	86
Table 4.3: Hansen Solubility Parameters of Moxidectin, PEO, PVP, and TEC, along with their solubility distances (Ra). .....	89

Table 4.4: HSP values of solvents used as well as their solvent scores .....	67
Table 4.5: Scoring criteria used for each solvent.....	67
Table 4.6: Onset of degradation of moxidectin and excipients .....	69
Table 4.7: Formulations Used for Extrusion and Microscopy Analysis .....	70
Table 4.8: DSC data of PVP, Moxidectin, PEO, and formulations ( $\Delta H_f = 197$ J/g for PEO) .....	71
Table 4.9: Injection Molded Tablets Mass Uniformity .....	74
Table 4.10: Content Uniformity and Degradation Analysis of Injection Molded Tablets	76

## LIST OF FIGURES

	Page
Figure 1.1: Diagram of tablet compression mechanism. ....	2
Figure 1.: (A) The relationship between particle size (mass) and the force exerted by gravity, which is responsible for powder flowability. (B) A depiction of the cohesive forces (FC) that additively contribute to poor flowability... ..	4
Figure 1.3. (A) Assuming equal particle volume, the green particle has greater surface roughness (surface area) compared to the blue bar which has more surface area compared to the smooth white sphere. Based on these morphologies, it is expected that flowability would also follow that trend as indicated by the blue arrow. (B) is an illustration of the impact of particle size dispersity and particle size on interparticulate interactions. Because of their small size, the blue particles pack very efficiently leading to more particle interactions and thus more friction and poorer flowability. When mixing particles of a large and small size (large dispersity of particle sizes), the smaller particles are fill the interparticulate space which increases the points of contact between particles generating more friction. The larger white particles have more interparticulate space meaning that there are fewer surface interactions between the particles to impeded flow, which is why it has the best flowability of all three samples. ....	8

Figure 2.1: Scanning electron microscopy of (a) BI-1 with scale bar 50  $\mu\text{m}$ , (b) BI-2 with scale bar 50  $\mu\text{m}$ , (c) BI-3 with scale bar 200  $\mu\text{m}$ , and (d) BI-4 with scale bar 500  $\mu\text{m}$ . Particle size distribution of (e) BI-1, (f) BI-2, (g) BI-3, and (h) BI-4.....38

Figure 2.2: Heckel Plots of BI-1 (a), BI-2 (b), BI-3 (c), and BI-4 (d). Red lines indicate the analysis region for the compression phase and blue lines indicate the analysis region for the decompression phase.....39

Figure 2.3: Analysis and comparison of formulation's impact on tensile strength as a function of compression pressure (tableability) for BI-1 (a), BI-2 (b), BI-3 (c), and BI-4 (d). The higher the LAC or DICAL percentage the lower the slope in the linear region leading into the onset of the plateau region... ..46

Figure 2.4: HPLC analysis of (a) BI-4 F1 tablets, (b)BI-4 F2, and (c) BI-3 F5 tablets stored under accelerated stability conditions. The red arrow in Fig.3b indicates the peak that is not present in the stock solution but is present in the tablets, which indicates the development of a degradation product.....51

Figure 3.1. Particle size distribution of granules measured manually via SEM images. Lengths of particles plotted and average distribution curve generated. Unmodified BI-2 particle size distribution with average particle size (A) has a more narrow and smaller average particle size compared to granules. 150 granules (B) have a narrower particle size distribution compared to 250 granules (C) and 425 granules (D). As expected, the average particle size increases with mesh size. ....65

Figure 3.2. SEM images of (A) 425-250  $\mu\text{m}$ , (B) 250-150  $\mu\text{m}$  granules and (C) <150  $\mu\text{m}$  granules. The morphology gets more irregular as granule size decreases. The 425  $\mu\text{m}$  granules (A) are predominately spherical in shape.. ....67

- Figure 3.3. (A) Comparison of tensile strength as a function of compression pressure (tableability) of F1\_150 (red) and F1\_250 (black) to determine if granule size impacted the tensile strength of the extragranular formulation. There is a slight deviation at higher compression pressures, but the formulas perform almost identically. (B) Comparison of tableability of the extragranular formulations (red and black) with powder blends made from unmodified BI-2 (blue). Tableability decreased with granulated BI-2 regardless of granule size.....70
- Figure 4.1: TGA thermograms of API and excipients.....91
- Figure 4.2: DSC thermograms of PVP and moxidectin samples. Left (a) – Glass transition of PVP and moxidectin. Right (b) – Glass transition of PVP and moxidectin plasticized with TEC-BHT.....92
- Figure 4.3: DSC thermograms of PEO, placebo, and API loaded formulations. Left (a) – 1st heating curve of the extrudate samples. Right (b) – Zoom in on the glass transition of the samples from the 2nd heating curve.. ....93
- Figure 4.4: Torque vs time plot of F1-Moxi formulation during extrusion. ....95
- Figure 4.5: (A) Graphic of the "G" SLA injection mold insert design embedded in the steel mold. The depressions at the edges were added to facilitate removal from the steel mold. (B) shows the SLA insert used to make the dog bone shaped tablets alongside one of the tablets. (C) shows the diversity of tablet geometries made in this study.....98
- Figure 4.6: HPLC chromatogram of content uniformity samples showing the increase in the degradant peak (red arrows) for extruded samples compared to pure

moxidectin stock and the blank mobile phase. The peak at 20.1 being the larger peak area was used to calculate percent degradation.....100

Figure 4.7: (A) The average dissolution profile of 2 mg tablets (n=3) made from F1\_moxi with error bars in black. (B) Dissolution profiles of 11 mg, F2\_moxi tablets at both 65 (n=1) and 100 (n=1) rpm paddle speed to highlight the difference that dissolution parameters have on the release profile. ....102

Figure 4.8: SEM of cross section of injection molded bars. F4 (A,D) formulation contains no effervescent granules, and the PVP/PEO phase separation is clearly visible as indicated by the navy blue arrow in D. F1-Moxi (B,E) contains moxidectin and effervescent granules. The effervescent granules are highlighted with black arrows. F1 (C,F) contains effervescent but no Moxi. The morphology of the Moxi and placebo formulation are identical. The porosity that develops as a result of bicarb decomposition is indicated with red arrows (E,F). ....104

Figure 4.9 POM images of injection molded samples in the melt at 120°C to show the phase separation between PEO (A) and F4 (C). Additionally, 40°C highlighting the morphology differences between the spherulite structures in pure PEO (B) and F4 (D). The spherulites in D are smaller and more numerous compared to the spherulites of pure PEO.: .....107



## CHAPTER 1

### INTRODUCTION AND LITERATURE REVIEW

#### *Pharmaceutical Market Analysis*

According to an IQVIA market report, the U.S. pharmaceutical market for 2022 was valued at \$429 Billion, including prescription and over-the-counter medications[1]. Of all the drug delivery systems, tablets are the most popular and comprise a large part of the global pharmaceutical market[2]. Compared to intravenous injections and other delivery forms, tablets are less invasive and easier to administer for patients, which makes it more likely for patients to comply with medication regimens. Tablets are also less expensive than other drug delivery forms because the excipients used in tableting are more affordable, and tablets can be rapidly produced in abundance[3].

#### *Tablet Manufacturing Challenges*

Tablets are typically made via powder compression. The mechanism of tablet formation is illustrated in Figure 1.1. The die and punches are the mold that will shape the tablet during compression. The powder is filled into the die, and a scraper removes excess powder. The upper tooling inserts into the die. The increasing insertion of the upper punch generates the pressure to make the tablet. The particles rearrange and densify as pressure is applied. If pressure continues to increase once there is no more room for the particles to move relative to one another, the pressure causes the particles to deform. Plastic deformation (permanent deformation) causes the tablet to become cohesive. After

maximum insertion of the upper punch, the tablet is ejected and conveyed to the next stage of processing to be coated or packaged for sale.

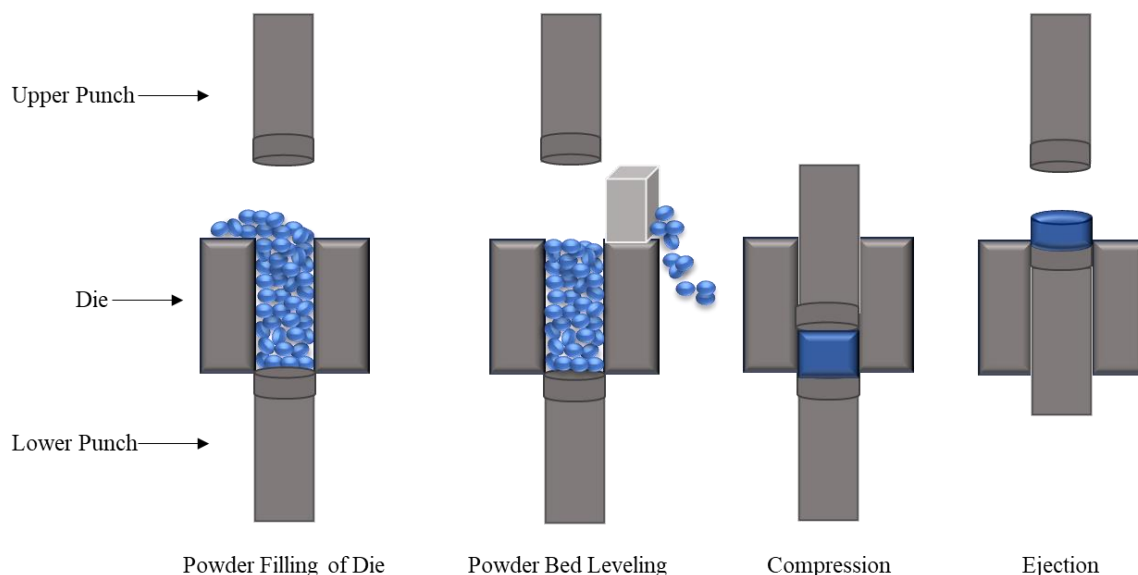


**Figure 1.1.** Diagram of tablet compression mechanism.

In industrial tablet production, a multi-barrel and multi-station tablet press can produce 1.6 million tablets an hour, translating to approximately one tablet produced every two milliseconds[4]. The entire mechanism illustrated in Figure 1.1 happens in 2 milliseconds and must produce a tablet that meets stringent standards for consistency in mass, strength, and disintegration time to ensure patient safety and tablet performance[5, 6]. Therefore, designing a powder formulation that can meet those rigorous demands while keeping production costs low is challenging[7]. Currently, tablet formulations are developed using trial and error to guide formulation, and formulas are often tested on large-scale equipment to ensure the final formula will be industrially manufacturable[8, 9]. This approach to formulation development is wasteful and time consuming. On average, a drug takes 12-15 years to go from discovery to the market[10, 11]. Of that timeline, 1-2 years is spent in development and pre-clinical research partially because of the

cumbersome techniques currently used for formulation development[12]. This large investment of time and billions of dollars in resources (drug synthesis, labor, and equipment) to do large scale formulation work is especially bad in light of the 90% failure rate of drug products during clinical trials[11, 13, 14]. Within the last decade, research into new techniques to improve the efficiency of pharmaceutical formulation development has gained traction in the literature, especially regarding materials science as a guide for formulation development[15-23]. The premise of the research is that if formulators understand the particle and material properties that impact powder and tablet performance (i.e., flowability, tabletability, compressibility, compactability, disintegration, and dissolution), then formulations can be designed to meet specified criteria rather than developed via trial and error. The quality-by-design approach of tablet formulation, also called material sparing tablet development, is possible because of the clearly defined parameters by the Food and Drug Administration (FDA) and the United States Pharmacopeia (USP) for acceptable tablet qualities. According to the FDA and USP, tablets must; have API loading between 90-110% label claim, disintegrate in under 45 minutes (under 15 min is preferred), have a dissolution release profile in accordance with the application (70-80% API release in under an hour for immediate release), have a mass loss of no more than 1% after friability testing (typically achieved by having tablets with a tensile strength of 2 MPa or greater)[24-27].

#### *Powder and Tablet Material Properties for Quality by Design Applications*

Achieving the tablet attributes listed above is facilitated by understanding the structure-function relationship between the powder morphology of the blends, the powder blend properties, and the resulting tablets[27]. The physical and chemical characteristics of the

powder used to make the blend directly impact the flowability, tabletability, compressibility, and compactability of the powder blend[28]. These properties of the powder blend are then linked to the tensile strength (friability), content uniformity, disintegration, and dissolution profile of the tablets made from that powder blend.

Looking at just one example of this complex structure-function relationship, flowability, the capacity for loose particulates to move, is a critical quality attribute for powder formulations. As mentioned above, tablets are produced at an incredibly high rate. Because the tableting equipment is operating on the order of milliseconds, the powder

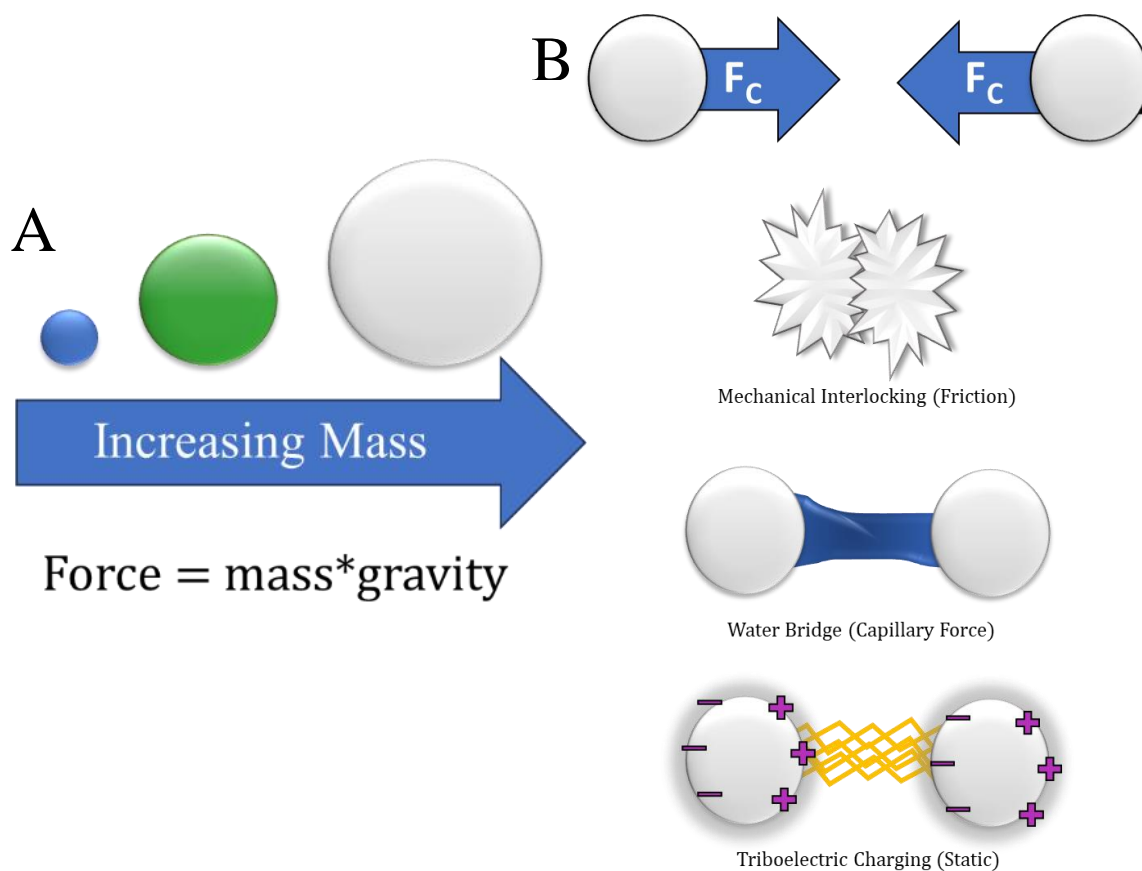


**Figure 1.2.** (A) The relationship between particle size (mass) and the force exerted by gravity, which is responsible for powder flowability. (B) A depiction of the cohesive forces ( $F_c$ ) that additively contribute to poor flowability.

formulation must be able to quickly and consistently fill the die so that tablet mass and, thus, drug dosing will be consistent. Achieving industrially relevant flowability is one of the most challenging aspects of formulations because most drugs intrinsically do not exhibit good flowability. Therefore, other ingredients, known as excipients, are added to the drug, also referred to as active pharmaceutical ingredient (API), to improve the flowability of the blended powder. Formulators can use materials science to determine how different excipients impact flowability and other powder attributes.

In general, powders will flow if the force exerted by gravity on the powder is larger than the cohesive forces between powder particles. Since acceleration due to gravity is a fixed value, there are only two mechanisms to improve flowability: increasing the mass of the particles or decreasing the cohesive forces between particles. To increase the particle's mass, the particle's size or true density must increase. True density is an inherent property of the material that composes the particle and cannot be altered via processing. Increasing particle size can be done by granulating, a general term for any technique that fuses smaller particles to form larger agglomerate granules.

There are more mechanisms by which to reduce cohesive forces than there are for increasing the force of gravity on the particles. The cohesive forces that impede flowability fall into the three categories listed in Figure 1.2 B [29]. Water bridge formation is caused by excessive moisture present in the powder [30]. The water on the surface of the powder particles can interact as the particles try to flow past one another, and the surface tension of the water acts like a glue to fuse the particles [31]. To reduce the cohesion caused by water bridging, powders must be dried to remove excess moisture, which can be challenging for hygroscopic powders. However, some moisture

content is needed to help reduce or prevent the next cause of cohesive force, triboelectric charging.

Triboelectric charging, also known as static or electrostatic energy, results from electron transfer between surfaces caused by friction[32]. The electron transfer results in a temporary charge on both surfaces. The charging of the particles results in attraction and repulsion within the powder as like charges interact, and opposite charges interact, respectively[33]. The repulsive force can lead to powder particles adhering to nearby conductive surfaces, thus leading to powder loss, while the attractive forces cause agglomeration and, thus, poorer flowability. Increasing the moisture content of the powder, usually by increasing the humidity in the processing room, will help the powder particles to be more conductive, which facilitates the dissipation of the charging[34]. Another way to combat triboelectric charging through formulation is to coat the particles with a material that reduces charging by modifying the surface energy of the particles. Such compounds include silica, alumina, and metal salts[32].

The final cohesive force is mechanical interlocking; also, a function of friction, which occurs anytime one surface moves over another surface, such as when particles try to flow past one another. Therefore, any morphological aspects about the particles that increase surface area (i.e., surface roughness, increased particle shape linearity, decreased particle size, increased particle size dispersity) will increase the force of friction and thus the total cohesive forces (Figure 1.3)[35-41]. In contrast, morphology features that minimize surface area and particle interactions will improve flowability. Many of the techniques used to increase flowability via the previously mentioned mechanisms will also reduce the friction experienced by particles. For example, granulation will increase

particle size, increasing the interparticulate space, as illustrated in Figure 1.3 B, but granulation also increases particles' circularity, reducing the surface area that could lead to mechanical interlocking (Figure 1.3 A)[42]. Additionally, coating the particles with silica to reduce charging will change the surface energy of the particles[43]. By coating with fumed silica, the surfaces become lubricated and lower the coefficient of friction so that the particles can flow past one another more easily.

All the mechanisms discussed apply to API and excipient modifications to improve flowability. To recap, increasing particle size, decreasing particle size dispersity, controlling moisture content, decreasing surface energy, and increasing the circularity of particles will improve flowability, and these principles can guide excipient selection to optimize the features of the individual excipients but also of the blended powders. As discussed, flowability is just one of several important powder blend characteristics needed to develop a robust and industrially relevant compression powder formulation. Though not relevant to this body of work, compactability, compressibility, disintegration, and dissolution are equally complex, and, like flowability, understanding the structure-function relationship between the physical/chemical properties of the particles and the resulting tablets can facilitate faster and more efficient formulation development.

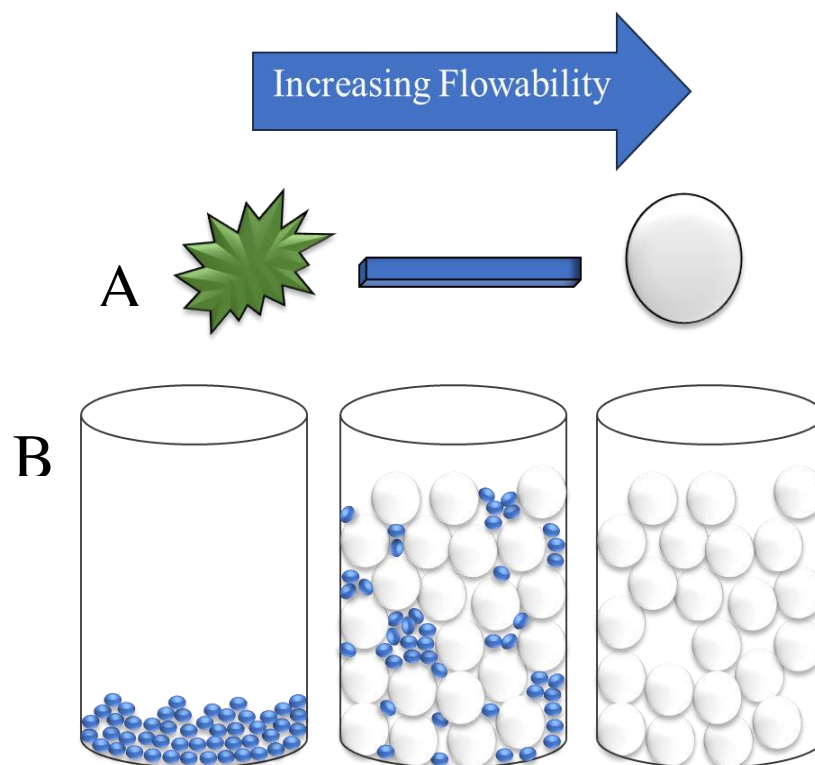


Figure 1.3. (A) Assuming equal particle volume, the green particle has greater surface roughness (surface area) compared to the blue bar which has more surface area compared to the smooth white sphere. Based on these morphologies, it is expected that flowability would also follow that trend as indicated by the blue arrow. (B) is an illustration of the impact of particle size dispersity and particle size on interparticulate interactions. Because of their small size, the blue particles pack very efficiently leading to more particle interactions and thus more friction and poorer flowability. When mixing particles of a large and small size (large dispersity of particle sizes), the smaller particles fill the interparticulate space which increases the points of contact between particles generating more friction. The larger white particles have more interparticulate space meaning that there are fewer surface interactions between the particles to impeded flow, which is why it has the best flowability of all three samples.



*Innovative Drug Delivery Methods, Continuous Manufacturing, and Overcoming Solubility/Bioavailability Limitations*

In addition to understanding material science as it relates to formulation development, another important focus of this body of work is the frontier of oral solid dosage drug delivery, including novel drug delivery methods and manufacturing methods. In the novel drug delivery category, a few examples of areas of interest are controlled release[44-46], micro tablets[47, 48], personalized medicine[49], polypills[50, 51], and smart pills[52-54], which are all intended to improve the patient experience. Controlled release is the ability to selectively release API either in a specific location in the gastrointestinal tract, for a prolonged period of time, or under specific physiological conditions. The ability to control the release of API can reduce the side effects experienced by patients by reducing API burst release and increasing site-specific absorption to reduce off-target effects[55, 56]. Micro tablets are easier to swallow and enable smaller doses for pediatric patients.

Personalized medicine acknowledges the metabolic and pharmacokinetic differences in different patients, and methods of manufacturing personalized dosages help to reduce side effects and improve the efficacy of the medication. Polypills arose from the large average number of medications consumed daily, especially in geriatric patients. Polypills combine multiple APIs into a single dosage to reduce the number of medications ingested. Polypills are beneficial for comorbidities where the same few APIs are often used in combination to treat illnesses like heart disease, high blood pressure, and diabetes.

Smart pills integrate technology, like microchips, microfluidic pumps, and sensors, with traditional tablet dosage forms. For example, silica microchips were embedded in

schizophrenia medications that linked to a phone or sensor on the patient to help ensure that the patient was taking their medication properly. Schizophrenia is a mental disorder that presents paranoia as one of the most common symptoms. During an episode, symptoms may induce the patient not to trust their medications and thus not comply with the prescription regimen, which will lead to further worsening of symptoms. The chip enables medical professionals to detect potential lapses, thus protecting patients from relapse. These novel drug delivery products improve patient experience and the efficacy of oral solid dosage forms.

At the frontier of oral solid dosage manufacturing, the predominant focus is on continuous manufacturing methods and industrially relevant methods of improving the solubility and bioavailability of APIs. Continuous manufacturing is a term used to describe the uninterrupted production of drug products instead of batch processing, which is incremental production. For example, there is interest in producing all-in-one equipment that can continuously granulate, blend powder, compress tablets, and coat tablets[57, 58]. Currently, each of these steps is done separately, and time and resources are wasted moving materials from one stage of processing to the next. Continuous manufacturing is inherently more efficient and can produce larger quantities of drug products[58, 59]. Therefore, advancements in continuous manufacturing are a particular area of interest to the pharmaceutical industry.

The other oral solid dosage manufacturing area of interest relevant to this work is industrially relevant methods of improving the solubility and bioavailability of APIs. The biopharmaceutical classification system (BCS) is a way of classifying the solubility and bioavailability of APIs. BCS 1 is highly soluble and highly bioavailable. BCS 2 has low

solubility but high bioavailability. BCS 3 has high solubility but low bioavailability. BCS 4 has low solubility and bioavailability. Most APIs coming out of the drug discovery phase of drug product development are BCS 2-4, meaning that these APIs have solubility challenges, bioavailability limitations, or both. Therefore, a key area of interest is modifying these APIs or formulating them in such a way as to improve those deficiencies. There are a variety of techniques that can improve solubility/bioavailability. Examples are milling, co-crystallization, self-emulsifying drug delivery systems (SEDDES), and amorphous solid dispersions. Milling is used to reduce the particle size of the API. Reducing the particle size increases the surface area ratio, increasing the API's dissolution rate. Co-crystallization is a technique whereby the API is dissolved and then recrystallized with another material that can integrate with the API to form a new crystal lattice structure[60]. Through crystal engineering, incorporating the new molecule into the crystal lattice will increase molecular flexibility, improving the API's dissolution and potentially bioavailability[61]. SEDDES are an oral solid dosage form made of oils, surfactants, and API, which will spontaneously form an oil-in-water emulsion when dissolved in water under mild agitation (like the peristaltic motion of the stomach during digestion)[62]. The surfactant and oil droplets solubilize the API and improve the API absorption (bioavailability) in the intestines. The last example, amorphous solid dispersions (ASD), is a method explored in this body of work. ASDs are the amorphous form of an active pharmaceutical ingredient (API) stabilized via a matrix such as a polymer or a wax. Amorphous APIs have a higher solubility and typically higher bioavailability than their crystalline counterparts[63]. The majority of ASD products on the market are capsules or tablets. It can be challenging to make ASDs because

amorphous APIs are metastable. If not stabilized via the matrix, the API can recrystallize over time, thus eliminating the solubility benefits. There are ways to evaluate molecules to determine their glass forming ability (GFA) and glass stability (GS), which is the ability of the molecule to remain amorphous[64]. Generally, larger, more complex molecules are more stable as an amorphous solid than smaller molecules and are thus better suited for ASD applications.

### *Manufacturing ASDs*

ASDs can be produced through two mechanisms: solvent or fusion. The solvent mechanism is done by dissolving API with excipients. The solvent is then rapidly evaporated, which does not allow the API sufficient time for molecular reorganization into crystals. An example of solvent-based ASD production is spray drying. The second mechanism is fusion, a solvent-free technique where the API is melted and mixed with a polymer or wax matrix. The combination of heat and shear melts the crystalline API to make it amorphous, and then, as the ASD cools, the matrix interactions stabilize the amorphous form of the API. Hot melt extrusion (HME) and spray congealing are two examples of fusion ASD methods.

HME is a popular fusion technique for making ASDs because large volumes of material can be processed quickly, and the solvent-free nature of the technique makes it more environmentally friendly than spray drying[65]. The production of ASD tablets via HME typically starts by blending ASD excipients, usually in the form of powders. The powders are then fed into an extruder using a gravity feeder or a motorized powder feeder, and the formulation is melt-mixed at elevated temperatures. After extrusion, the cooled extrudate is milled. The powdered extrudate is then sieved to collect particles in an appropriate size

range. The particles of the desired size range are then blended with other powder excipients needed for compression. The powder blend is then fed into a tablet press, where the powder will be compressed into a solid compact[66-70]. While this extensive process can be done continuously, the additional grinding, sieving, blending, and compression steps add time, resources, and equipment to the production process, increasing the product's cost.

Injection molding is already being used prevalently in other sectors to produce large volumes of products rapidly and inexpensively. In this study, ASD tablets were injection molded to eliminate the additional processing steps used in traditional ASD tablet production. Since injection molding can be coupled directly to HME, tablets could be continuously produced faster than the current ASD tablet production methodology.

Despite the widespread usage of injection molding in other applications, there are only a handful of studies using injection molding for the production of tablets[71-75]. Of those studies, only two achieved immediate release (I.R.) criteria[76, 77]. This is because injection molding produces a dense compact made of polymers that, if soluble in water, has a high viscosity at the dissolution interface, which retards API diffusion. Therefore, this work is timely and beneficial in a research area that is understudied and of interest industrially for its continuous manufacturing focus and the novelty of producing an immediate release ASD injection molded tablet.

#### *Objectives and Outlines of this dissertation:*

The objective of this dissertation's first two research chapters was to use the material science principles aforementioned to rapidly and efficiently develop formulations for APIs selected at random to demonstrate the universality of these principles for all APIs. The APIs were characterized using material sparing tests, and then formulations were

designed based on each API's unique needs and characteristics. Powder blends were then tested against the FDA and USP standards to ensure the blends could be used to produce high-quality and functional tablets. In the latter chapter, material sparing granulation was added to modify one of the aforementioned APIs. The particle morphology of that API had led to content uniformity issues in the work done in the former chapter.

The last research chapter highlighted a new and more efficient method of producing ASD tablets via injection molding, which is a continuous manufacturing method unlike current batch production methods used to make ASDs. The goal of this work was to create an ASD injection molding formulation for the manufacture of immediate release tablets that conformed to all USP standards. Less than 10 g of model API and material sparing test methods were used to demonstrate the feasibility of quality-by-design in all areas of formulation development, even with novel drug delivery methods.

## References

1. Incorporated, I., *The Use of Medicines in the U.S. 2023 Usage and Spending Trends and Outlook to 2027*. 2023.
2. Sohail Arshad, M., et al., *A review of emerging technologies enabling improved solid oral dosage form manufacturing and processing*. *Adv Drug Deliv Rev*, 2021. **178**: p. 113840.
3. Cole, G.C. *Evaluating Development and Production Costs: Tablets Versus Capsules*. 1998.
4. Compacting, F., *Next generation Tableting Technology FE75*, F. Compacting, Editor.
5. Žagar, J. and J. Mihelič, *Big data collection in pharmaceutical manufacturing and its use for product quality predictions*. *Scientific Data*, 2022. **9**(1): p. 99.
6. French, W.N., et al., *Pharmacopeial standards and specifications for bulk drugs and solid oral dosage forms. Similarities and differences*. *Journal of Pharmaceutical Sciences*, 1967. **56**(12): p. 1622-1641.
7. van der Merwe, J., et al., *The Role of Functional Excipients in Solid Oral Dosage Forms to Overcome Poor Drug Dissolution and Bioavailability*. *Pharmaceutics*, 2020. **12**(5).
8. Zakowiecki, D., et al., *Exploiting synergistic effects of brittle and plastic excipients in directly compressible formulations of sitagliptin phosphate and sitagliptin hydrochloride*. *Pharmaceutical Development and Technology*, 2022. **27**(6): p. 702-713.

9. LaMarche, K., et al., *The distribution of Drucker-Prager Cap model parameters for pharmaceutical materials*. Powder Technology, 2023. **425**: p. 118528.
10. McNamee, L.M., M.J. Walsh, and F.D. Ledley, *Timelines of translational science: From technology initiation to FDA approval*. PLoS One, 2017. **12**(5): p. e0177371.
11. Hughes, J.P., et al., *Principles of early drug discovery*. Br J Pharmacol, 2011. **162**(6): p. 1239-49.
12. Thomas, F. *Formulating the Best Approach for Tablets*. Pharmaceutical Technology, 2022.
13. Subbiah, V., *The next generation of evidence-based medicine*. Nature Medicine, 2023. **29**(1): p. 49-58.
14. Smietana, K., M. Siatkowski, and M. Møller, *Trends in clinical success rates*. Nature Reviews Drug Discovery, 2016. **15**(6): p. 379-380.
15. Yamashita, H. and C.C. Sun, *Material-Sparing and Expedited Development of a Tablet Formulation of Carbamazepine Glutaric Acid Cocrystal– a QbD Approach*. Pharmaceutical Research, 2020. **37**(8).
16. Vreeman, G. and C.C. Sun, *Mean yield pressure from the in-die Heckel analysis is a reliable plasticity parameter*. International Journal of Pharmaceutics: X, 2021. **3**: p. 100094.
17. Wang, C. and C.C. Sun, *The efficient development of a sildenafil orally disintegrating tablet using a material sparing and expedited approach*. International Journal of Pharmaceutics, 2020. **589**: p. 119816.



18. Sun, C.C. and P. Kleinebudde, *Mini review: Mechanisms to the loss of tabletability by dry granulation*. European Journal of Pharmaceutics and Biopharmaceutics, 2016. **106**: p. 9-14.
19. Cunningham, J.C., I.C. Sinka, and A. Zavaliangos, *Analysis of tablet compaction. I. Characterization of mechanical behavior of powder and powder/tooling friction*. Journal of Pharmaceutical Sciences, 2004. **93**(8): p. 2022-2039.
20. Procopio, A.T., A. Zavaliangos, and J.C. Cunningham, *Analysis of the diametrical compression test and the applicability to plastically deforming materials*. Journal of Materials Science, 2003. **38**(17): p. 3629-3639.
21. Hassan, L., et al., *Simulation of roller compaction by combination of a compaction simulator and oscillating mill – A material sparing approach*. International Journal of Pharmaceutics, 2023. **644**: p. 123281.
22. Chiang, C.W., et al., *Development of an Amorphous Solid Dispersion Formulation for Mitigating Mechanical Instability of Crystalline Form and Improving Bioavailability for Early Phase Clinical Studies*. Molecular Pharmaceutics, 2023. **20**(5): p. 2452-2464.
23. Shah, H.S., et al., *Accelerating pre-formulation investigations in early drug product life cycles using predictive methodologies and computational algorithms*. Therapeutic Delivery, 2021. **12**(11): p. 789-797.
24. Pharmacopeia, U.S., *General Chapter Dissolution <711>*. 2023.
25. French, W.N., et al., *Pharmacopeial standards and specifications for bulk drugs and solid oral dosage forms. Similarities and differences*. Journal of Pharmaceutical Sciences, 1967. **56**(12): p. 1622-1641.

26. Wheless, J.W. and S.J. Phelps, *A Clinician's Guide to Oral Extended-Release Drug Delivery Systems in Epilepsy*. J Pediatr Pharmacol Ther, 2018. **23**(4): p. 277-292.
27. Khan, A., *Prediction of quality attributes (mechanical strength, disintegration behavior and drug release) of tablets on the basis of characteristics of granules prepared by high shear wet granulation*. PLoS One, 2021. **16**(12): p. e0261051.
28. Schulze, D., *Flow Properties of Bulk Solids*, in *Powders and Bulk Solids: Behavior, Characterization, Storage and Flow*, D. Schulze, Editor. 2021, Springer International Publishing: Cham. p. 57-100.
29. Cordova, L., et al., *Measuring the spreadability of pre-treated and moisturized powders for laser powder bed fusion*. Additive Manufacturing, 2020. **32**: p. 101082.
30. Crouter, A. and L. Briens, *The effect of moisture on the flowability of pharmaceutical excipients*. AAPS PharmSciTech, 2014. **15**(1): p. 65-74.
31. Sandler, N., et al., *Effect of Moisture on Powder Flow Properties of Theophylline*. Pharmaceutics, 2010. **2**(3): p. 275-290.
32. Matsusaka, S., et al., *Triboelectric charging of powders: A review*. Chemical Engineering Science, 2010. **65**(22): p. 5781-5807.
33. Zhang, L., X. Bi, and J.R. Grace, *Measurements of Electrostatic Charging of Powder Mixtures in a Free-fall Test Device*. Procedia Engineering, 2015. **102**: p. 295-304.

34. Biegaj, K.W., et al., *Surface Chemistry and Humidity in Powder Electrostatics: A Comparative Study between Tribocharging and Corona Discharge*. ACS Omega, 2017. **2**(4): p. 1576-1582.
35. Podczec, F. and Y. Mia, *The influence of particle size and shape on the angle of internal friction and the flow factor of unlubricated and lubricated powders*. International Journal of Pharmaceutics, 1996. **144**(2): p. 187-194.
36. Nan, W., M. Ghadiri, and Y. Wang, *Analysis of powder rheometry of FT4: Effect of particle shape*. Chemical Engineering Science, 2017. **173**: p. 374-383.
37. Ferrari, F., et al., *The surface roughness of lactose particles can be modulated by wet-smoothing using a high-shear mixer*. AAPS PharmSciTech, 2004. **5**(4): p. 60.
38. Pohlman, N.A., et al., *Surface roughness effects in granular matter: Influence on angle of repose and the absence of segregation*. Physical Review E, 2006. **73**(3): p. 031304.
39. Tay, J.Y.S., et al., *Effects of Particle Surface Roughness on In-Die Flow and Tableting Behavior of Lactose*. Journal of Pharmaceutical Sciences, 2019. **108**(9): p. 3011-3019.
40. Liu, L.X., et al., *Effect of particle properties on the flowability of ibuprofen powders*. International Journal of Pharmaceutics, 2008. **362**(1): p. 109-117.
41. Habibnejad-korayem, M., J. Zhang, and Y. Zou, *Effect of particle size distribution on the flowability of plasma atomized Ti-6Al-4V powders*. Powder Technology, 2021. **392**: p. 536-543.

42. Kudo, Y., M. Yasuda, and S. Matsusaka, *Effect of particle size distribution on flowability of granulated lactose*. Advanced Powder Technology, 2020. **31**(1): p. 121-127.
43. Alizadeh, M., et al., *The effect of particle shape on predicted segregation in binary powder mixtures*. Powder Technology, 2017. **319**: p. 313-322.
44. Mirvakili, S.M. and R. Langer, *Wireless on-demand drug delivery*. Nature Electronics, 2021. **4**(7): p. 464-477.
45. Almoshari, Y., *Osmotic Pump Drug Delivery Systems-A Comprehensive Review*. Pharmaceuticals (Basel), 2022. **15**(11).
46. Varde, N.K. and D.W. Pack, *Microspheres for controlled release drug delivery*. Expert Opin Biol Ther, 2004. **4**(1): p. 35-51.
47. Klingmann, V., et al., *Acceptability of Multiple Uncoated Minitablets in Infants and Toddlers: A Randomized Controlled Trial*. The Journal of Pediatrics, 2018. **201**: p. 202-207.e1.
48. Mitra, B., et al., *Decoding the small size challenges of mini-tablets for enhanced dose flexibility and micro-dosing*. International Journal of Pharmaceutics, 2020. **574**: p. 118905.
49. Schork, N.J., *Personalized medicine: Time for one-person trials*. Nature, 2015. **520**(7549): p. 609-611.
50. Janczura, M., S. Sip, and J. Cielecka-Piontek, *The Development of Innovative Dosage Forms of the Fixed-Dose Combination of Active Pharmaceutical Ingredients*. Pharmaceutics, 2022. **14**(4).

51. Khaled, S.A., et al., *3D printing of five-in-one dose combination polypill with defined immediate and sustained release profiles*. Journal of Controlled Release, 2015. **217**: p. 308-314.
52. Sutradhar, K.B. and C.D. Sumi, *Implantable microchip: the futuristic controlled drug delivery system*. Drug Delivery, 2016. **23**(1): p. 1-11.
53. *Abilify MyCite summary review*. 2017.
54. *Smart pills to help diagnose gut disorders*, in *National Science Foundation*.
55. Hagan, A., et al., *Predicting pharmacokinetic behaviour of drug release from drug-eluting embolization beads using in vitro elution methods*. European Journal of Pharmaceutical Sciences, 2019. **136**: p. 104943.
56. Marvola, M., et al., *Enteric polymers as binders and coating materials in multiple-unit site-specific drug delivery systems*. European Journal of Pharmaceutical Sciences, 1999. **7**(3): p. 259-267.
57. Portier, C., C. Vervaet, and V. Vanhoorne, *Continuous Twin Screw Granulation: A Review of Recent Progress and Opportunities in Formulation and Equipment Design*. Pharmaceutics, 2021. **13**(5).
58. National Academies of Sciences, E., et al., in *Innovations in Pharmaceutical Manufacturing on the Horizon: Technical Challenges, Regulatory Issues, and Recommendations*. 2021, National Academies Press (U.S.)

Copyright 2021 by the National Academy of Sciences. All rights reserved.: Washington (DC).

59. Yoon, H.-S., et al., *A comparison of energy consumption in bulk forming, subtractive, and additive processes: Review and case study*. International Journal

- of Precision Engineering and Manufacturing-Green Technology, 2014. **1**(3): p. 261-279.
60. Kuminek, G., et al., *Cocrystals to facilitate delivery of poorly soluble compounds beyond-rule-of-5*. Adv Drug Deliv Rev, 2016. **101**: p. 143-166.
  61. Tehler, U., et al., *Optimizing Solubility and Permeability of a Biopharmaceutics Classification System (BCS) Class 4 Antibiotic Drug Using Lipophilic Fragments Disturbing the Crystal Lattice*. Journal of Medicinal Chemistry, 2013. **56**(6): p. 2690-2694.
  62. Salawi, A., *Self-emulsifying drug delivery systems: a novel approach to deliver drugs*. Drug Deliv, 2022. **29**(1): p. 1811-1823.
  63. Wilson, V.R., et al., *Amorphous solid dispersions of enzalutamide and novel polysaccharide derivatives: investigation of relationships between polymer structure and performance*. Scientific Reports, 2020. **10**(1): p. 18535.
  64. Baird, J.A., B. Van Eerdenbrugh, and L.S. Taylor, *A classification system to assess the crystallization tendency of organic molecules from undercooled melts*. J Pharm Sci, 2010. **99**(9): p. 3787-806.
  65. Pandi, P., et al., *Amorphous solid dispersions: An update for preparation, characterization, mechanism on bioavailability, stability, regulatory considerations and marketed products*. Int J Pharm, 2020. **586**: p. 119560.
  66. Agrawal, A., et al., *Development of Tablet Formulation of Amorphous Solid Dispersions Prepared by Hot Melt Extrusion Using Quality by Design Approach*. AAPS PharmSciTech, 2016. **17**(1): p. 214-232.

67. Lima, A.L., et al., *Hot-Melt Extrusion as an Advantageous Technology to Obtain Effervescent Drug Products*. Pharmaceutics, 2020. **12**(8).
68. Verreck, G., et al., *The effect of pressurized carbon dioxide as a temporary plasticizer and foaming agent on the hot stage extrusion process and extrudate properties of solid dispersions of itraconazole with PVP-VA 64*. European Journal of Pharmaceutical Sciences, 2005. **26**(3): p. 349-358.
69. Triboandas, H., et al., *Itraconazole Amorphous Solid Dispersion Tablets: Formulation and Compaction Process Optimization Using Quality by Design Principles and Tools*. Pharmaceutics, 2022. **14**(11).
70. Sarabu, S., et al., *Hypromellose acetate succinate based amorphous solid dispersions via hot melt extrusion: Effect of drug physicochemical properties*. Carbohydrate Polymers, 2020. **233**: p. 115828.
71. Xu, H., et al., *Hybrid Manufacturing of Oral Solid Dosage Forms via Overprinting of Injection-Molded Tablet Substrates*. Pharmaceutics, 2023. **15**(2).
72. Walsh, E., et al., *Manufacture of tablets with structurally-controlled drug release using rapid tooling injection moulding*. International Journal of Pharmaceutics, 2022. **624**: p. 121956.
73. Quinten, T., et al., *Evaluation of injection moulding as a pharmaceutical technology to produce matrix tablets*. European Journal of Pharmaceutics and Biopharmaceutics, 2009. **71**(1): p. 145-154.
74. Almeida, A., et al., *Ethylene vinyl acetate as matrix for oral sustained release dosage forms produced via hot-melt extrusion*. European Journal of Pharmaceutics and Biopharmaceutics, 2011. **77**(2): p. 297-305.

75. Quinten, T., et al., *Sustained-release and swelling characteristics of xanthan gum/ethylcellulose-based injection moulded matrix tablets: in vitro and in vivo evaluation*. J Pharm Sci, 2011. **100**(7): p. 2858-70.
76. Desai, P.M., et al., *Integrated hot-melt extrusion – injection molding continuous tablet manufacturing platform: Effects of critical process parameters and formulation attributes on product robustness and dimensional stability*. International Journal of Pharmaceutics, 2017. **531**(1): p. 332-342.
77. Melocchi, A., et al., *Evaluation of Hot-Melt Extrusion and Injection Molding for Continuous Manufacturing of Immediate-Release Tablets*. Journal of Pharmaceutical Sciences, 2015. **104**(6): p. 1971-1980.



## CHAPTER 2

### ***5 GRAMS IN 2 WEEKS: MATERIAL SAVING TABLET DEVELOPMENT OF DIRECT COMPRESSION FORMULATIONS FOR IMMEDIATE RELEASE APPLICATIONS***

Wood, C.; Manovacia, N.; Drewke, J.; Bell, S.; Bramhall, J.; Locklin J, To be  
submitted to The Journal of Controlled Release

**Abstract:**

Material sparing tablet development describes a new approach to tablet formulation development that uses the material properties of the active pharmaceutical ingredient (API) to guide formulation design. This work expands on the methods and demonstrates its application with any API. Four APIs were randomly selected from Boehringer Ingelheim's platform opnMe. The APIs exhibited different morphologies, densities, flowability, and compression behaviors, which presented unique formulation challenges. Small batches of each API ( $\leq 5$  g) were used to mimic early-phase development. Each API was analyzed for particle morphology, compression behavior, and flowability. Formulations were then designed to complement these API properties. Powder blends were tested for flowability ( $\leq 12$  mm Flodex) and tensile strength ( $> 2$  MPa). To ensure manufacturability, tablet disintegration ( $< 15$  min), and friability were verified. Accelerated stability testing was done to determine excipient compatibility and overall drug product stability (NMT 0.3 % API loss). This work demonstrated that for any API, formulations could be designed and tested for critical manufacturing attributes, and possible failure points determined using less than 5 g of API in less than 14 days.

**Introduction:**

Tablets are the most popular method of drug delivery due to their high patient compliance, high production capacity, and comparatively lower manufacturing cost. Tablets are made via compression of powder blends. If an API is viable for direct compression (DC), meaning no additional modification of the API is needed, then the API can be blended with other excipients and directly tableted. In cases where an API is unsuitable for direct compression (i.e., cases of poor flowability or a tendency to

segregate), additional modification of the API might be needed prior to compression to enable the API to form a stable and well-flowing powder blend[1]. API modification methods include granulation, Würster coating, and spray drying[2]. Modifications of the API increase the time, resources, and cost needed to produce tablets. Therefore, DC is the simplest and most economical approach to tableting, but developing a DC formulation is not without its challenges. Tableting formulations require sufficient flowability to ensure good content uniformity and dosage size while operating tableting equipment at industrial speeds (up to 450 tablets per second)[3]. The powder blends must also form cohesive tablets at pressures that are feasible for industrial tableting equipment (tableability). Additionally, the resulting tablets must be mechanically strong enough to withstand processing conditions but as per guidelines for immediate release tablets, disintegrate in less than 15 minutes.

Due to these challenges, formulation development is often conducted on a large scale to ensure the scalability and industrial viability of the final product. Unfortunately, this approach, coupled with the common trial-and-error methods, usually requires kilograms of API and months to years of development work.[4, 5]. To improve the efficiency of this process, reduce costs, and shorten the timeline of getting medications to patients, a quality-by-design approach known as material-sparing tablet development was discussed by Sun and coworkers[6, 7].

The work described herein expands on the material-sparing tablet formulation development approach by demonstrating that regardless of the physical-chemical properties of the API, a successful formulation can be achieved using less than 5 g of API in approximately two weeks. Additionally, this work improved upon the methodology

discussed by Sun *et al.* through the addition of excipient compatibility and accelerated API stability testing with only moderate increases to the timeline and API usage. The key to this material sparing tableting approach is to utilize the material properties of the API and excipients to develop formulations that complemented the API, reducing both the amount of time and API required. By utilizing small-scale test methods and formulating based on material properties, the limited API was used more efficiently while still assessing the quality of the powder blends and tablets and evaluating manufacturing feasibility.

The nominated DC formulations exhibited good flowability, chemical stability, and homogeneity and yielded mechanically robust tablets that delivered API effectively. Setting these criteria as thresholds allowed for rapid screening and elimination of formulations that were not feasible, which shortened the timeline for formulation development and allowed for the use of less than 5 g of API. This study primarily focused on the mechanical properties of the formulations and how they can be optimized for DC or identify reasons why certain APIs may not be suitable candidates for DC.

### **Materials and Methods:**

#### *Materials*

BI 638683 (BI-0001), BI 639667 (BI-0002), BI 666877 (BI-0003), and BI 729802 (BI-0004) (were donated by Boehringer Ingelheim and used as received. Fastflo® 316 (LAC) (Kerry Inc.), Avicel® PH-102 (MCC) (Dupont), Emcompress Anhydrous® (DICAL) (JRS Pharma), and Explotab® (SSG) (JRS Pharma) were donated and used as received. Magnesium stearate (MS) (LFA) was purchased and used as received.

#### *Flowability of Pure API and Powder Blends with Flodex*

Intrinsic powder flowability tester (Flodex, Hansen) was used to quantify the flowability of pure API for formulation development and the powder blends for manufacturability. Flodex testing is helpful for quantifying the flowability, but visual observations of the intrinsic powder flowability of the pure API are sufficient for formulation development. For pure API, 20 g of powder was sieved with a # 20 sieve (850  $\mu\text{m}$  pore size) and loaded via funnel into the Flodex apparatus. All API was recovered after the test to be used for formulation development since flodex is a non-destructive test. The Flodex value was reported as the smallest orifice the powder would freely flow through 3 consecutive times. The same procedure was used for blend analysis, except only 10-15 grams of each blend, minus magnesium stearate, was used for testing to prevent lubricant overmixing. Avicel PH-102 was used to determine the threshold for successful flowability. Avicel PH-102 is a common tableting excipient and has been reported as the standard for flowability that is industrially viable[8]. Therefore, powders with flowability comparable to or better than Avicel PH-102 were classified as successful flowability.

#### *Particle Morphology and Size Distribution via Scanning Electron Microscopy (SEM)*

1-3 mg of API was sprinkled onto conductive carbon tape and dispersed with compressed air to remove excess powder. This sample was prepared in a level 1000 clean room to minimize contamination. Samples were sputter coated with 10 nm of gold/palladium and imaged on a scanning electron microscope (FEI Teneo, Thermo-Fisher). Images for each API were taken at different magnifications due to the diversity in particle sizes. ImageJ software was used to measure discrete particles for length and width. Particle lengths were plotted to determine the particle size distribution of the pure APIs. Particle

morphologies were classified using the Handbook of Mineralogy published by the Mineralogical Society of America[9].

#### *Bulk and Tapped Density*

Bulk and tapped density testing were performed with a 100 ml graduated cylinder and an automated tap tester (PT TD200, Pharmatest). The powder was sieved through a #20 sieve before being gently added to the graduated cylinder. The cylinder was sealed and tapped according to ISO 3953 until the powder bed volume changed by less than 2%. Final mass and volume were measured to calculate the tapped density.

#### *True Density Measurement and Compression Behavior (Heckel Analysis)*

The true densities of pure APIs were measured using a 10 cm<sup>3</sup> insert on a helium pycnometer (AccuPyc II 1345, Micromeritics). Sample mass was between 1-6 grams for all APIs tested due to the difference in bulk density. The test was set for ten purges and ten test cycles, but run precision was used to stop the experiment when the variation between five consecutive measurements was below 0.05%. The average of all five cycles is the true density of the sample listed in Table 2.4. Pressure and equilibration rates were 19.5 psig and 0.005 psig/min, respectively.

Heckel plots were generated for pure APIs using the constant “true” volume method [10]. The mass of powder needed to reach a volume of 0.104 cm<sup>3</sup> was calculated using Equation 1.

*Equation 1. mass of API = true density \* desired volume*

API powder was manually loaded into the tablet press (XP-1, Korsch) with 6mm flat circle tooling. Tablets were compressed at ten tablets per minute. Displacement and force readouts for the upper and lower tooling during the entire compression and decompression cycle were recorded and used to calculate the change in porosity [11].

Volume change and compression pressure were calculated from the raw displacement and force data. The resulting Heckel plots were initially analyzed from 20-80 MPa of the compression and decompression phases to calculate the slope of the line. The analysis regions were adjusted until a linear fit of  $\geq 0.98$  was achieved. The inverse of the slope of the compression and the decompression curves are the plastic and elastic yield pressures, respectively.

#### *Preparation of Powder Blends*

10-15 gram batches of each formulation were made (Table 2.4). All excipients except magnesium stearate were mixed in a Turbula® mixer for 5 minutes and then sieved with # 20 and a #40 or #60 sieve (850, 425, 250  $\mu\text{m}$  pore size respectively). Three grams of the powder blend were aliquoted for making tablets, and the remainder was used to test flowability. Before tableting, magnesium stearate was added to the powder aliquot and mixed in the Turbula® mixer for an additional minute.

#### *Tabletability of Powder Blends*

100 mg of powder blend was weighed and manually loaded into the die. Tablets were made from 50 MPa to at least 500 MPa of compression pressure for all formulations. For tensile strength analysis, the dimensions of each tablet were measured using digital calipers (547-500S, Mitutoyo) after ejection. Tablets were then tested for diametrical breaking force (TBH 125, Erweka). Equation 2 was used to calculate the tensile strength of tablets, and results were plotted as a function of compression pressure. To conserve powder, only one tablet per compression pressure was tested for tensile strength.

*Equation 2. tensile strength =  $(2 \cdot \text{breaking force}) / (\pi \cdot \text{tablet thickness} \cdot \text{tablet width})$*

#### *Friability*

Tablets made at varying compression pressures were dusted and then weighed. Three tablets per formulation per compression pressure were analyzed instead of the traditional ten tablets to keep with the material sparing nature of the work. In compliance with USP <1216>, tablets were loaded into a friabilator (45-2100, Vankel) and rotated for 4 minutes at 25 rpm. Tablets were dusted and weighed again, and the percentage mass loss was calculated.

#### *Disintegration Testing*

If tablets passed friability, the same tablets were used for disintegration testing according to USP standard <701> for uncoated tablets. Immersion fluid was reverse osmosis water at 37 °C. Basket oscillations were 30 strokes per minute with a standard six-tube sample basket (PTZ-S, Pharmatest). The timer started when the bottom of the basket touched the water and stopped when all pieces of the tablet had passed through the wire mesh. Three tablets per formulation were tested, but the disintegration times were identical within the resolution limits for this analysis method, so no standard deviations were reported.

#### *Content Uniformity Testing*

HPLC analytical methods were provided by Boehringer Ingelheim. HPLC calibration curves were made for each API (1100, Agilent), and all curves had  $\geq 0.999$  linearity. Each API required different gradient and HPLC conditions (Table 2.1, 2.2, and 2.3). The flow rate for all HPLC methods were 1 ml/min. Tablets were randomly selected for content uniformity analysis. The majority of the HPLC mobile phases contain trifluoroacetic acid (TFA) to improve HPLC resolution.

The average and standard deviation for each formulation were calculated from the quantification of API in 5 individual tablets. Tablets were weighed and then placed in a



100 mL volumetric flask before disintegrating using either 90:10 acetonitrile-water or 90:10 methanol-water. Samples were sonicated for 15 minutes and filtered with a 0.2  $\mu\text{m}$  PTFE syringe filter before HPLC analysis. API concentration was calculated using the standard curve. Acceptance criteria of no more than 15 passes USP <905> standards for acceptable consistency in dosage form. Since acceptance criteria (AV) (Equation 3) is calculated using both the average API loading ( $\bar{x}$ ) and the relative standard deviation (SD), it takes into account both the amount of API added to the formulation and the tendency for a blend to segregate.

$$\text{Equation 3 } AV = |\bar{x} - 98.5| + (2.4 * SD)$$

**Table 2.1. HPLC Methods for Each API**

BI	Method	Mobile Phase(s)	Wavelength (nm)	Column	Column temp (° C)	Injection volume ( $\mu\text{L}$ )
1	Gradient	0.1% TFA in water, 0.1% TFA in acetonitrile	250	ACE 50 X 4.6 mm, 5 $\mu\text{m}$ , C18, 100 Å	50	5
2	Isocratic	70:30, 0.1% TFA in water, 0.1% TFA in acetonitrile	238	ACE 50 X 4.6 mm, 5 $\mu\text{m}$ , C18, 100 Å	35	2
3	Gradient	0.05 M phosphate buffer (pH 7.5), acetonitrile	260	ACE 50 X 4.6 mm, 5 $\mu\text{m}$ , C18, 100 Å	40	15
4	Isocratic	50:50, 0.1% TFA in water, acetonitrile	330	Agilent Eclipse XBD-C18, 150 x 4.6 mm, 5 $\mu\text{m}$ , 80 Å	40	10

**Table 2.2 BI-1 HPLC Method Mobile Phase Gradient**

Time (Min)	0.1% TFA in ACN (%)	0.1% TFA in Water (%)	Flow Rate (mL/min)
0	30	70	1
2	30	70	1
5	70	30	1
Post run (4 minutes)	30	70	1

**Table 2.3 BI-3 HPLC Method Mobile Phase Gradient**

Time (Min)	ACN (%)	0.05 M Phosphate Buffer (%)	Flow Rate (mL/min)
0	20	80	1
1	20	80	1
6	95	5	1
8	95	5	1
8.01	20	80	1
10	20	80	1

### *Accelerated Stability Studies*

Tablet samples were placed in humidity chambers with different saturated salt solutions to achieve specified temperature and humidity conditions (20°C/65% RH, 20°C/43% RH, and 70°C/75% RH). After five days, samples were analyzed via HPLC using the same sample preparation method outlined in content uniformity testing. Tablets tested at 70°C /75% RH required 15 additional minutes of sonication to disintegrate fully. Percent degradation was calculated via Equation 4 to normalize for API content and HPLC variation. Degradant peak areas were reported as a percentage of the area of the main API peak area. Degradant peaks greater than 0.3% of the area of the API peak had sufficient degradation to signal an excipient incompatibility or API instability.

*Equation 4. degradation percent= (area of degradation peak)/ (area of API peak) \*100*

### **Results and Discussion:**

#### *Particle Shape, Size, and Size Distribution*

As seen in Table 2.4 and Figure 2.1, the morphologies of the APIs selected for this study cover a range of shapes and sizes, which directly impact compressibility and flowability. The particle size distribution of each API is plotted in Figure 2.1. Identifying the particle properties that impact the flowability and compressibility of the powder is beneficial for selecting the best excipients and determining maximum API loading. For this study, particle size classifications are as follows: average particle size <20 µm is ultrafine, <75 µm is fine, <150 µm is medium, and >150 µm is coarse/large particles.

**Table 2.4. Synopsis of API Particle Morphology**

API	Particle Morphology	Average Particle Size (l x w) ( $\mu\text{m}$ )	True Density (g/mL)	Bulk Density (g/mL)	Tapped Density (g/mL)	Compressibility Index	Flodex Value (mm)
<b>BI-1</b>	Thin tabular	10 x 3	1.443	0.14	0.33	136	>34
<b>BI-2</b>	Random	13 x 8	1.508	0.35	0.61	74	22
<b>BI-3</b>	Bladed	43 x 6	1.424	0.16	0.32	100	28
<b>BI-4</b>	Coxcomb	150	1.369	0.55*	0.77*	136	8

\*Bulk and tapped density measured with 10 mL graduated cylinder because of low powder volume

*BI-1 (Tabular):* Tabular is a plate-like structure defined as broad and thin with two well-developed parallel faces. As shown in Figure 2.1a, aggregate stacks of the tabular plates are more abundant than discrete particles, which could suggest high surface energy of BI-1 leading to large cohesive forces between particles. BI-1 has a relatively narrow particle size distribution, with the lengths of the particles ranging from 3 - 24  $\mu\text{m}$ . The average particle size is 10  $\mu\text{m}$  x 3  $\mu\text{m}$ , which is an ultra-fine particle. The tabular morphology and small particle size lends itself to high packing density as can be seen by the substantial number of particles per aggregate stack (Figure 2.1a).

*BI-2 (Random):* As the name implies, random particles have no observable shape pattern. BI-2 is an ultra-fine particle with an average particle size of 13  $\mu\text{m}$  x 8  $\mu\text{m}$ . This API also has a slightly wider particle size range from 0.3 - 36  $\mu\text{m}$  compared to BI-1. There are actually numerous particles in the 0.3  $\mu\text{m}$  range, but most of those particles are adhered to the surface of larger particles (Figure 2.1b). This inherent morphology is extremely beneficial for formulation because the small particles act as a coating on the larger irregularly shaped particles, making them in effect behave like spherical particles. This phenomenon is actually a common technique employed by formulators to improve flowability of sticky or irregularly shaped APIs. A glidant, like fumed silica, is milled

with the API to coat the individual particles and decrease the interparticulate friction, which drastically improves flowability. BI-2 inherently exhibits this behavior.

*BI-3 (Bladed):* Bladed is a habit that is flat, elongated, and often comes to a point on the ends. BI-3 has a wide particle size distribution with particle lengths ranging from 12 -124  $\mu\text{m}$ . This API is a fine particle with an average particle size of 43  $\mu\text{m}$  x 6  $\mu\text{m}$ . As can be seen in Figure 2.1c, the texture of the bladed particles is rough on the surface, which will likely increase the interparticle friction and impact the intrinsic flowability of this API.

*BI-4 (Coxcomb):* Coxcomb is a habit defined as closely spaced aggregated tabular crystals. Since BI-4 particles are predominately spherical due to the agglomerated tabular structure (Figure 2.1d), diameters of the spheres sufficed for size measurement. The average particle size is 150  $\mu\text{m}$ . The particle size distribution of BI-4 is the largest of all the APIs studied, ranging from 94 - 263  $\mu\text{m}$ . BI-4 therefore is predominately composed of large particles with some medium particles.

#### *True Density, Bulk Density, Tapped Density, and Compressibility Index*

True density is the measurement of the density of a material excluding pores and is an intrinsic property of the material. Bulk and tapped density are measurements of the density of the powder under static and dynamic conditions and are meant to simulate conditions that might be experienced during processing. Bulk and tapped density are largely dependent on the morphology and surface chemistry of the particles, which are influenced by the production and storage conditions of the API[12, 13]. Compressibility index (CI) is a measurement of the ratio between the bulk and tapped density and has historically been used as a predictive tool for flowability.

As presented in Table 2.4, the true density of BI-1 is  $1.4426 \pm 0.0023$  g/mL. The high compressibility index of BI-1 is caused by the small particle size and tabular structure of the particles which increases particle packing efficiency under dynamic conditions. Despite having the second largest true density, this API had the smallest bulk density. The true density of BI-2 is  $1.5084 \pm 0.0008$  g/mL. BI-2 has a higher bulk density than BI-1, likely caused by the higher true density, and is less compressible than any of the other APIs investigated. The true density of BI-3 is  $1.4243 \pm 0.0017$  g/mL. BI-3 has a similar bulk and tapped density to BI-1 and is also highly compressible. The true density of BI-4 is  $1.3690 \pm 0.0010$  g/mL. The large average particle size and uniform particle shape of BI-4 leads to the high bulk density despite the true density being the lowest of all APIs in this study. BI-4 has a wide distribution of particle sizes, which leads to a greater packing efficiency and thus a higher compressibility index.

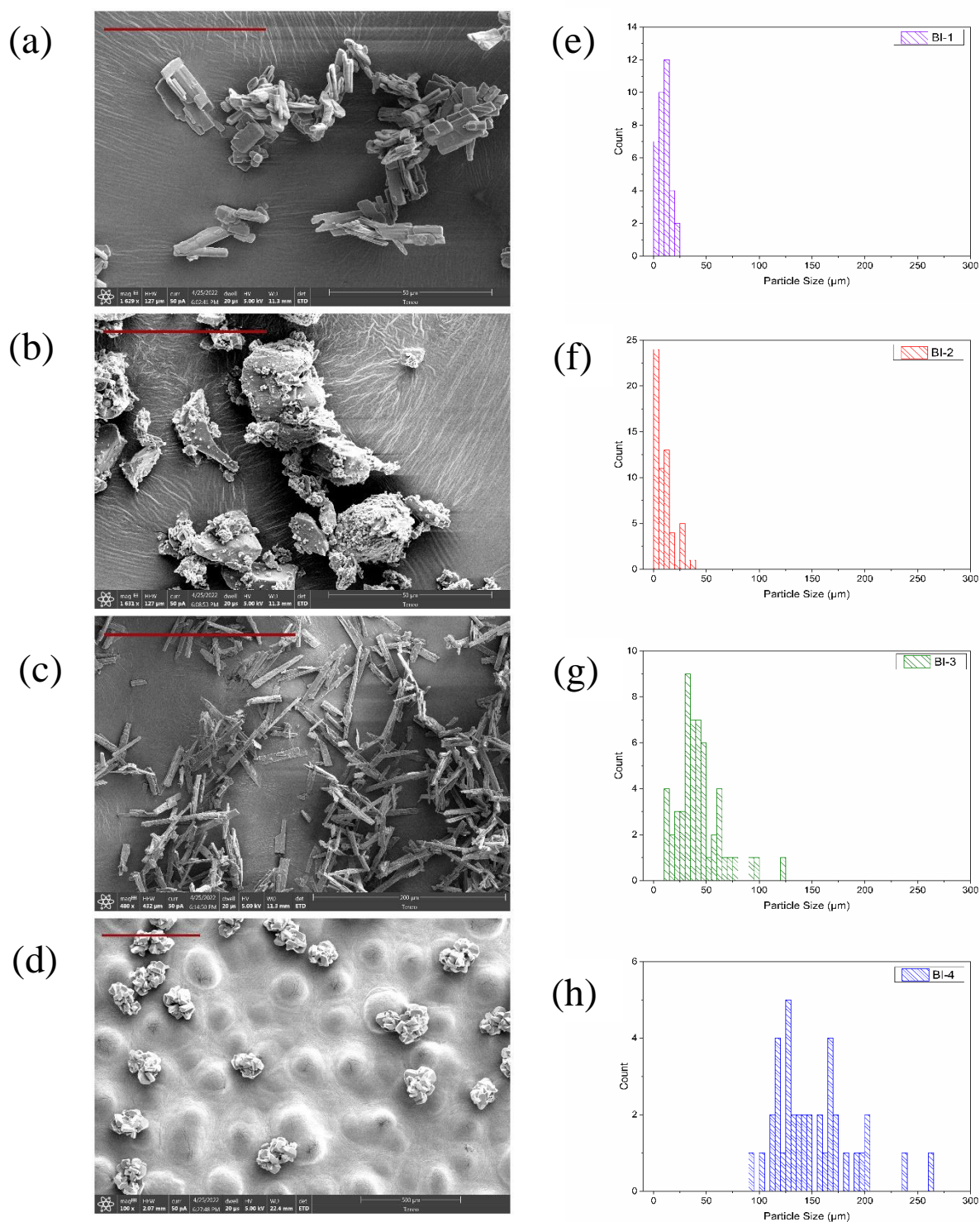


**Figure 2.1.** Scanning electron microscopy of (a) BI-1 with scale bar 50  $\mu\text{m}$ , (b) BI-2 with scale bar 50  $\mu\text{m}$ , (c) BI-3 with scale bar 200  $\mu\text{m}$ , and (d) BI-4 with scale bar 500  $\mu\text{m}$ .

Particle size distribution of (e) BI-1, (f) BI-2, (g) BI-3, and (h) BI-4

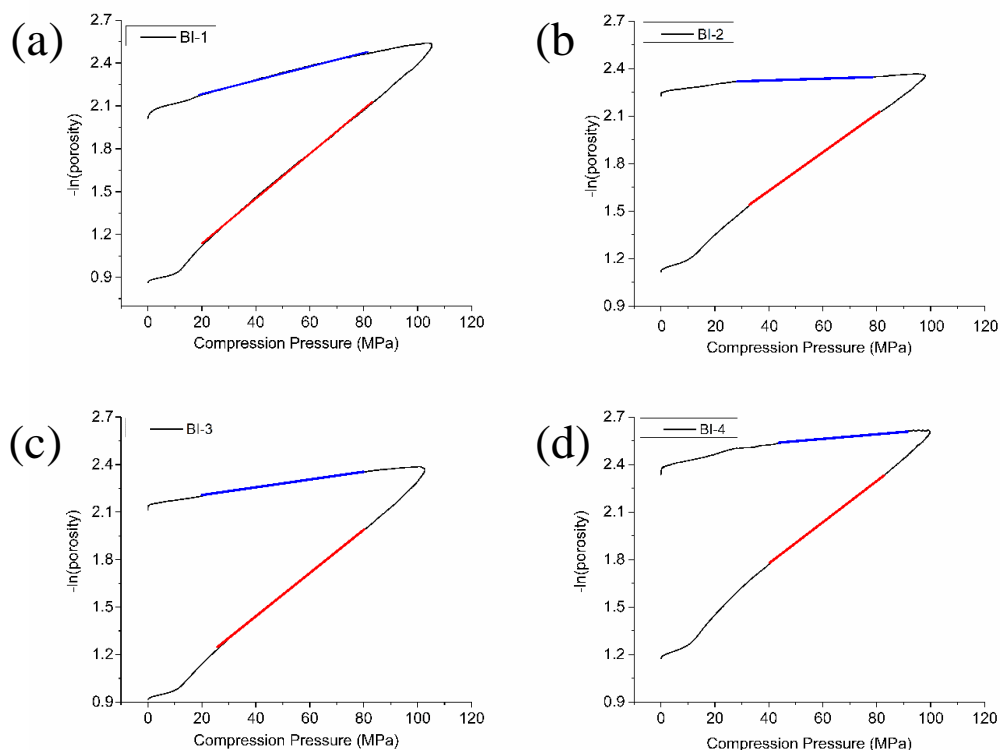


**Figure 2.2.** Heckel Plots of BI-1 (a), BI-2 (b), BI-3 (c), and BI-4 (d). Red lines indicate the analysis region for the compression phase and blue lines indicate the analysis region for the decompression phase.

### *Flowability*

The lower the intrinsic flowability value the better the flowability of the powder. Avicel PH 102 has an intrinsic flowability value of 12 mm and is considered the threshold for industrially feasible flowability. Therefore, any powders with a flowability through  $\leq 12$  mm should have sufficient flowability to be used on industrial tableting equipment at full speed without complications.

The intrinsic flowability of BI-1 is extremely poor with the powder not flowing through the largest aperture test disk available (34 mm diameter). Therefore, the Flodex value for

this API is unmeasurable and poor flowability is evident. The poor intrinsic flowability of this API will make it particularly challenging to formulate because even at low API loading ( $<15\%$  w/w) it will likely impact the overall powder blend flowability. Despite having small particle size, BI-2 has the second lowest intrinsic flowability with a Flodex value of 22 mm. The high true density and low compressibility of this API is likely the reason that the flowability of it is improved when compared to BI-1 despite having similar particle sizes. The intrinsic flowability of BI-3 is 28 mm. Despite having larger particles on average than BI-1 and BI-2, the flowability of this API is hindered by the large distribution of particle sizes and the lower true density of the material compared to the first two APIs. Thus, the flowability of this API is moderately poor and will be challenging to develop a powder blend formulation that achieves industrially relevant flowability. The intrinsic flowability of BI-4 is 8 mm which is unusually low for a pure API. The excellent flowability is due to the large average particle size which overcomes the low true density, large particle size distribution, and high compressibility.

Compressibility index has historically been used as a predictive tool for flowability. The rationale was that powders with higher compressibility had poorer flowability. As can be seen in Table 2.4, BI-4 has the same compressibility as BI-1, but the flowability of BI-4 is superior. Compressibility is not a reliable predictor of flowability because it does not consider true density, average particle size, and other factors that contribute to flowability. Particle flow happens when the force of gravity times the mass of the particle is sufficiently large to overcome the cohesive forces of the particles. The larger the particle mass, the more likely a particle is to exhibit good flowability. Therefore, large particles or particles with a high true density will often have good powder flowability.



### *Compression Behavior (Heckel Analysis)*

Table 2.5 shows the plastic yield pressures ( $YP_p$ ) and elastic yield pressures ( $YP_e$ ) of each API calculated from the linear fit of the Heckel plots. Heckel, Kawakita, and numerous other methods of evaluating compression behavior have been explored in the literature and have been criticized for oversimplifying material classification[14-20].

Conventionally,  $YP_p$  values  $< 100$  MPa are classified as plastic/ductile, while values  $> 100$  Mpa are brittle[15]. For a DC powder formulation, a 2:1 or 3:1 ratio of brittle to ductile (high yield pressure to low yield pressure) excipients has been found to give optimal tabletability profiles[21]. In this study, all of the APIs are classified as plastic, so the ratio of brittle (DICAL/LAC) to ductile (MCC) will be similar for all formulations. If any of the APIs had been brittle, the MCC content would have been increased so that optimal brittle to ductile ratios would be maintained.

Additionally, materials with low  $YP_e$  values have potential for high elastic recovery during and after tableting. However, this is not always the case. One example commonly used in formulation work is MCC which has a low  $YP_e$  value but minimal elastic recovery[15]. It can be challenging to distinguish between plastic and elastic materials using Heckel analysis, but in this study visual observations during tableting helped identify APIs with a propensity for elastic recovery.

BI-1 has the lowest  $YP_p$ . By conventional Heckel classification, this API would be classified as a plastic material with a high potential for elastic recovery. Cohesive failure caused by high elastic recovery was not observed in tablets made of pure BI-1 despite having the lowest  $YP_e$  value. BI-2 has the highest  $YP_p$  and  $YP_e$  values of the APIs studied, which indicates that it is the least plastic API and has no elastic recovery. BI-3

has a small  $Y_{P_p}$  value and is thus classified as a plastic material. The  $Y_{P_e}$  is moderately high, so it would typically be classified as having minimal elastic recovery. However, during Heckel analysis, tablets made from pure BI-3 underwent cohesive failure during ejection. When compressed at lower pressures, tablets remained intact during ejection, but would soon cap or laminate when exposed to minimal shear stress. This behavior is highly indicative of elastic recovery as well as a lack of cohesion between BI-3 particles. BI-4 has a low  $Y_{P_p}$  and a high  $Y_{P_e}$ , so it is classified as plastic with little to no elastic recovery.

<b>Table 2.5. Compression Behavior of API</b>			
<b>API</b>	Yield Pressure Plastic (Compression Phase) (MPa)	Yield Pressure Elastic (Decompression Phase) (MPa)	Compression Behavior Classification*
<b>BI-1</b>	64	208	Plastic
<b>BI-2</b>	82	1822	Plastic
<b>BI-3</b>	73	408	Plastic, high elastic recovery
<b>BI-4</b>	77	685	Plastic
<b>*Unless indicated otherwise, samples are classified as having little to no elastic recovery</b>			

Elastic recovery after tableting leads to a reduction in solid fraction after ejection and subsequently, weaker tablets. Being able to accurately identify and quantify the propensity of a material to cap or laminate after ejection is crucial for formulation development. Material sparing methods of compression behavior classification are an ongoing area of research that will enable better and more efficient formulation development.[5, 22]

### *Formulation Design*

Formulations tested for each API and flowability of the powder blends are listed in Table 2.6. Having more than 15% fine particles in a formulation reduces the number of particles that overlap between layers of compressed powder as a result the tablet can undergo cohesive failure at the interfaces of the layers, which leads to capping and lamination.

Since most of the APIs are ultra-fine/fine particles, the maximum API loading for those APIs would be 15%. However, since MS and SSG are also ultrafine particles, the maximum API loading of all the formulations was set at 10% to leave room for additional disintegrant or lubricant if needed. Additionally, since the majority of the APIs studied have poor flowability, increasing the API loading would be detrimental to the overall flowability of the blends.

BI-1 is an ultra-fine API with terrible flowability, and thus, the most challenging part of formulation design is achieving industrial flowability without having blend homogeneity issues. Choosing excipients with larger particle sizes will improve the flowability of the powder blend but will increase the tendency for segregation. The decision was made to focus on achieving flowability rather than preventing segregation. As seen in Table 2.6, even with most of the formulation made of excipients with excellent flowability, industrial flowability of the blend was not achieved. Additional content of DICAL or LAC would have been detrimental to the tableability of the powder blend and therefore was not added to try and further improve flowability.

**Table 2.6. Powder Blend Formulations and Flowability Evaluation**

<b>API</b>	<b>Formula ID</b>	<b>API (%w/w)</b>	<b>MCC (%w/w)</b>	<b>LAC (%w/w)</b>	<b>DICAL (%w/w)</b>	<b>SSG (%w/w)</b>	<b>MS (%w/w)</b>	<b>Flodex Value (mm)</b>
<b>BI-1</b>	F1	10	22	66	0	1	1	<b>20</b>
<b>BI-1</b>	F2	10	22	0	66	1	1	<b>16</b>
<b>BI-2</b>	F1	10	30	58	0	1	1	<b>10</b>
<b>BI-2</b>	F2	10	44	44	0	1	1	<b>12</b>
<b>BI-3</b>	F1	10	87	0	0	2	1	<b>16</b>
<b>BI-3</b>	F2	10	0	87	0	2	1	<b>8</b>
<b>BI-3</b>	F3	10	43.5	43.5	0	2	1	<b>14</b>
<b>BI-3</b>	F4	10	58	29	0	2	1	<b>14</b>
<b>BI-3</b>	F5	10	29	58	0	2	1	<b>12</b>
<b>BI-4</b>	F1	10	30	58	0	1	1	<b>6</b>
<b>BI-4</b>	F2	10	30	0	58	1	1	<b>5</b>

Since BI-2 has ultra-fine particles, it too is likely to segregate if excipient particle sizes are drastically different. The better intrinsic flowability of BI-2 enables a lower portion of the large particle size excipients, enabling lower DICAL and LAC loading to modify the compression behavior of the powder blend. Addition of more low-yield pressure (plastic) excipients lowers the compression pressure needed to achieve high tensile strength tablets, thus reducing wear and tear on tableting equipment and increasing tablet production rate. Both formulations tested achieved industrial flowability (Table 2.6).

BI-3 had significant cohesive failure during Heckel analysis with an extreme tendency to laminate during and after ejection. More formulations with varying ratios of low and high-yield pressure excipients were tried for this API than any other to see how formulation can impact the tablet strength of an API with high elastic recovery. F2 and F5 achieved industrial flowability (Table 2.6) because they had a higher percentage of LAC, an excipient with excellent flowability, which improved the flowability of the overall blend. BI-3 has more SSG than other formulations because it was the first sample to be formulated, and after seeing that the disintegration times were extremely low for BI-3, SSG concentrations were lowered for the remaining formulations.

The excellent intrinsic flowability and large particle size of BI-4 makes it suitable for use with a wide range of formulations and could have had higher API loading without negatively impacting flowability but was kept at 10% loading in this study to remain consistent with the other APIs. The excellent flowability of the powder blends for BI-4 compared to BI-2 and BI-3 is a testament to the influence the API has on powder blends even at low percent loading in the formulation.

### Tabletability

When analyzing tabletability curves, the target tensile strength is  $\geq 2$  MPa using less than 500 MPa of compression pressure. As can be seen in Figure 2.3, all formulations tested not only met those requirements but were able to achieve much higher tensile strength within an industrially relevant compression window. The optimal manufacturing compression pressure is the onset of the plateau region of the tabletability curve. This region optimizes tablet strength, and because of the lower slope, minor changes in force

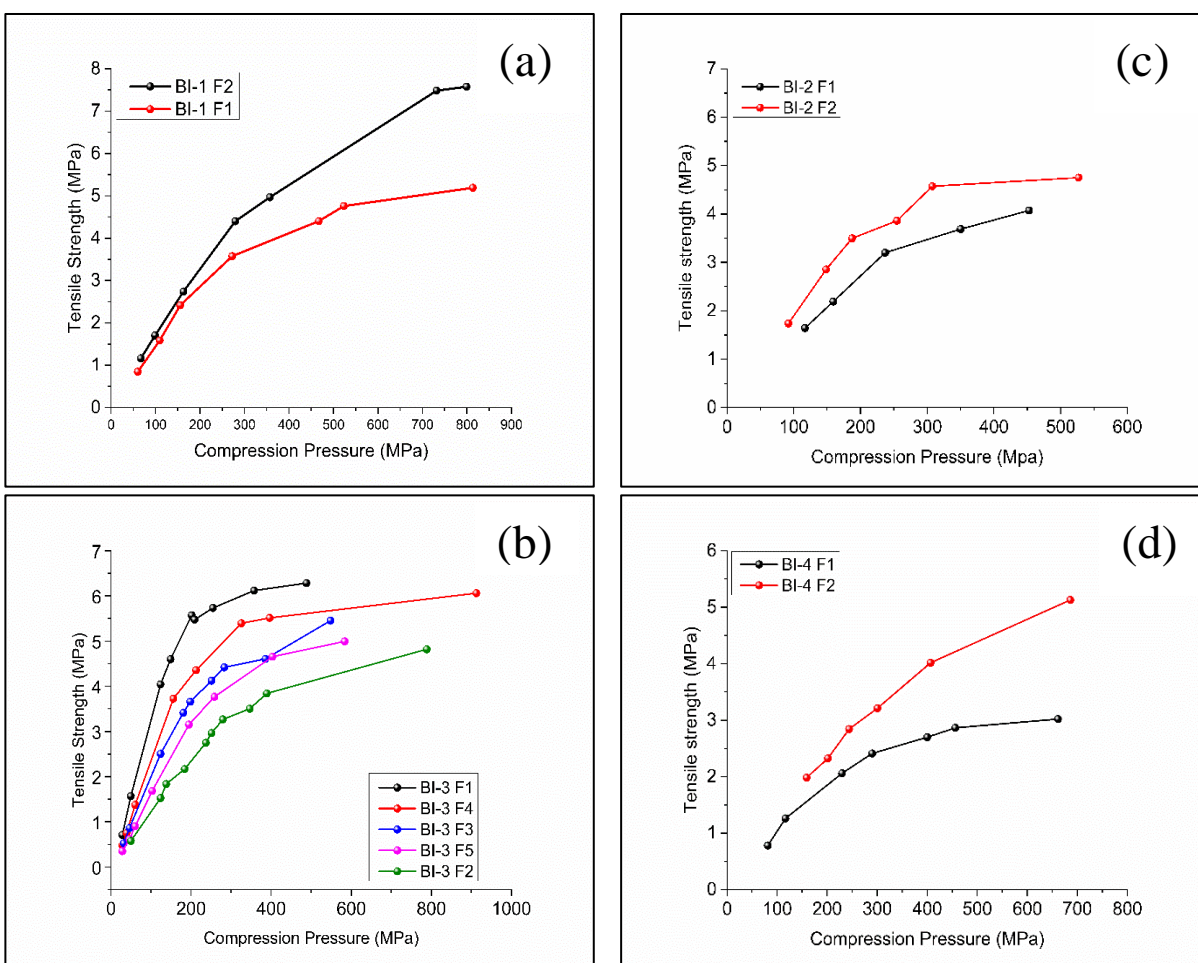


**Figure 2.3.** Analysis and comparison of formulation's impact on tensile strength as a function of compression pressure (tabletability) for BI-1 (a), BI-2 (b), BI-3 (c), and BI-4 (d). The higher the LAC or DICAL percentage the lower the slope in the linear region leading into the onset of the plateau region.

during production do not result in significant tablet performance variation. Therefore, it is also preferable for the formulation to have an onset of plateau < 500 MPa, which is the maximum compression pressure typically used for pharmaceutical products.

For BI-1, the shift of the plateau onset to lower compression pressures for F1 (500 MPa) compared to F2 (700 MPa) is a function of the lower yield pressure of LAC compared to DICAL.

BI-2 F1 has more LAC than F2. Since LAC has a higher yield pressure than MCC, the onset of plateau of F1 (400 MPa) is higher than F2 (300 MPa).

As shown in BI-3, the tabletability curves' slope and onset of plateau correlates perfectly with the formulation's ratio of plastic (low yield pressure) to brittle (high yield pressure) excipients. With decreasing yield pressure of the blend, the compression pressure at which the formulation achieves 2 MPa tensile strength and the onset of plateau region shifts lower. Of the formulations that had industrial flowability (F2 and F5), the onset of plateau for F2 (~600 MPa) is significantly higher than F5 (400 MPa), which makes F2 less industrially feasible, since the onset of plateau was not achieved in <500 MPa.

The slope of the tabletability for BI-4 F1 is lower and thus changes more gradually than any of the other formulations tested. Therefore, the onset of plateau and optimal tableting condition is a region from 300-500 MPa. F2 does achieve 2 MPa tensile strength in >500 MPa, but even at 700 MPa, it had not started to plateau. Therefore, F2 would not be the preferred formulation to use in manufacturing and would require more extensive formulation development to be successful.

### *Friability, Disintegration*

Using the tableability curve as a guide for desired compression pressure, tablets were made for each API blend that had passed all previous testing. Tablets were made in the onset of the plateau range, which is ideal for industrial tableting conditions. Table 2.7 shows that all tablets for all formulations passed friability and disintegration testing. As expected, the disintegration time increased with increasing compression pressure due to an increase in solid fraction. There was also a general trend with mass loss decreasing as a function of increasing compression pressure.

which was also expected.

<b>Table 2.7. Friability and Disintegration Analysis of Tablets</b>			
<b>Formulation</b>	<b>Compression Pressure (Mpa)</b>	<b>Friability Mass Loss (%) (n=3)</b>	<b>Disintegration Time (Sec) (n=3)</b>
<b>BI-2 F1</b>	269	0.3	67
<b>BI-2 F1</b>	318	0.1	89
<b>BI-2 F1</b>	386	0.1	127
<b>BI-2 F2</b>	230	0.2	63
<b>BI-2 F2</b>	297	0.2	102
<b>BI-3 F5</b>	386	0.1	142
<b>BI-4 F1</b>	279	0.4	78
<b>BI-4 F1</b>	400	0.3	176
<b>BI-4 F2</b>	290	0.3	88
<b>BI-4 F2</b>	403	0.0	175

### *Content Uniformity*

Tablets with an acceptance criterion of no more than 15 pass USP content uniformity <905>. Therefore, BI-1 and BI-2 formulations fail content uniformity (Table 2.8). A closer look at the average API loading and standard deviation (SD) of BI-1 and BI-2



reveals that in addition to the average API loading being low (except F1), the SD is also high. BI-1 and BI-2 generated more aerosolized particles during sieving and had more powder residue clinging to the sieving equipment than the other APIs, which likely led to the lower average loading. The large SD is the result of segregation of the API and is caused by particle size or density disparity between the excipients and the API. After one week, and two grams of each API, no further analysis is needed, and it is concluded that BI-1 and BI-2 are not suitable for direct compression due to issues with flowability and

<b>Table 2.8. Content Uniformity and Segregation Analysis</b>		
Formulation	Percent Label Claim (%) $\pm$ SD (n=5)	Acceptance Criteria
BI-1 F1	90 $\pm$ 8.7	29
BI-1 F2	77 $\pm$ 6.8	38
BI-2 F1	82 $\pm$ 7.6	35
BI-2 F2	82 $\pm$ 7.0	33
BI-3 F5	99 $\pm$ 2.6	7
BI-4 F1	94 $\pm$ 2.6	11
BI-4 F2	92 $\pm$ 2.8	13

content uniformity.

As can be seen in Table 2.8, the content uniformity for BI-3 and BI-4 are on average greater than 90% label claim. The SD for BI-4 is comparable to BI-3, so the increase in acceptance criteria is the result of the lower average API loading. This could be human error when weighing out API or BI-4 could have a slight preference for the sieving equipment compared to BI-3. Regardless, BI-3 and BI-4 formulations pass content uniformity and do not show a tendency to segregate.

### *Accelerated Stability*

There were no observable degradation peaks for BI-3 F5 under any of the accelerated stability conditions (Figure 2.4c) BI-4 F1 (Figure 2.4a) had no observable degradation peaks, but BI-4 F2 (indicated by the red arrow in Fig. 2.4b) had 0.18% degradation (Table 2.9). While BI-4 F2 had less than 0.3% degradation, BI-4 F1 having no degradation makes it the preferable formulation since it also had the preferable tabletability profile and sufficient flowability. After two weeks of analysis using less than five grams of API, successful tablet formulations have been identified for BI-3 and BI-4.

**Table 2.9. Quantification of Percent Degradation After Accelerated Stability Testing at 70°C/75% RH temp and humidity**

Sample	Main Peak Area (mAU)	Main Peak Retention Time (min)	Main Degradation Peak Area (mAU)	Degradation Peak Retention Time (min)	Percent Main Band (%)
BI-4 F2	765.6	4.712	1.4	2.051	0.18

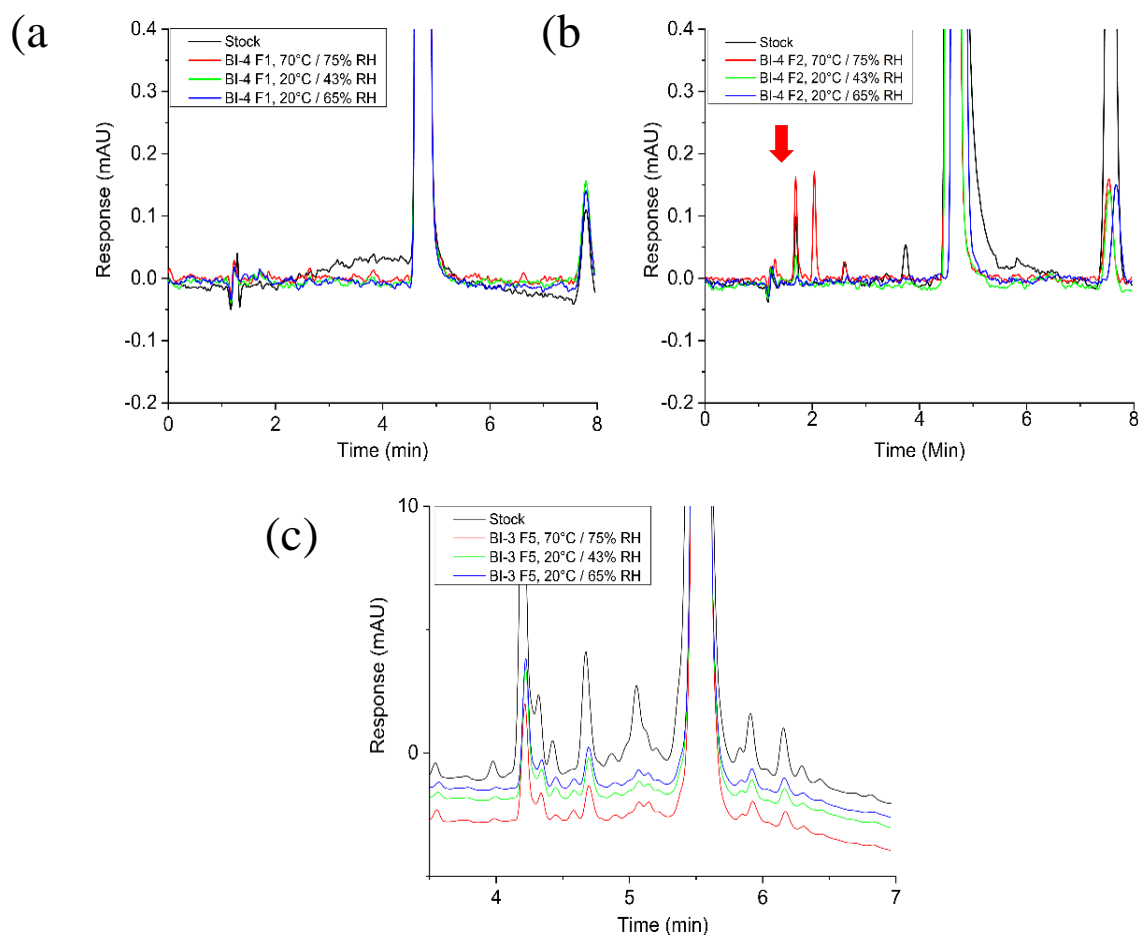


**Figure 2.4.** HPLC analysis of (a) BI-4 F1 tablets, (b)BI-4 F2, and (c) BI-3 F5 tablets stored under accelerated stability conditions. The red arrow in Fig.3b indicates the peak that is not present in the stock solution but is present in the tablets, which indicates the development of a degradation product.

### Conclusion:

The material sparing and expedited development technique was applied to four different APIs. Critical failure criteria were identified in BI-1 and BI-2 using minimal API and time. BI-3 and BI-4 are ready to proceed to scale-up knowing that these intended formulations should scale to manufacturing smoothly. In all cases tested in this study,

less than 5 g of the API were consumed, and successful direct compression tablet formulations or identification of critical failure attributes were obtained in less than two weeks.

*BI-1:* After applying the material sparing approach to this API, it was concluded that the small particle size and poor flowability led to an inability to meet industrial acceptable flowability. Also, the small API particles tended to adhere to sieves and aerosolize when the powder was handled, causing the API loading to drop over time. The small particle size also led to segregation of the powder blend even under mild handling conditions. This tendency would be exaggerated under the mechanical agitation experienced by powders operating on large tablet presses at high speed. To overcome these challenges, granulation or other additional processing is required for this API to be feasible for compression formulations.

*BI-2:* Due to its small particle size, BI-2 also tended to segregate. Granulation or other additional processing is required for this API to overcome the issue of segregation and be feasible for industrial scale compression. Despite the small particle size, formulations were designed that achieved industrially relevant flowability, tabletability, and disintegration.

*BI-3:* BI-3 exhibited elastic recovery and a propensity to laminate after ejection. Despite this drawback, a successful formulation was identified, and the resulting tablets met all necessary criteria for industrial manufacturing. This formulation could be industrially scaled and have successful tablet manufacturing.

*BI-4:* BI-4 had no major drawbacks to overcome, and the resulting formulations are superb candidates for industrial tablet manufacturing. BI-4 formulations could have higher drug loading without sacrificing manufacturability if so desirable during scaleup. This work highlights the universal applicability of material sparing development for direct compression formulation design regardless of API properties. Instituting these methods can save time and resources, but also enables life-saving drug products to reach patients sooner. This study primarily focused on the mechanical properties of the formulations and how they can be used to optimize or eliminate APIs or formulations as candidates for direct compression. It did not include work on solubility enhancement or granulation. However, these two aspects could be included in future work and would not significantly increase the timeline or API requirements.

## References

1. Gaik, J., *Go with the flow: The critical issue of powder flow in tablet production*, in *European Pharmaceutical Manufacturer*. 2018.
2. Wang, B., et al., *A critical review on granulation of pharmaceuticals and excipients: Principle, analysis and typical applications*. Powder Technology, 2022. **401**: p. 117329.
3. Compacting, F., *Next generation Tableting Technology FE75*, F. Compacting, Editor.
4. Zakowiecki, D., et al., *Exploiting synergistic effects of brittle and plastic excipients in directly compressible formulations of sitagliptin phosphate and sitagliptin hydrochloride*. Pharmaceutical Development and Technology, 2022. **27**(6): p. 702-713.
5. LaMarche, K., et al., *The distribution of Drucker-Prager Cap model parameters for pharmaceutical materials*. Powder Technology, 2023. **425**: p. 118528.
6. Yamashita, H. and C.C. Sun, *Material-Sparing and Expedited Development of a Tablet Formulation of Carbamazepine Glutaric Acid Cocrystal– a QbD Approach*. Pharmaceutical Research, 2020. **37**(8).
7. Wang, C. and C.C. Sun, *The efficient development of a sildenafil orally disintegrating tablet using a material sparing and expedited approach*. International Journal of Pharmaceutics, 2020. **589**: p. 119816.
8. Sun, C.C., *Setting the bar for powder flow properties in successful high speed tableting*. Powder Technology, 2010. **201**(1): p. 106-108.

9. Anthony, J.W., et al., *Handbook of Mineralogy*. 2003, Mineralogical Society of America: Chantilly, VA 20151-1110, USA.
10. Patel, D., et al., *Negative porosity issue in the Heckel analysis: A possible solution*. International Journal of Pharmaceutics, 2022. **627**: p. 122205.
11. Heckel, R., *An analysis of powder compaction phenomena*. Trans. Metall. Soc. AIME, 1961. **221**: p. 1001-1008.
12. Ding, H., et al., *Effects of Morphology on the Bulk Density of Instant Whole Milk Powder*. Foods, 2020. **9**(8): p. 1024.
13. Kunnath, K., et al., *Assessing predictability of packing porosity and bulk density enhancements after dry coating of pharmaceutical powders*. Powder Technology, 2021. **377**: p. 709-722.
14. Yost, E., et al., *Beyond Brittle/Ductile Classification: Applying Proper Constitutive Mechanical Metrics to Understand the Compression Characteristics of Pharmaceutical Materials*. Journal of Pharmaceutical Sciences, 2022. **111**(7): p. 1984-1991.
15. Hooper, D., et al., *A Modern Approach to the Heckel Equation: The Effect of Compaction Pressure on the Yield Pressure of Ibuprofen and its Sodium Salt*. Journal of Nanomedicine & Nanotechnology, 2016. **7**: p. 2157-7439.
16. Sonnergaard, J.M., *A Simplified Model Structure for Compression Characterization of Pharmaceutical Tablets*. Journal of Pharmaceutical Sciences, 2022. **111**(11): p. 3088-3095.

17. Sun, C.C. and P. Kleinebudde, *Mini review: Mechanisms to the loss of tabletability by dry granulation*. European Journal of Pharmaceutics and Biopharmaceutics, 2016. **106**: p. 9-14.
18. Sonnergaard, J., *A Critical Evaluation of the Heckel Equation*. International journal of pharmaceutics, 2000. **193**: p. 63-71.
19. Cunningham, J.C., I.C. Sinka, and A. Zavaliangos, *Analysis of tablet compaction. I. Characterization of mechanical behavior of powder and powder/tooling friction*. Journal of Pharmaceutical Sciences, 2004. **93**(8): p. 2022-2039.
20. Procopio, A.T., A. Zavaliangos, and J.C. Cunningham, *Analysis of the diametrical compression test and the applicability to plastically deforming materials*. Journal of Materials Science, 2003. **38**(17): p. 3629-3639.
21. Ali, H.H.M., et al., *Investigating Variation in Compressional Behavior of a Ternary Mixture from a Plastic, Elastic and Brittle Fracture Perspective in the Context of Optimum Composition of a Pharmaceutical Blend*. Polymers (Basel), 2023. **15**(5).
22. Casian, T., et al., *In-Depth Understanding of Granule Compression Behavior under Variable Raw Material and Processing Conditions*. Pharmaceutics, 2022. **14**(1): p. 177.



CHAPTER 3

**MATERIAL SAVING GRANULATION AND DEVELOPMENT OF  
COMPRESSION FORMULATIONS FOR IMMEDIATE RELEASE TABLET  
APPLICATIONS**

Wood, C.; Bell, S.; Bramhall, J.; Locklin J, To be submitted to The Journal of

Controlled Release

**Abstract:**

Material sparing tablet development (MSTD) is a new approach to tablet formulation development that uses the material's properties of the active pharmaceutical ingredient (API) to guide formulation design and material sparing test methods to use API more efficiently. This work expands on the previous work completed by this group to demonstrate the use of the material sparing approach for rapid and efficient formulation development, especially as it relates to preparing for clinical trials. In the previous study, BI-2 was deemed unsuitable for direct compression due to its small average particle size and propensity to adhere to surfaces via electrostatic interaction, which led to blend inhomogeneity and lower average API loading under dynamic conditions. In this work, material sparing dry granulation techniques were employed to explore particle size impact on content uniformity. After granulating, API was characterized and incorporated into powder blends. The blends and resulting tablets were tested against industry standards to gauge manufacturability and product quality. Powder blends were tested for flowability ( $\leq 12$  mm Flodex) and tensile strength ( $> 2$  MPa), while tablets were tested for disintegration ( $< 15$  min) and friability (no more than 1% mass loss). Powder blends made with granulated API had improved flowability but reduced tensile strength compared to the formulations made with unmodified API. However, tablets made with granulated formulations achieved sufficient tensile strength to pass friability and disintegration testing. Granulation improved blend homogeneity, and selection for particles  $\leq 150$   $\mu\text{m}$  had better blend homogeneity than 250-150  $\mu\text{m}$  particles due to the narrower particle size distribution of the powder blend. Unfortunately, granulation increased the electric potential of the granules, so API was more likely to adhere to

processing equipment and vessels, which led to lower average API loading despite the better homogeneity of the blend. The formulations for BI-2 are sufficiently consistent to move to clinical trials. However, more work is needed to explore the impact of formulation and processing for optimizing API loading during granulation of BI-2.

### **Introduction:**

Tablets are the most popular method of drug delivery due to their high patient compliance, high production capacity, and comparatively lower manufacturing cost.

Tablets are made via compression of powder blends. If an API is viable for direct compression (DC), meaning no additional modification of the API is needed, then the API can be blended with other excipients and directly tableted. In cases where an API is unsuitable for direct compression (i.e., cases of poor flowability or a tendency to segregate), additional modification of the API might be needed prior to compression to enable the API to form a stable and well-flowing powder blend[1].

Granulation, the process of fusing numerous particles to make one larger particle, can be done via dry, wet, or melt processing to modify the API. Wet granulation is accomplished by gluing particles together using a liquid binder which must be dried then milled. Melt granulation is accomplished by mixing a melted excipient, usually polymeric, with the API to fuse the particles. Dry granulation is achieved by compressing API with another excipient then grinding the resulting compact, termed a slug, to the appropriate size range. In all cases, the resulting granules are larger than the original API which is beneficial for flowability and preventing segregation. Melt granulation is a relatively new technique which is becoming more popular since it is a continuous manufacturing method[2]. However, it is not suitable for APIs that are sensitive to temperature or shear

stress. Dry granulation is a popular granulation method industrially since it does not use solvent and does not need to be dried prior to milling, unlike wet granulation[3].

Formulation development and API modifications, even for clinical trials, are often conducted on a large scale to ensure the scalability and industrial viability of the final product. Unfortunately, this approach, coupled with the common trial-and-error methods used in formulation, usually requires kilograms of API and months to years of development work.[4, 5]. To improve the efficiency of this process, reduce costs, and shorten the timeline of getting medications to patients, a quality-by-design approach known as MSTD was discussed by Sun and coworkers[6, 7].

The work described herein expands on the MSTD approach by demonstrating that small scale granulation can be done to develop a formulation suitable for clinical testing without the need of kilograms of API. This work and these methods are not a replacement for the formulation development that would be needed to granulate and tablet at an industrial scale because the methods used herein are not representative or translatable to large scale roller compaction. However, only a small quantity of tablets, approximately 100-1000, are needed for clinical testing[8, 9]. The benefit and novelty of this work is that material sparing granulation is faster and uses less API compared to large scale formulation development. In the pre-clinical formulation stage, even 1 kg of API is a huge resource and time investment, especially considering the 90% average failure rate in clinical trials[10]. Using MSTD, the resources that would have been spent on large scale formulation can be devoted to exploring a larger portfolio of candidate molecules or pursuing alternative delivery routes, thus increasing the efficiency and capacity of product development.

### **Materials and Methods:**

Materials: BI 639667 (BI-0002) was donated by Boehringer Ingelheim and used as received. Fastflo® 316 (LAC) (Kerry Inc.), Avicel® PH-102 and PH-101 (Dupont), (JRS Pharma), and Explotab® (SSG) (JRS Pharma) were donated and used as received.

Magnesium stearate (MS) (LFA) was purchased and used as received.

#### *Flowability of Pure API, Granulated API, and Powder Blends with Flodex*

Intrinsic powder flowability tester (Flodex, Hansen) was used to analyze the flowability of pure API for formulation development and the powder blends for manufacturability. For pure API, 20 g of powder was sieved with a # 20 sieve (850 µm pore size) and loaded via funnel into the Flodex apparatus. The Flodex value was reported as the smallest orifice the powder would freely flow through 3 consecutive times. The same procedure was used for blend analysis, except only 10 grams of powder blend minus magnesium stearate, was used for testing to prevent lubricant overmixing. Avicel® PH-102 was used to determine the threshold for successful flowability. Avicel® PH-102 is a common tableting excipient and has been reported as the standard for flowability that is industrially viable[11]. Therefore, powders with flowability comparable to or better than Avicel® PH-102 were classified as successful flowability. Since there was not sufficient quantity of granulated material to test flowability using the flodex, qualitative assessments were made about the flowability of granulated material.

#### *Material Sparing Dry Granulation:*

BI-2 was blended with Avicel® PH-101 (50 µm average particle size) and SSG. The powder was compressed on a single station tablet press at 65 MPa (XP-1, Korsch) using flat 25 mm circle D-type tooling (Natoli). The slug was milled with a mortar and pestle

then poured onto sieves of increasingly smaller mesh size. The granules were forced through the mesh with a spatula to mill the granules  $> 425 \mu\text{m}$  to the appropriate size range. #20, #40, #60, and #100 sieve (850, 425, 250, and  $150 \mu\text{m}$  pore size respectively) were used, but only granules in the  $250\text{-}150 \mu\text{m}$  range and the  $\leq 150 \mu\text{m}$  range were used to make powder blends.

#### *Preparation of Powder Blends*

10 gram batches of formulation were made for each granule size. All excipients except magnesium stearate were mixed in a Turbula mixer for 5 minutes and then sieved with #20 and a #40 sieve. Before tableting, magnesium stearate was added to the powder and mixed in the Turbula mixer for an additional minute.

#### *Tabletability of Powder Blends*

100 mg of powder blend was weighed and manually loaded into the die. Tablets were made from 50 MPa to 550 MPa of compression pressure. For tensile strength analysis, the dimensions of each tablet were measured using digital calipers (547-500S, Mitutoyo) immediately after ejection. Tablets were then tested for diametrical breaking force (TBH 125, Erweka). Equation 2 was used to calculate the tensile strength of tablets, and results were plotted as a function of compression pressure. To conserve powder, only one tablet per compression pressure was tested for tensile strength.

*Equation 2. tensile strength =  $(2 * \text{breaking force}) / (\pi * \text{tablet thickness} * \text{tablet width})$*

#### *Friability*

Tablets made at varying compression pressures were dusted and then weighed. Three tablets per formulation were analyzed instead of the traditional ten tablets to keep with the material sparing nature of the work. In compliance with USP <1216>, tablets were

loaded into a friabilator (45-2100, Vankel) and rotated for 4 minutes at 25 rpm. Tablets were dusted and weighed again, and the percentage mass loss was calculated.

#### *Particle Morphology and Size Distribution via Scanning Electron Microscopy (SEM)*

1-3 mg of API or granulated API was sprinkled onto conductive carbon tape and dispersed with compressed air to remove excess powder. Unmodified API samples were sputter coated with 10 nm of gold/palladium while granules were coated with 15 nm of gold/palladium. Samples were imaged on a scanning electron microscope (FEI Teneo, Thermo-Fisher). ImageJ software was used to measure discrete unmodified BI-2 particles and BI-2 granules for length. Particle lengths were plotted to determine the particle size distribution of the unmodified API and granules.

#### *Disintegration Testing*

If tablets passed friability, the same tablets were used for disintegration testing according to USP standard <701> for uncoated tablets. Immersion fluid was reverse osmosis water at 37 °C. Basket oscillations were 30 strokes per minute with a standard six-tube sample basket (PTZ-S, Pharmatest). The timer started when the bottom of the basket touched the water and stopped when all pieces of the tablet had passed through the wire mesh. Three tablets per formulation were tested, but the disintegration times were identical within the resolution limits for this analysis method, so no standard deviations were reported.

#### *Content Uniformity Testing*

Calibration curve of pure BI-2 was made to quantify BI-2 content uniformity (1100, Agilent). The calibration curve had  $\geq 0.999$  linearity. BI-2 HPLC method is an isocratic method of 70:30 mixture of 0.1% trifluoroacetic acid (TFA) in water and 0.1% trifluoroacetic acid in acetonitrile. Tablets were randomly selected for content uniformity

analysis. The average API loading and standard deviation for both formulations were calculated from the quantification of API in five individual tablets. Tablets were weighed and then placed in a 100 mL volumetric flask before disintegrating using either 90:10 acetonitrile-water. Samples were sonicated for 15 minutes and filtered with a 0.2  $\mu\text{m}$  PTFE syringe filter before HPLC analysis. Granules were tested for content uniformity in the same way as tablets, but due to limited powder availability, only two granule samples were tested per granule size. The content uniformity of granules is an average of the four samples analyzed. For powder residue testing, a spatula was used to scrape powder residue from the sides of the container used to blend the intragranular formulation. Powder was transferred from container directly into a 10 mL volumetric flask. The mass of the recovered powder residue (11.4 mg) was recorded and brought to volume with 90:10 acetonitrile-water. The sample was analyzed via HPLC and BI-2 concentration calculated.

### **Results and Discussion:**

#### *Granulated Particle Morphology*

Of the 3.91 g of intragranular formulation (Table 3.1) weighed out for granulation, 3.12 g of granules were recovered for a yield of 79.7%. Most of the loss occurred prior to compaction since the powder adhered to the container. Of the 3.12 g, 1.36 g of 250-150  $\mu\text{m}$  granules (250 granules) were recovered and 1.75 g of <150  $\mu\text{m}$  granules (150 granules) were recovered. A few milligrams of 425-250  $\mu\text{m}$  granules (425 granules) were collected, but not enough to formulate a powder blend. As can be seen in Figure 3.1, the distribution of particle size increases with increasing sieve size. While all the granules are larger than the unmodified BI-2, the average granule size, excluding the 425 granules, does not correspond to the mesh opening sizes used to separate the granules. This is



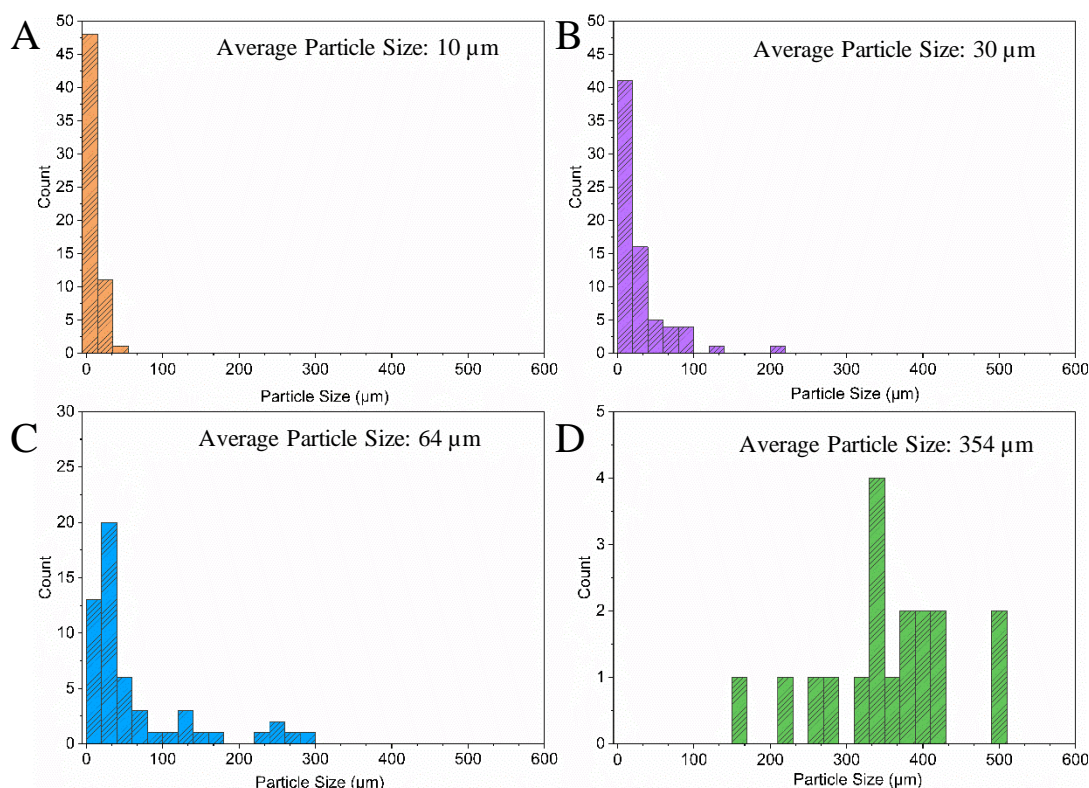


**Figure 3.1.** Particle size distribution of granules measured manually via SEM images.

Lengths of particles plotted and average distribution curve generated. Unmodified BI-2 particle size distribution with average particle size (A) has a more narrow and smaller average particle size compared to granules. 150 granules (B) have a narrower particle size distribution compared to 250 granules (C) and 425 granules (D). As expected, the average particle size increases with mesh size.

caused by the abundant fine particulates in the 250 and 150 granules as can be seen in the SEM images in Figure 3.2, which skews the average particle size to be smaller. These particles, probably due to static, adhered to the sieve rather than passing through even though they

are smaller than the mesh opening. Modifying environmental conditions, formulation, and processing during granulation could improve the dispersity of the granules collected in future work.

#### *Powder Blend Formulation and Flowability*

Formulations for the intragranular portion used to make the slug and resulting granules as well as the powder blend formulation (extragranular formulation) are listed in Table 3.1 and Table 3.2 respectively. Since the granules would only contain 49% BI-2, the granule loading in the powder blend was set to 10.2% to achieve 5% BI-2 loading. Explotab was added to the intragranular and extragranular formulas to enable the granules to disintegrate as well as the tablet. Avicel® PH 101 was used to achieve better homogeneity of the slug since the particle size of PH 101 is 50  $\mu\text{m}$  which is much closer to the average API size of unmodified BI-2 than PH-102. The flowability of the intragranular formulation was poor as expected based on the particle size and inherent flowability of the components. The powder had to be manually fed into the tablet press and pre-compressed to fit all the low-density powder into the die to make the slug. The slug was compressed to 65 MPa, which is above the compression yield point of PH-101, to ensure plastic deformation of the Avicel PH 101. As the PH-101 deforms, new surfaces are generated and the compressed PH-101 conforms around the BI-2 particles nearby to create numerous contact points that should stabilize the cohesion of the granules even through milling and sieving.

After granulation, qualitative assessment of the granules revealed a remarkable difference in the flowability. As expected, the 450 granules had superb flowability due to their large

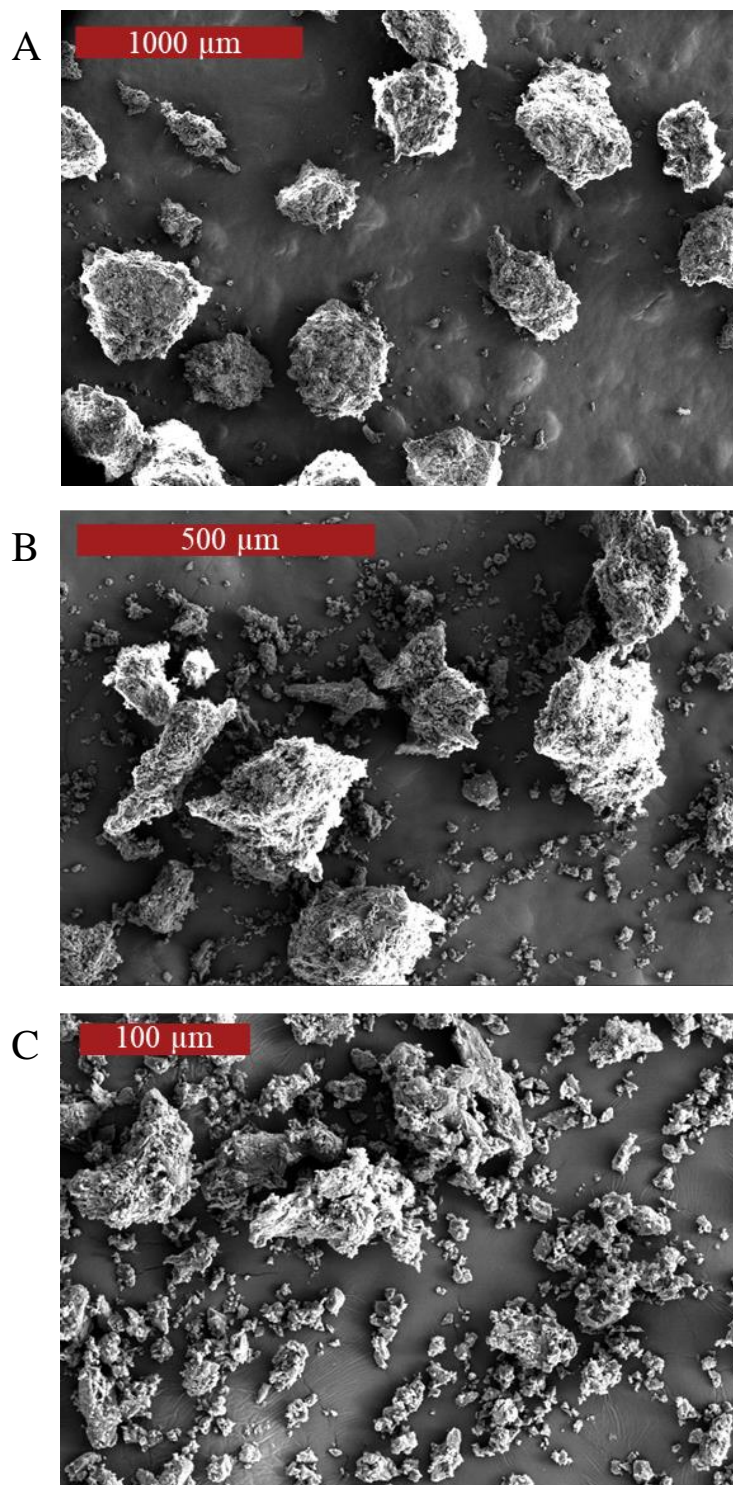


**Figure 3.2.** SEM images of (A) 425-250  $\mu\text{m}$ , (B) 250-150  $\mu\text{m}$  granules and (C) <150  $\mu\text{m}$  granules. The morphology gets more irregular as granule size decreases. The 425  $\mu\text{m}$  granules (A) are predominately spherical in shape.

size and spherical shape. The 250 granules had great flowability, but not as good as the 450 granules, due to their smaller average particle size. The 150 granules had moderate flowability, comparable to Avicel Ph-102. A video recording of the powder flowability of the granules accompanies this document and is available on ProQuest. Even at low loading, granules impacted the flowability of the blends. Due to the better intrinsic flowability of the 250 granules compared to the 150 granules, F1\_250 had a slightly better flowability (9mm) compared to F1\_150 (10 mm). Both granulated formulations had better flowability than the unmodified BI-2 formulation (12 mm), though no conclusions can be drawn from this about the impact of granulation on flowability, since the API loading of the granules and thus the overall blend is less than in the unmodified BI-2 formulation.

The excipients for extragranular formulation were selected based on the predicted size of the granules. The target particle size range was 100-250  $\mu\text{m}$  for excipients to minimize the chance of granular segregation in the powder blend. The extragranular formulation was based on the F2 formulation for BI-2 from previous work since it had a better tabletability profile than F1 and comparable performance in other tests.

<b>Table 3.1. Intragranular Formulation</b>		
<b>Excipient</b>	<b>Weight Percent (% w/w)</b>	<b>Average Particle Size (<math>\mu\text{m}</math>)</b>
<b>Avicel PH 101</b>	49	50
<b>BI-2</b>	49	13
<b>SSG</b>	2	42

**Table 3.2. Extragranular Formulation**

Formulation	Unmodified BI-2 (% w/w)	150 Granules (% w/w)	250 Granules (% w/w)	Avicel PH 102 (% w/w)	LAC (% w/w)	SSG (% w/w)	MS (%w/w)
Unmodified BI-2 (F2)	10	0	0	44	44	1	<b>1</b>
F1_150	0	10.2	0	41.3	46.5	1	<b>1</b>
F1_250	0	0	10.2	41.3	46.5	1	<b>1</b>
<b>Avg. Particle Size (µm)</b>	<b>10</b>	<b>30</b>	<b>64</b>	<b>80-140</b>	<b>129</b>	<b>38-42</b>	<b>Not Listed</b>

### *Tabletability*

As seen in Figure 3.3 A, the tabletability of the F1\_150 and F1\_250 formulations are practically identical with only a slight deviation at higher compression pressures. In Figure 3.3 B, the tabletability of unmodified BI-2 formulation is compared to the granulated formulations. The unmodified formulation was able to achieve a higher maximum tensile strength, but the curve for unmodified BI-2 is more disjointed because of the blend inhomogeneity of the formulation. Segregation of the blend led to tablets with varying ratios of API and excipients which impacted the tabletability from one tablet to another. The granulated tablets produced more consistent tablets and thus the tabletability curve clearly depicts the ideal tabletability behavior with a linear region leading to a clear onset of plateau followed by a maximum compression plateau. Reduction in tensile strength of granulated formulations is a documented phenomenon in the literature[12]. It is hypothesized that work hardening and increasing particle size is responsible for the reduction in tensile strength.

### *Friability and Disintegration*

Tabletability curves were used to determine the optimal compression pressure for each formulation. Tablets were made in the onset to plateau region to maximize tensile

strength and prevent over compression. Despite lower tensile strength, the tablets made from granulated BI-2 passed friability and disintegration testing with ease. The standard

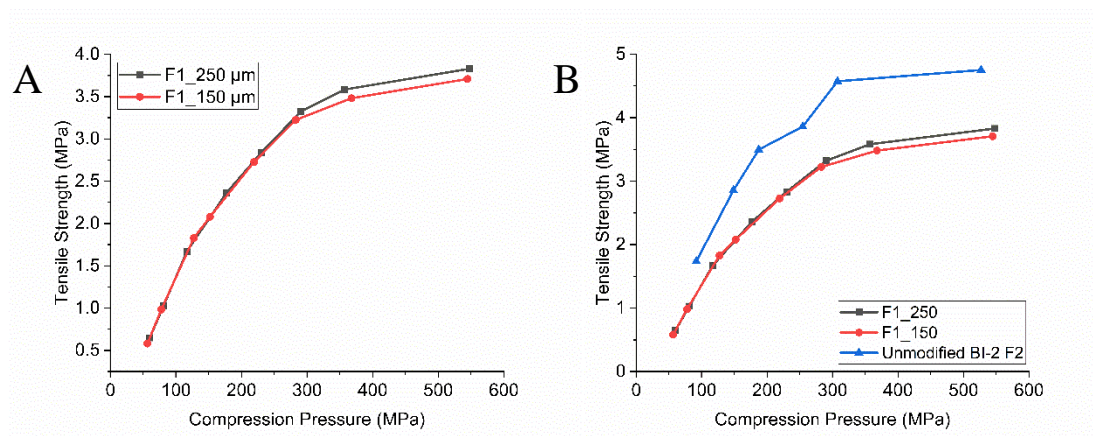


**Figure 3.3.** (A) Comparison of tensile strength as a function of compression pressure (tableability) of F1\_150 (red) and F1\_250 (black) to determine if granule size impacted the tensile strength of the extragranular formulation. There is a slight deviation at higher compression pressures, but the formulas perform almost identically. (B) Comparison of tableability of the extragranular formulations (red and black) with powder blends made from unmodified BI-2 (blue). Tableability decreased with granulated BI-2 regardless of granule size.

for friability testing is no more than 1% mass loss, and both formulations were well below that threshold (Table 3.3). Disintegration testing is considered a success if tablets fall apart in less than 15 minutes, though less than 45 minutes is still passable. Both formulations dissolved in well under 15 minutes (Table 3.3).

#### *Content Uniformity*

Content uniformity of the granules were tested to gauge BI-2 encapsulation efficiency. Granules, both the 250 and 150, contained only 89% of the expected BI-2 based on

intragranular formulation target loading (Table 3.4). Therefore, the calculation of percent label claim in tablets was adjusted to reflect the lower BI-2 content of the granules.

Unmodified BI-2, as well as the resulting granules, exhibited static adhesion to containers and processing equipment. To highlight the impact of static, powder residue taken from the container used to blend the intragranular formulation was analyzed for BI-2 content.

The powder adhered to the wall of the container contained 200% more BI-2 than would be present if intragranular formulation had uniformly coated the vessel.

**Table 3.3. Friability and Disintegration Analysis of Tablets**

<b>Formulation</b>	<b>Compression Pressure (Mpa)</b>	<b>Friability Mass Loss (%) (n=3)</b>	<b>Disintegration Time (Sec) (n=3)</b>
<b>F1_250</b>	300	0.31	109
<b>F1_150</b>	300	0.25	114

**Table 3.4 . Content Uniformity of Granules, Unmodified BI-2 Formulation Tablets, and Granulated Formulation Tablets**

<b>Formulation</b>	<b>Average API loading (n=5) (% label claim)</b>	<b>Standard Deviation (n=5)</b>
<b>Granules</b>	89*	0.9*
<b>Unmodified BI-2 ( F2)</b>	82**	7.0
<b>F1_250</b>	89**	3.6
<b>F1_150</b>	78**	1.2

\* n=4 samples tested due to limited powder availability

\*\* label claim adjusted to normalize for actual API loading in granules measured via HPLC

As seen in Table 3.4, the average API loading for all formulations is below the desired 90-110% label claim. Static is exacerbated by mixing, milling, sieving, and other mechanical agitations that induce friction between powder particles[13]. The transfer of electrons between the two surfaces as the grate past one another generates a temporary

charge, known as triboelectric charging, on the surface of the powder particles. The generation of numerous positive and negatively charged particles in the powder results in repulsion of like charges and attraction of opposite charges, known as bipolar charging, and can lead to agglomeration, adherence to surfaces, and spark generation[14]. The charge will eventually dissipate, but the longevity of the charged surface is a function of the conductivity of the materials that makes the particle. The more conductive a material is, the more quickly the static will dissipate, and conversely, insulating materials such as glass and plastics will maintain the charge for longer[15]. As static is generated through friction of surfaces, the more a powder is agitated (i.e., milling and sieving) the more static will be generated. Therefore, it would be expected that BI-2 granules would have more triboelectric charge than unmodified BI-2 due to the increased amount of mechanical agitation and thus lower average API loading. However, particle size impacts the ability to dissipate triboelectric charge, and small particles are more subject to electrostatic interactions with vessels than large particles due to their smaller mass[16-19]. It is possible that the larger particles present in 250 granules were able to dissipate the additional charging more efficiently, which led to lower API loss compared to the 150 granules. The average API loading of F1\_150 being lower than unmodified BI-2 suggests that the static charge generated by milling and sieving increased the API loss of the smaller granules compared to unmodified BI-2 (Table 3.4).

Despite the lower average API loading in the tablets, the consistency of the API loading for granulated formulations did improve compared to the unmodified BI-2, as evidenced by the decrease in deviation of API loading in F1\_250 and F1\_150 shown in Table 3.4. The deviation in the of F1\_250 is above the 2.5 standard deviation target, so F1\_150



would be the preferred for moving to clinical trials. F1\_150 granules are in a similar particle size range, both average particle size and particle size distribution, to the excipients used for the extragranular formulation, which is giving rise to the improved consistency in BI-2 loading. Given the consistency of the API loading, tablets for clinical trials can be produced from the remaining 9.6 g of F1\_150 powder blend, and target dosing can be achieved by adjusting the tablet mass to account for the lower API loading in the powder blend.

### **Conclusion:**

Building off the work previously done by this group and using only 2 g of API, material sparing granulation was applied and a successful tablet formulation with improved consistency of API loading was developed. Compared to the 1 kg or more of API needed for large scale formulation development, material sparing granulation reduced the API consumption to develop a formulation for clinical trial testing by almost three orders of magnitude. Additionally, the complete timeline for material sparing tablet development including the addition of the material sparing granulation took less than a month. The increase in efficiency and the reduction of time for formulation development of new APIs using this approach reduces the opportunity cost for pharmaceutical companies at such an early phase of drug product development where failure rate is high. The manual milling method used in this work disproportionally created small particles compared to the target particle size ranges. In future work, other material sparing milling methods will be explored to improve upon the creation of granules in a certain size range. Also, formulation and processing conditions (i.e., humidity, grounding, mixing times) will be modified to test how these factors impact the generation of static in powders.

## References

1. Gaik, J., *Go with the flow: The critical issue of powder flow in tablet production*, in *European Pharmaceutical Manufacturer*. 2018.
2. Záhonyi, P., et al., *Integrated continuous melt granulation-based powder-to-tablet line: Process investigation and scale-up on the same equipment*. *European Journal of Pharmaceutics and Biopharmaceutics*, 2023. **189**: p. 165-173.
3. Jaspers, M., et al., *A novel approach to minimize loss of compactibility in a dry granulation process using superdisintegrants*. *Powder Technology*, 2022. **408**: p. 117773.
4. Zakowiecki, D., et al., *Exploiting synergistic effects of brittle and plastic excipients in directly compressible formulations of sitagliptin phosphate and sitagliptin hydrochloride*. *Pharmaceutical Development and Technology*, 2022. **27**(6): p. 702-713.
5. LaMarche, K., et al., *The distribution of Drucker-Prager Cap model parameters for pharmaceutical materials*. *Powder Technology*, 2023. **425**: p. 118528.
6. Yamashita, H. and C.C. Sun, *Material-Sparing and Expedited Development of a Tablet Formulation of Carbamazepine Glutaric Acid Cocrystal– a QbD Approach*. *Pharmaceutical Research*, 2020. **37**(8).
7. Wang, C. and C.C. Sun, *The efficient development of a sildenafil orally disintegrating tablet using a material sparing and expedited approach*. *International Journal of Pharmaceutics*, 2020. **589**: p. 119816.
8. An, M.-W., et al., *Principles of Good Clinical Trial Design*. *Journal of Thoracic Oncology*, 2020. **15**(8): p. 1277-1280.

9. Sakpal, T.V., *Sample size estimation in clinical trial*. Perspect Clin Res, 2010. **1**(2): p. 67-9.
10. Hampson, L.V., et al., *A New Comprehensive Approach to Assess the Probability of Success of Development Programs Before Pivotal Trials*. Clinical Pharmacology & Therapeutics, 2022. **111**(5): p. 1050-1060.
11. Sun, C.C., *Setting the bar for powder flow properties in successful high speed tableting*. Powder Technology, 2010. **201**(1): p. 106-108.
12. Skelbæk-Pedersen, A.L., et al., *The relevance of granule fragmentation on reduced tableability of granules from ductile or brittle materials produced by roll compaction/dry granulation*. Int J Pharm, 2021. **592**: p. 120035.
13. Deng, T., V. Garg, and M.S.A. Bradley *Electrostatic Charging of Fine Powders and Assessment of Charge Polarity Using an Inductive Charge Sensor*. Nanomanufacturing, 2023. **3**, 281-292 DOI: 10.3390/nanomanufacturing3030018.
14. Zhang, L., X. Bi, and J.R. Grace, *Measurements of Electrostatic Charging of Powder Mixtures in a Free-fall Test Device*. Procedia Engineering, 2015. **102**: p. 295-304.
15. Biegaj, K.W., et al., *Surface Chemistry and Humidity in Powder Electrostatics: A Comparative Study between Tribocharging and Corona Discharge*. ACS Omega, 2017. **2**(4): p. 1576-1582.
16. Ramirez-Dorronsoro, J.-C., R.B. Jacko, and D.O. Kildsig, *Chargeability measurements of selected pharmaceutical dry powders to assess their electrostatic charge control capabilities*. AAPS PharmSciTech, 2014. **7**(4): p. 103.

17. Karner, S., E.M. Littringer, and N.A. Urbanetz, *Triboelectrics: The influence of particle surface roughness and shape on charge acquisition during aerosolization and the DPI performance*. Powder Technology, 2014. **262**: p. 22-29.
18. Cruise, R.D., et al., *The effect of particle size and relative humidity on triboelectric charge saturation*. Journal of Physics D: Applied Physics, 2022. **55**(18): p. 185306.
19. Mukherjee, R., et al., *Effects of particle size on the triboelectrification phenomenon in pharmaceutical excipients: Experiments and multi-scale modeling*. Asian Journal of Pharmaceutical Sciences, 2016. **11**(5): p. 603-617.

## CHAPTER 4

# **DEVELOPMENT OF IMMEDIATE RELEASE AMORPHOUS SOLID DISPERSION FORMULATION FOR MANUFACTURING INJECTION MOLDED SOLID DOSAGE PRODUCTS**

Wood, C.; Patel, K.; Bledsoe, J.; Weber, V.; Bell, S.; Bramhall, J.; Locklin J, To be  
submitted to The Journal of Controlled Release

**Abstract:**

Amorphous solid dispersion (ASD) tablets are beneficial for improving the solubility and bioavailability of BCS 2-4 drugs, which makeup the majority of drugs coming out of drug discovery. Immediate release ASD tablets are currently manufactured via extrusion, grinding of the extrudate, sieving to achieve narrow particle size, blending with other excipients, then compression with a tablet press. In this work, a new and more efficient method of ASD tablet production via direct injection molding of extruded formulations was explored as a viable alternative for the industrial production of ASD tablets.

Moxidectin is a high potency active pharmaceutical ingredient (API) and was used as a model API for formulation development. Formulations with and without moxidectin were extruded and injection molded into a variety of shapes. Stereolithography (SLA) molds were printed to prototype both traditional and unique tablet geometries. Tablets were measured against United State Pharmacopeia (USP) quality standards for immediate release tablets (i.e., dissolution rate, friability, and content uniformity) and were found to perform as well as if not better than tablets made via traditional manufacturing methods. By utilizing material sparing test methods, a formulation was developed that produced an immediate release ASD, using less than 10 g of API. This work demonstrated the viability and benefits of this innovative ASD tablet manufacturing method as well as the benefits of material sparing formulation development.

**Introduction:**

ASD as they relate to pharmaceuticals are the amorphous form of an active pharmaceutical ingredient (API) stabilized via a matrix such as a polymer or a wax. Amorphous APIs have higher solubility and typically higher bioavailability than their

crystalline counterparts[1] can improve the delivery and uptake of BCS II, III, and IV APIs. The majority of ASD products on the market are capsules or tablets. It can be challenging to make ASDs because amorphous APIs are in a metastable state. If not stabilized via a matrix, the API can re-crystallize over time, thus eliminating the solubility benefits. There are ways to evaluate molecules to determine their glass forming ability (GFA) and glass stability (GS), or the ability for the molecule to remain amorphous[2]. Generally, larger, complex molecules are more stable in the amorphous state than smaller molecules and are thus better suited for ASD applications.

ASDs can be produced through two mechanisms: solvent or fusion. The solvent mechanism is done by dissolving API with excipients. The solvent is then rapidly evaporated, which does not allow the API sufficient time for molecular reorganization into crystals. An example of solvent based ASD production is spray drying. The second mechanism is fusion, a solvent-free technique where the API is melted and mixed with a polymer or wax matrix. The combination of heat and shear melts the crystalline API to make it amorphous then as the ASD cools the matrix interactions stabilize the amorphous form of the API. Hot melt extrusion (HME) and spray congealing are two examples of fusion ASD methods.

HME is a popular fusion technique for making ASDs because large volumes of material can be processed quickly and the solvent-free nature of the technique makes it more environmentally friendly than spray drying[3]. The production of ASD tablets via HME typically starts by blending ASD excipients, usually in the form of powders. The powders are then fed into an extruder using a gravity feeder or a motorized powder feeder, and the formulation is melt mixed at elevated temperatures. After extrusion, the cooled extrudate

is milled. The powderized extrudate is then sieved to collect particles in an appropriate size range. The particles of desired size range are then blended with other powder excipients needed for compression. The powder blend is then fed into a tablet press where the powder will be compressed into a solid compact[4-8]. While this extensive process can be done continuously, the additional grinding, sieving, blending, and compression steps add time, resources, and equipment to the production process, which increases the cost of the product.

This work was done to highlight a new and more efficient method of producing ASD tablets, which is already being used prevalently in other sectors to produce large volumes of products rapidly and inexpensively. In this study ASD tablets were injection molded to eliminate the additional processing steps used in traditional ASD tablet production. Since injection molding can be coupled directly to HME, tablets could be continuously produced at a higher rate than the current ASD tablet production methodology. Injection molding could also be more energy/resource efficient since it requires fewer pieces of equipment for tablet production. Despite the widespread usage of injection molding in other applications, there are only a handful of studies using injection molding for the production of tablets[9-13]. Of those studies, only two were able to achieve immediate release (IR) criteria[14, 15], which is >85% API release in under an hour United States Pharmacopeia (USP) <711>[16]. This is because injection molding produces a dense compact made of polymers that, if soluble in water, has a high viscosity at the dissolution interface which retards API diffusion. To overcome this challenge, effervescent powders were analyzed as disintegrants to accelerate the erosion of the interfacial gel layer and increase API diffusion rates.



The goal of this work was to create an ASD injection molding formulation for the manufacture of IR tablets that conformed to all USP standards. Moxidectin, a BCS II anti-parasitic drug used to treat onchocerciasis, was used as a model API[17]. The typical dosing for onchocerciasis treatment is 2-8 mg, which is achieved by taking multiple 2 mg IR tablets to reach correct dosing. Relevant USP standards for this work include content uniformity <905>, tablet friability <1216>, and dissolution <711>. Additionally, stereolithography (SLA) inserts were made to highlight the ability to create unique tablet geometries with injection molding. Traditional tablets made via powder compression are often circles or ovals because sharp points and extensions from the tablet body create manufacturing problems. However, injection molding of these types of shapes can be accomplished without sacrificing manufacturability or tablet strength. The expanded range of shape options would be beneficial for modifying surface area to control release profiles and potentially help patients more easily distinguish between medications.

### **Materials and Methods:**

#### *Materials*

Polyox<sup>TM</sup> WSR N80 (PEO) was donated by Dupont. Poly(vinyl pyrrolidone) K-30 (PVP) was purchased from Spectrum® Chemical MFG Corp. Sodium bicarbonate (bicarb) was purchased from VWR. Citric acid monohydrate and triethyl citrate (TEC) were purchased from Sigma-Aldrich. Moxidectin was donated by Boehringer Ingelheim. All materials were used as received.

### *Solubility Study of Moxidectin*

Hansen Solubility Parameters (HSP) of moxidectin were measured by conducting a solubility study. 10-15 mg of API was loaded into a scintillation vial and solvent was added with a Pasteur pipette until the API was dissolved. The mass of solvent added was recorded and converted to volume using the solvent density. The saturation concentration of the solutions prepared were determined by dividing the mass of API by volume of solvent added. Based on the saturation concentration, the solvents were assigned a score from 1 to 6, where 1 is the best performing solvent and 6 is worst. By assigning 5 as the inside value for the genetic algorithm in the HSPiP® software, the solubility parameters of moxidectin were determined. Further details on the solvent scoring method in HSPiP® software is provided by ([18]). The HSP values and scores of solvents used are listed in Table S.3. The criteria used to assign the solvent scores are listed in Table 4.

Using the databases on HSPiP® software, several GRAS plasticizers were compared and evaluated with the API and polymeric excipients to determine the best plasticizer for the formulation. HSP values of PVP and PEO were also obtained from the polymer database in HSPiP® and used for comparison.

### *Thermogravimetric Analysis (TGA)*

TGA analysis of excipients was conducted on TA Instruments Discovery TGA. 7-11 mg samples were loaded on platinum TGA pans and heated from 40°C to 600°C at 20°C/min under a nitrogen purge of 25 mL/min. Due to the low density of moxidectin, a 600 mg/mL solution of moxidectin in acetone was prepared and solvent cast onto the

platinum TGA pan. The solution cast pan was dried in a vacuum chamber (< 5 torr) for 4 hours at ambient temperature before TGA analysis.

#### *Differential Scanning Calorimetry (DSC)*

DSC analysis of the API, excipients, and injection molded samples were conducted on TA Instruments Discovery DSC 250 equipped with a RCS90 cooling system under a 50 mL/min nitrogen purge. Samples weighing 4-8 mg were enclosed in aluminum Tzero® pans. PVP and moxidectin samples were heated from 25°C to 200°C at 10°C/min to erase thermal history followed by a cooling ramp to 25°C and were subsequently reheated to 200°C. PEO, PVP-TEC, Moxi-TEC, and extruded samples were heated from -80°C to 120°C at 10°C/min to erase thermal history. The samples were cooled to -80°C at 10°C/min followed by another heating to 120°C.

#### *Flowability*

Intrinsic powder flowability tester (Flodex, Hansen) was used to analyze the industrial feasibility of this formulation for ease of powder feeding during extrusion. Powder blend was loaded via funnel into the Flodex apparatus. Thirty seconds after complete powder loading, the latch on the trap door was opened to enable the powder to flow out of the orifice. Disks with different diameter orifices were exchanged, and the Flodex value was reported as the smallest orifice the powder would freely flow through 3 consecutive times. The smaller the orifice, the better the intrinsic flowability of the powder. The TEC was not added to the powder blend during flowability testing because in industrial HME, Moxidectin and TEC would be precisely pumped in via a liquid feed port instead of mixed with the powder, which would improve consistency in API loading.

### *Extrusion and Injection Molding*

Samples were extruded using a ThermoFischer HAAKE MiniLab II conical twin screw extruder set at 120°C with 50 RPM screw speed. The samples were cycled for 4 minutes to ensure even mixing before being collected for injection molding using a HAAKE MiniLab II ram injection molder. The samples were injection molded into a 45°C mold at 700 Bar to form a 1.0mm x 10.0mm x 60.0 mm bar (DMA bar), a 3.2mm x 12.6mm x 64.0 mm bar (Izod Bar), and custom tablet geometries (circular, hexagonal, heart, and dog bone shaped tablets). A PVP-TEC (67% PVP and 33% TEC-BHT) blend was also prepared by the same conditions described above, but with 2 minutes of mixing time instead of 4 minutes. Changes in torque and pressure inside of the extruder were monitored and recorded through ThermoFischer PolySoft OS.

A larger batch of placebo formulation was extruded using a ThermoFischer Process 11 parallel co-rotational twin screw extruder ( $D = 11\text{mm}$  and  $L/D = 40$ ). The standard screw profile used consists of conveying and distributive mixing elements. The temperature profile (Table 1) of the heating zones is listed in Table 1. Placebo was extruded at a 50 RPM speed and the recorded melt temperature was 118°C. The extrudate was flushed through the HAAKE MiniLab II extruder and injection molded to produce tablets of desired geometry using the conditions described above.

<b>Table 4.1. Temperature profile for Process 11.</b>								
<b>Zone</b>	<b>2</b>	<b>3</b>	<b>4</b>	<b>5</b>	<b>6</b>	<b>7</b>	<b>8</b>	<b>Die</b>
<b>Temperature (°C)</b>	20	40	80	120	120	120	120	120

### *Tablet Geometry*

In the early phase of formulation optimization, tablets were made by hole punching circles of different diameters from injection molded DMA or Izod bars. To highlight the variety of geometries that can be made using this technology, SLA resin was used to 3D print inserts for the Izod mold to manufacture traditional circle tablets as well as unique tablet geometries that would be challenging to achieve with powder compression. The average weight and standard deviation were reported for 6 tablets. The tablet's thickness and diameter were measured using a force-controllable micrometer (547-S, Mitutoyo) with a resolution of 0.001 mm. The average thickness and diameter were reported for three tablets.

### *SLA Printed Injection Mold Insert*

Injection mold inserts were designed using Fusion360 Computer-Aided Design (CAD) software and exported into 3D stereolithography mesh (.stl) files for printing. The mesh files were uploaded into Formlabs Preform software for model slicing. Formlabs' Rigid 10K resin was used for mold insert production. All recommended printing parameters were used, and printing was conducted on a Form 3 printer (Formlabs, Sommerville, MA) at a layer height of 100 microns. After printing, support structures were removed, and the parts were washed with isopropanol using a Form Wash washing station. The washed parts were dried and post-cured in a Form Cure station set to 45°C for 10 minutes. The final printed inserts were gently sanded to achieve an appropriate fit for the injection mold. Silicon mold release was applied to the inserts to make removal from the steel mold easier. After injection, inserts were removed from the steel mold and put in

liquid nitrogen to facilitate tablet removal while minimizing tablet deformation during extraction.

#### *Content Uniformity*

Individual tablets were weighed and placed in 100 mL volumetric flasks. Tablets were dissolved and moxidectin was extracted using 50:50 acetonitrile-water as the diluent. Tablets were sonicated for 15 minutes or until all extrudate had dissolved. Samples were filtered with 0.2  $\mu$ m PTFE filters before analyzing via HPLC (1100 MWD detector, Agilent). Moxidectin concentration was calculated using a standard curve with a linear fit of  $> 0.9999$ . Concentration of degradation products were calculated as a percentage of the area of the moxidectin peak. The area of the degradant peak was divided by the area of the moxidectin peak and multiplied by 100. This method enables quantification of small quantities of degradation and normalizing for the run-to-run variation of the HPLC.

The moxidectin HPLC method was a gradient method (Table 2). The column was an Eclipse XDB-C18 150 mm x 4.6 mm with 5  $\mu$ m particle size set at 55°C. Detector wavelength was 245 nm. Injection volume was 35  $\mu$ L including a needle wash step in methanol after each injection.

<b>Table 4. 2. Moxidectin HPLC Method Mobile Phase Gradient</b>			
Time (Min)	Methanol (%)	0.05% H <sub>3</sub> PO <sub>4</sub> in Water (%)	Flow Rate (mL/min)
0	75	25	1
14	80	20	1
15	80	20	1
15.10	80	20	2
19	85	15	2
21	90	10	2
Post run (9 minutes)	75	25	1

### *Moisture Content*

Moisture content was analyzed via mass loss on drying. The moisture content of placebo extrudates were measured immediately after extrusion. A separate placebo powder blend sample was made and tested to analyze moisture content prior to extrusion. Samples were weighed then put in an oven at 70°C and 0.2 bar for seven days. Samples were allowed to cool to room temperature under vacuum before measuring the final mass. The percent mass loss corresponds to the percent moisture of the sample.

### *Dissolution Profile*

Dissolution was carried out at 37°C in a USP 2 apparatus (2500, Distek). Dissolution media was 0.74% v/v Tween 20 in water. Small tablets were dissolved in 500 mL of water and large tablets in 900 mL of water to ensure sink conditions. Two small tablets per vessel were used corresponding to 70 mg of total mass. Only one large tablet per vessel was tested. Dissolution was carried out at 65 rpm and 100 rpm to analyze the impact that paddle speed had on dissolution. Small tablets were run in triplicate to assess the reproducibility of dissolution profiles. At specified time intervals, 1 mL of dissolution media was sampled and filtered through a 0.2  $\mu$ m PTFE filter before being analyzed via HPLC. Media was not replaced. Moxidectin concentration was calculated using the standard curve and release rate calculated as a function of the percent label claim. The Food and Drug Administration (FDA) states that for immediate release of a BCS II molecule, products must release  $\geq 85\%$  of the API in under an hour and thus was used as the standard to assess success of immediate release API delivery in tablets[16].

### *Scanning Electron Microscopy (SEM)*

A ThermoFischer FEI Teneo field emission scanning electron microscope was used to generate electron micrograph images. Cryofractured cross-sections of the injection molded samples were imaged with an 8 kV acceleration voltage. Surface and internal cross-section of extrudates were adhered to a metal puck using conductive carbon tape then sputter coated with 10 nm of gold/palladium.

### *Polarized Optical Microscopy (POM)*

A Nikon Eclipse LV100N POL (Nikon USA, USA) polarized optical microscope equipped with TMHS600 temperature-controlled stage and LINK (ver.1.2.5.1300, Linkam Scientific Instrument, UK) were used to analyze the spherulite morphology and phase separated domains in the extrudate. The extrudate was heated at 100°C/min from ambient to 120°C then cooled at 40°C/min to 40°C.

### *Friability Analysis*

USP <1216> states that a passable variation is less than 1 % mass loss after friability testing. 8 large geometry placebo tablets were weighed (XS105 Dual Range, Mettler Toledo) then rotated at 25 rpm for 4 min (10805R, Vankel). Tablets were then re-weighed and mass loss after friability was calculated.

## **Results and Discussion:**

### *HSP Analysis*

Hansen Solubility Parameters of moxidectin are reported in Table 4.3 along with HSP values of the excipients. The scoring criteria used for HSP values and scores assigned to



each sample are listed in Tables 4.4 and 4.5. Compatibility of PEO, PVP, and TEC with moxidectin was determined by calculating their HSP distance from moxidectin (Table 4.5). Specifically, understanding the compatibility of TEC with moxidectin was crucial as moxidectin has a  $T_g$  above the extrusion temperature used. As shown by Table 4.5, moxidectin has a small distance ( $R_a$ ) of 4.67 from TEC and 4.23 from PEO indicating good compatibility between moxidectin and these materials. Whereas PVP has a higher  $R_a$  of 7.41 from moxidectin, which indicates poorer compatibility. However, the  $R_a$  with PVP is well within moxidectin's radius of interaction, which suggests that the drug should be soluble in all three excipients.

<b>Table 4.3. Hansen Solubility Parameters of Moxidectin, PEO, PVP, and TEC along with their solubility distances (<math>R_a</math>).</b>					
<b>Compound</b>	<b><math>\delta_D</math></b>	<b><math>\delta_P</math></b>	<b><math>\delta_H</math></b>	<b><math>R_a</math> (Moxidectin)</b>	<b><math>R_a</math> (TEC)</b>
<b>Moxidectin</b>	17.0	6.9	7.9	0.0	4.67
<b>PEO</b>	17.0	10.0	5.0	4.23	8.72
<b>PVP</b>	18.3	12.9	11.4	7.41	8.79
<b>TEC</b>	16.5	4.9	12.0	4.67	0.00

Additionally, the high compatibility of TEC and moxidectin was readily observed during sample preparation for extrusion. Moxidectin was dissolved in the plasticizer before extrusion to ensure that the drug can be melt processed at 120°C and dissolved into the matrix. TEC compatibility with the polymer excipients was also investigated to ensure that TEC is melt miscible and does not phase separate or leach out of the polymers over time. The TEC distances with respect to other compounds are listed in Table 4.3, which shows that TEC has limited compatibility with the polymeric excipients as indicated by the large  $R_a$ . Less compatible plasticizers have been known to leach out of the polymer

<b>Table 4.4.</b> HSP values of solvents used as well as their solvent scores				
<b>Solvent</b>	<b><math>\delta_D</math></b>	<b><math>\delta_P</math></b>	<b><math>\delta_H</math></b>	<b>Score</b>
Acetone	15.5	10.4	7.0	2
Chloroform	17.8	3.1	5.7	3
Methyl Ethyl Ketone	16.0	9.0	5.1	3
2-Propanol	15.8	6.1	16.4	4
Benzene	18.4	0.0	2.0	3
Tetrahydrofuran	16.8	5.7	8.0	3
Acetonitrile	15.3	18.0	6.1	3
N-Methyl-2-Pyrrolidone	18.0	12.3	7.2	5
1,3-Dioxolane	18.1	6.6	9.3	4
Heptane	15.3	0.0	0.0	4
Ethanol	15.8	8.8	19.4	4
Dimethyl Sulfoxide	18.4	16.4	10.2	5
<i>o</i> -Dichlorobenzene	19.2	6.3	3.3	5
Cyclohexanone	17.8	8.4	5.1	6
Morpholine	18.0	4.9	11.0	5
Ethyl Acetate	15.8	5.3	7.2	3
Anisole	17.8	4.4	6.9	5
Toluene	18.0	1.4	2.0	3
<i>p</i> -Xylene	17.8	1.0	3.1	3
Methylene Dichloride	17.0	7.3	7.1	1

<b>Table 4.5.</b> Scoring criteria used for each solvent.	
<b>Score</b>	<b>Concentration (g/mL)</b>
1	>3
2	2 to 3
3	1 to 2
4	0.5 to 1
5	0.25 to 0.5
6	<0.25

matrix at higher concentrations[19]. However, the DSC shows that TEC reduces the glass transition temperature ( $T_g$ ) of both PEO and PVP significantly despite the limited compatibility suggested by HSP values (Figures 4.2b, 4.3b, and Table 4.8).

Incompatible plasticizers can still have a significant impact on  $T_g$  until a saturation concentration is reached and significant phase separation occurs[18, 20-22]. For this work, TEC is a minor component in the formulation relative to the polymer excipient and in all likelihood none of the plasticized materials will reach saturation concentration.

#### *Thermogravimetric Analysis (TGA)*

Thermogravimetric analysis of excipients was used to determine the thermal degradation temperatures and behavior of the API and excipients. The thermograms are shown in Figure 4.1 and the onset of degradation is listed in Table 4.6. The TGA data suggests that moxidectin, PEO, PVP, and citric acid are thermally stable well above the extrusion temperature of 120°C. The PVP sample has an initial mass loss starting at 47.8°C which is attributed to moisture loss due to its hygroscopic nature. The onset of mass loss in TEC and bicarb samples was observed to be approximately 130°C.

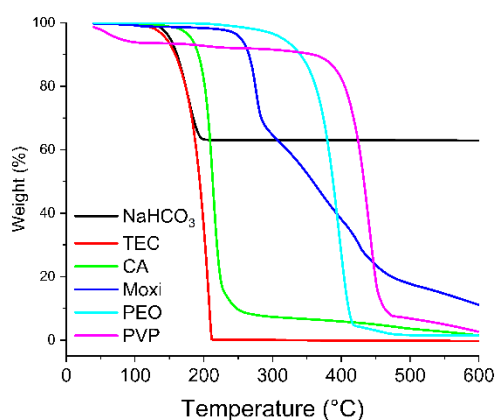


**Figure 4.1.** TGA thermograms of API and excipients.

<b>Table. 4.6. Onset of degradation of moxidectin and excipients</b>	
<b>Compound</b>	<b>Temperature (°C)</b>
Bicarb	131.7
TEC	135.2
CA	184.5
Moxidectin	255.1
PEO	345.0
PVP	395.6

### *Differential Scanning Calorimetry (DSC)*

DSC thermograms show that the PVP has a  $T_g$  well above the extrusion temperature.

Moxidectin's  $T_g$  was observed to be near the extrusion temperatures as well. To decrease the  $T_g$  of both materials and allow for successful extrusion at the given processing conditions, TEC was added to the formulation as a plasticizer. Plasticization of PVP and moxidectin by TEC (PVP-TEC and Moxi-TEC) are shown by  $T_g$  shifts in Figure 4.2.a

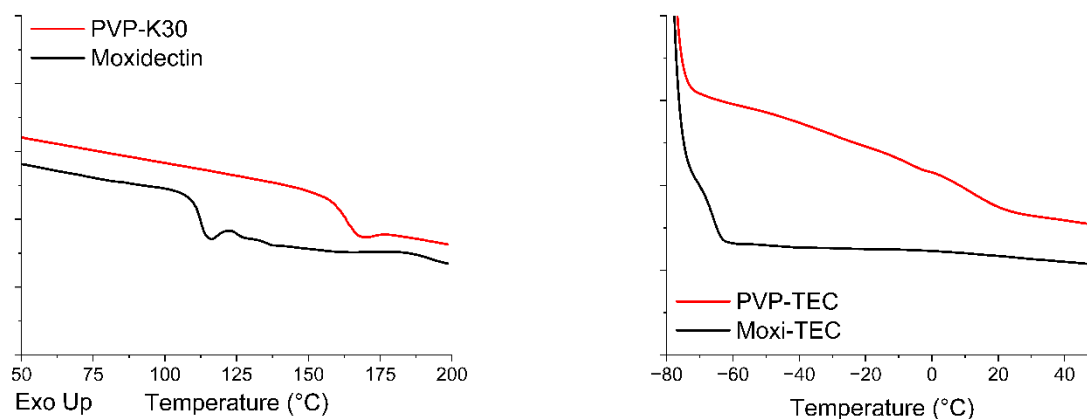


**Figure 4.2.** DSC thermograms of PVP and moxidectin samples. Left (a) – Glass transition of PVP and moxidectin. Right (b) – Glass transition of PVP and moxidectin plasticized with TEC-BHT.

and Table 4.7. PVP  $T_g$  is reduced drastically from 164.2°C to 11.2°C, similarly moxidectin's  $T_g$  is also reduced from 112.4°C to -65.8 °C (Figure 4.2.b and Table 4.7). PEO and formulations were also analyzed by DSC to determine the thermal

**Table 4.7. Formulations Used for Extrusion and Microscopy Analysis**

Formula	PEO (%w/w)	PVP (%w/w)	Bicarb (%w/w)	Citric Acid (%w/w)	Moxi (%w/w)	TEC (%w/w)	BHT (%w/w)
<b>PVP-TEC</b>	-	67	-	-	-	32.7	0.3
<b>Moxi-TEC</b>	-	-	-	-	38	61.3	0.7
<b>F1</b>	40	20	20	10	0	10	0
<b>F1 Moxi</b>	40	18	18	9	5.7	9.3	0
<b>F2</b>	40	20	20	10	0	9.9	0.1
<b>F2 Moxi</b>	40	18	18	9	5.7	9.2	0.1
<b>F3</b>	57	29	0	0	0	14	0

transitions from PEO, PVP and API in the extrudate. As shown in Figure 4. 3.a and Table 4.7. the melting point ( $T_m$ ) of PEO has drastically been reduced from 60.4°C to ~46°C-50°C, which can be attributed to reduction in lamellar thickness of PEO in the presence of other excipients. Thermal transitions of PVP were not identified from the extrudate thermograms due to its lower mass fractions in the formulation and potential overlap

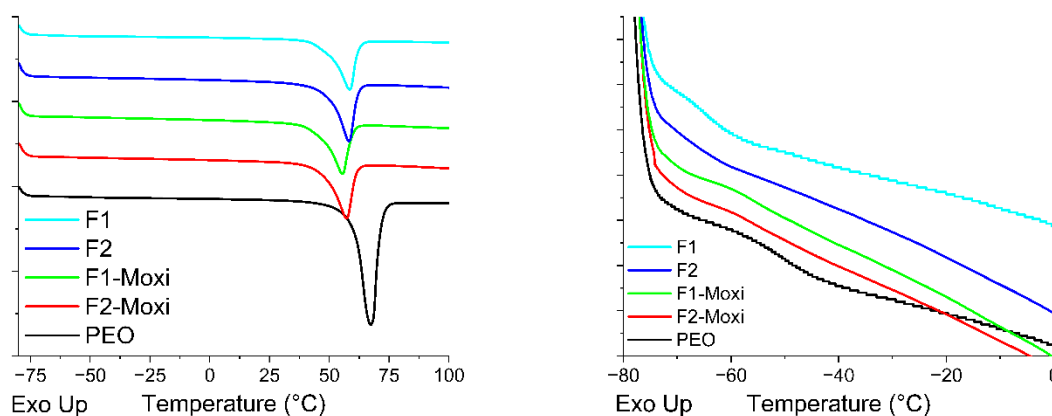


**Figure 4.3.** DSC thermograms of PEO, placebo, and API loaded formulations. Left (a) – 1st heating curve of the extrudate samples. Right (b) – Zoom in on the glass transition of the samples from the 2nd heating curve.

between the melting transition of PEO and  $T_g$  of PVP. As predicted by HSP, the  $T_g$  of PEO shifts in F1 and F2 placebo formulations, however due to the temperature limitation on the instrument, the exact  $T_g$  value wasn't verified. Interestingly, the  $T_g$  of PEO in F1-Moxi and F2-Moxi is not as drastic and observed to be  $\sim 4^\circ\text{C}$  lower than PEO's  $T_g$  (Figure 4.3.b and Table 4.7). The limited  $T_g$  shift of PEO with moxidectin containing formulations (F1-Moxi and F2-Moxi) could be explained by the high compatibility of moxidectin with PEO. According to the Fox equation,  $T_g$  shift in polymers due to plasticization is a function of the mass fraction of each component and their inherent  $T_g$ . Given that moxidectin has a much higher  $T_g$  than PEO and TEC, the presence of moxidectin in the samples counters the  $T_g$  reduction by TEC.

<b>Table 4.8. DSC data of PVP, Moxidectin, PEO, and formulations (<math>\Delta H_f = 197 \text{ J/g}</math> for PEO[23])</b>				
<b>Sample</b>	<b><math>T_g</math> (<math>^\circ\text{C}</math>)</b>	<b><math>T_m</math> (<math>^\circ\text{C}</math>)</b>	<b><math>T_c</math> (<math>^\circ\text{C}</math>)</b>	<b>% <math>X_c</math> of PEO</b>
<b>PEO</b>	-50.3	60.4	43.0	79.1
<b>PVP</b>	164.2	-	-	-
<b>PVP-TEC</b>	11.2	-	-	-
<b>Moxidectin</b>	112.4	-	-	-
<b>Moxi-TEC</b>	-65.8	-	-	-
<b>F1</b>	n.d.	49.4	42.1	83.5
<b>F2</b>	n.d.	50.0	41.3	93.2
<b>F1-Moxi</b>	-54.2	46.4	41.5	86.1
<b>F2-Moxi</b>	-54.1	48.2	42.4	91.2

#### *Intrinsic Flowability, Extrusion, and Injection Molding*

Moxidectin loading in this study was kept low in accordance with the target therapeutic dosing for this product (Table 8). Moxidectin availability was limited to less than 10 g, so the material-sparing and expedited formulation development technique[24, 25] was employed to simulate pre-clinical development conditions and conserve API. Therefore,

duplicate testing was minimized, and extrusion and injection molding optimization was done with placebo material.

The intrinsic flowability of the powder, as measured via Flodex, is  $< 4$  mm. The powder flows extremely well even through the smallest aperture test disk available. This is mostly due to the high flowability of the primary excipient, PEO, which contains the glidant fumed silica. This formulation will have no feeding problems when scaled up for manufacturing, even if only using a gravity feeder.

The extrudability of the formulation is highlighted by the consistent torque value observed during melt-mixing on Haake Minilab II in Figure 4.4. The sharp peaks earlier in the plot are observed as material is fed into the extruder. The last feeding peak at 6-minute was taken as the starting point for mixing and the sample was blended into the extruder until being ejected at the 10-minute mark for injection molding. The torque

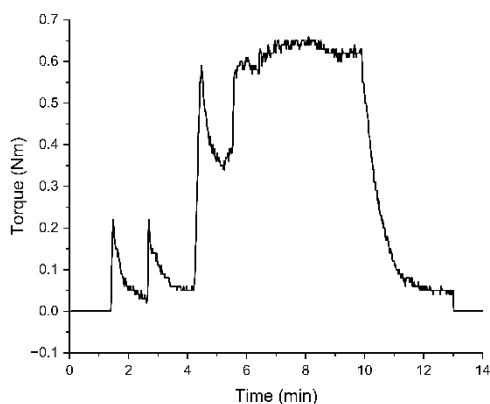


**Figure 4.4.** Torque vs time plot of F1-Moxi formulation during extrusion.

values during the mixing region are relatively consistent indicating even mixing of the formulation during extrusion. Due to the excellent nucleation efficiency of PEO, injection

molded bars could be removed from the mold immediately and without difficulty. No mold release was needed to extract the bars from the mold, which is beneficial for industrial processing of these formulations. Flashing occurred around the edges of the mold, but that can be mitigated by modifying injection mold conditions or applying clamp force to the mold during injection.

### *Moisture Content*

The moisture content prior to extrusion of the formulation including TEC was 1.33% based on loss on drying. F2 immediately following extrusion had a moisture content of 4.3 %. Bicarb decomposition as well as bicarb's reaction with citric acid produces water in addition to CO<sub>2</sub>, which is why the extruded product has a higher moisture content than the pre-extruded powder. Since the higher moisture content is coupled to the reaction that provides the higher porosity in the injection molded tablet, APIs sensitive to hydrolytic degradation must be extruded at a lower temperature to prevent bicarb decomposition, which could impact the dissolution profile of the formulation.

The higher moisture content of effervescent ASD formulations after extrusion was a surprising finding because in work done by Lima et.al, effervescent thermoplastic formulations went from 10% moisture content to 2.5-5% moisture content after extrusion at 100°C[5]. The study suggested that extrusion above the boiling point of water facilitated drying of the extrudate, which would be beneficial for effervescent tablets. In traditional tableting of effervescent, excipients must be dried prior to blending and the tableting/packaging must be done in low humidity conditions to protect effervescent components. Therefore, if extrusion doubles as a drying step, extrusion could make



tableting effervescent more efficient, and could provide some moisture barrier properties to prevent effervescent from absorbing water from the atmosphere post extrusion.

### *Tablet Geometry*

Tablets made via punchout from injection molded bars had consistent mass and geometry as expected for injection molded products (Table 4.9). The density of the tablets therefore is also constant, which indicates that if extrusion conditions are held constant, the porosity generated via bicarb decomposition is also constant. These findings also suggest a homogenous distribution of the effervescent throughout the matrix to evolve CO<sub>2</sub> consistently throughout the molten matrix. Porosity of the tablets impacts dissolution rate and could be leveraged for dissolution optimization in future work.

**Table 4.9. Injection Molded Tablets Mass Uniformity**

<b>Formulation</b>	<b>Avg. Mass (mg, n=6)</b>	<b>Avg. Thickness (mm, n=3)</b>	<b>Avg. Width (mm, n=3)</b>
<b>F1</b>	35.37 ± 0.49	1.03 ± 0.02	5.91 ± 0.02
<b>F1_Moxi Extrusion 1</b>	36.44 ± 0.82	1.07 ± 0.02	5.91 ± 0.02
<b>F1_Moxi Extrusion 2</b>	35.95 ± 0.36	1.03 ± 0.01	5.90 ± 0.02

SLA printed inserts were made to fit inside stainless steel Izod molds (Figure 4.5, A and B). SLA inserts were useful in prototyping unique tablet geometries, but the surface roughness of the printed insert made removing tablets difficult. Additionally, the inserts could only withstand a few injections before cracks developed. The limited lifetime of the inserts and difficulty removing tablets is why all testing was done on tablets punched out from injection molded bars. Given the highly consistent results from Table 6, it is expected that tablet consistency will only increase once these formulations are tested on

steel molds made to produce tablet geometries. The prototype geometries were picked to highlight the range of shapes that can be made with injection molding that would be challenging to produce with powder compression. Traditional tablets made via powder compression are often circles or ovals because sharp points and extensions from the tablet body create manufacturing problems such as picking and sticking[26]. Because of the cohesive nature of the thermoplastic resin, the polymer matrix does not adhere to the mold as much as it adheres to itself thus preventing picking-like behavior when extracting from the injection mold. Additionally, the G has a free-standing appendage off the main body of the tablet. In powder compression, this shape would create a mechanical weakness in the tablet which would likely lead to failing friability. The cohesion and

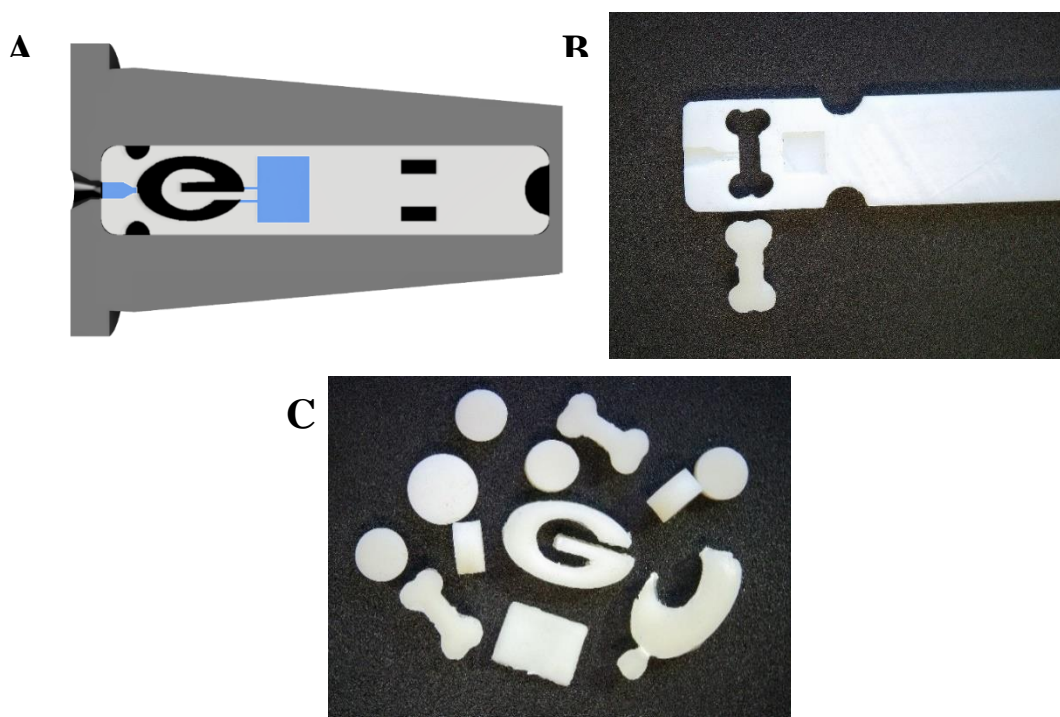


**Figure 4.5.** (A) Graphic of the "G" SLA injection mold insert design embedded in the steel mold. The depressions at the edges were added to facilitate removal from the steel mold. (B) shows the SLA insert used to make the dog bone shaped tablets alongside one of the tablets. (C) shows the diversity of tablet geometries made in this study.

flexibility of the thermoplastic polymer matrix enables the tablet to hold its shape even when stress is applied.

#### *Content Uniformity*

USP <905> is the industry standard for what is considered acceptable deviation from the target API loading (label claim) in pharmaceutical dosage forms. As a simplification of acceptance criteria, 85-115% of the label claim is acceptable for API loading in dosage forms in clinical phase development. Content uniformity is fundamental for assuring a therapeutic concentration systemically and for minimizing the risk of adverse events in patients. This requirement is particularly important in the case of low-dose, highly potent drugs like moxidectin, where small variations in the API amount due to the dosage form variation may result in a significant impact on safety and efficacy. As can be seen in Table 4.10, the injection molded tablets have extremely consistent and accurate API loading. Moxidectin solubilization in the plasticizer enables precise liquid feeding into the extruder and thus precise and homogenous distribution of moxidectin throughout the injection molded tablets. High precision and homogeneous API loading are an additional advantage of injection molding over traditional powder compression for tablet production.

<b>Table 4.10. Content Uniformity and Degradation Analysis of Injection Molded Tablets</b>		
<b>Formula</b>	<b>Content Uniformity (% label claim) (n=3)</b>	<b>Percent Degradation (%) (n=3)</b>
<b>F1_Moxi</b>	103.3 ± 0.9	1.9 ± 0.09
<b>F2_Moxi</b>	99.9 ± 1.8	3.4 ± 0.02

#### *Degradation Analysis via HPLC*

Figure 4.6 shows an HPLC chromatogram for injection molded tablets made with and without the antioxidant BHT compared to a pure moxidectin stock solution. The red arrows indicate the two degradant peaks which are not present, or present to a lesser degree, in the stock solution. The degradant peak at 20.1 min is elevated in the extruded samples but is present as evidenced by the shoulder at 20.1 on the main moxidectin peak in the stock solution. The stock solutions were made immediately prior to HPLC analysis,

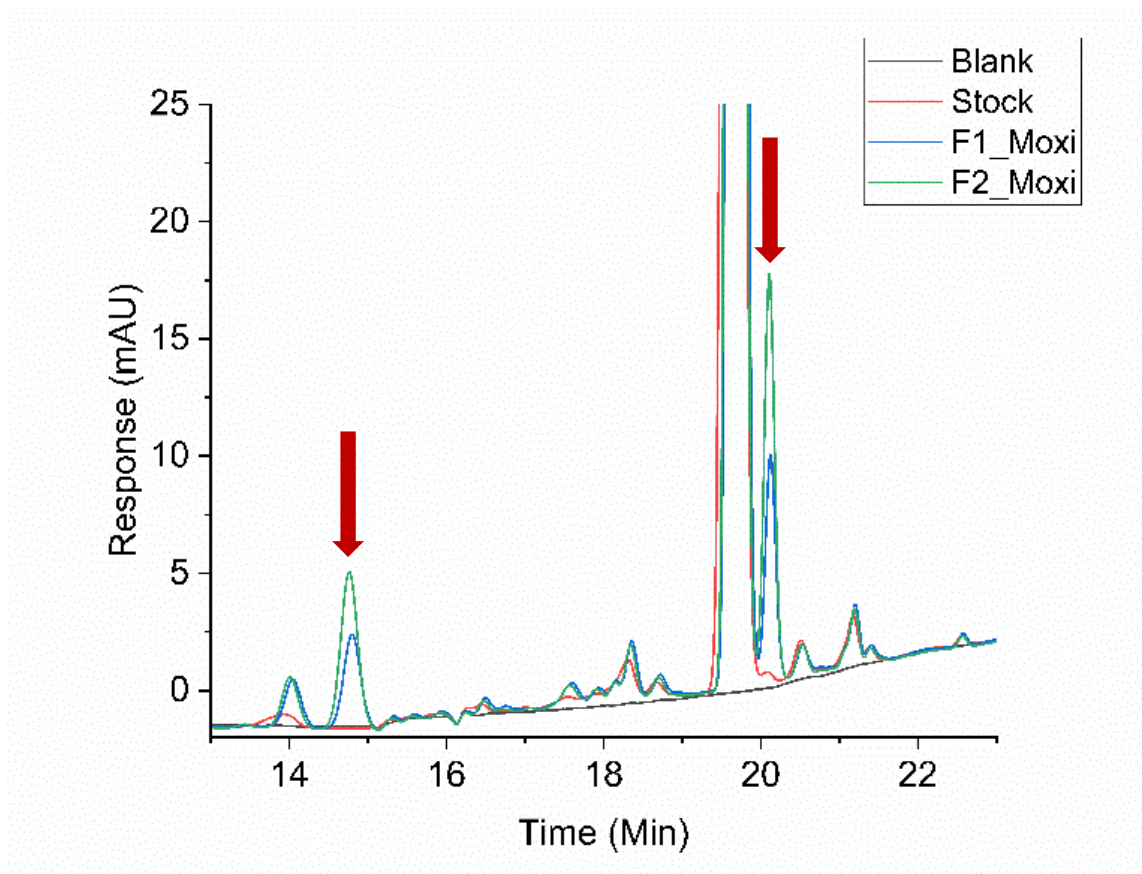


**Figure 4.6.** HPLC chromatogram of content uniformity samples showing the increase in the degradant peak (red arrows) for extruded samples compared to pure moxidectin stock and the blank mobile phase. The peak at 20.1 being the larger peak area was used to calculate percent degradation.

so no degradation of the stock occurred. Moxidectin typically is between 94-95%

pure[27], meaning some trace contaminants remain after production and purification as

can be seen in the stock solution in Figure 4.6. Moxidectin is reported to be susceptible to

oxidative degradation, so BHT was added to improve stability[28]. However, the percent degradation of F2 with BHT was higher than F1 which contained no BHT (Table 4.10). The degradant peaks were normalized against the amount of moxidectin present and were run in triplicate to enable comparison of the formulations and the amount of degradation. Further studies will be done to isolate and identify the structures of the two degradation peaks to enable formulation and extrusion processing changes to improve API stability. The HPLC chromatogram from F1 and F2 placebo samples. Dissolution samples from those formulations were analyzed via HPLC and no degradant peaks appeared for the placebo samples, which indicates that the degradant peak is the result of moxidectin and not an excipient degrading.

#### *Dissolution Profile*

To have a measurable quantity of moxidectin, 2x 2mg tablets were used per dissolution test, which mimics how moxidectin is currently prescribed for the treatment of onchocerciasis. Due to the consistency of the tablet geometry, tablet mass, and moxidectin content uniformity, the dissolution profiles of the triplicate tested samples are practically identical (Figure 4.7 A). F1 Moxidectin was able to achieve 85% release in 45 minutes, which classifies it as a successful immediate release tablet. Larger diameter and thickness circle tablets were punched out of Izod bars to determine the impact of tablet volume on dissolution. The average geometry of the 2 mg tablets was 1.07 mm x 5.91 mm weighing 36 mg. The larger tablets were 3.14 mm x 7.86 mm weighing 186 mg. The active dose of larger tablets was ~ 11 mg, which is larger than the maximum 8 mg dose needed to treat onchocerciasis. Given the high reproducibility of the smaller tablets, only one tablet per paddle speed was tested for larger tablets. As seen in Figure 4.7 B, the

larger tablets fail to meet 85% release by 1 hour, but do achieve 85% release in under two hours, which is close enough to immediate release for this technology to still be beneficial for some BCS 2, 3, and 4 applications. As expected, increasing the paddle speed to 100 rpm increases dissolution rate, but *in vivo* studies would need to be done to verify the bio relevance of the dissolution methods. Furthermore, modifying the tablet geometry to increase surface area and increasing the effervescent concentration can be explored in future studies to improve dissolution profiles for applications where higher dosing is needed.

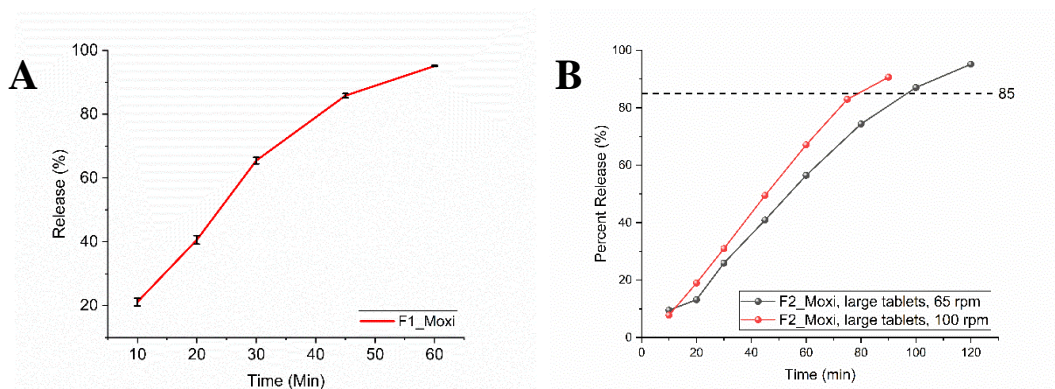


**Figure 4.7.** (A) The average dissolution profile of 2 mg tablets (n=3 made from F1\_moxi with error bars in black. (B) Dissolution profiles of 11 mg, F2\_moxi tablets at both 65 (n=1) and 100 (n=1) rpm paddle speed to highlight the difference that dissolution parameters have on the release profile

### *Friability Analysis*

Large diameter tablets weighing 1.63036 g total were tested for friability. The tablets increased in mass by 0.00042 g which is an increase in mass of 0.03%. This mass change could be caused by the formulation absorbing moisture from the atmosphere during friability testing, but this minor change is also near the  $\pm 0.0002$  g resolution limit of the scale. In either case, the tablets passed USP <1216> standard of less than 1% mass loss during friability testing.

To further confirm the strength of the injection molded tablet formulation, an injection molded bar was hit with a hammer to see if chipping or cracking would occur. After multiple hits, the bar remained unchanged unlike powder compression tablets which disintegrated into back into powder. The reason that the injection molded tablets are much stronger than traditional powder compression tablets is that compressed powder tablets rely on interparticulate surface interactions to form a cohesive tablet. The mechanical and chemical interactions at the contact points between particles prevent them from gliding past one another when stress is applied. The compression process forces more particles to interact thus generating a stronger tablet. In injection molded tablets the same principle applies, except when molten polymers are mixed then injected under pressure, the number of entanglements and contact points are more abundant for the polymer matrix compared to the compressed powder. The formulation and injection molding process therefore produce a stronger and likely a higher solid fraction tablet than powder compression.

One of the potential application benefits of the high strength injection molded tablets is in abuse deterrence of opioids. Schedule 2 opioids are notoriously misused and abused. Formulations to deter abuse of opioids is an active area of pharmaceutical research[29-32]. Two prominent methods of abuse are crushing the tablet either to snort or to extract the opioids from crushed tablets for intravenous injection[31, 33]. In either of these cases, the injection molded tablet formulations would deter abuse without delaying API release in patients using these products as intended. The injection molded tablets as discussed are impervious to crushing even by smashing with a hammer, so the tablets cannot be powderized via crushing or grinding for snorting. The high molecular weight of the



water-soluble PEO/PVP would form a viscous gel if dissolved in a small quantity of water, which would hinder opioid extraction for intravenous injection as well as impede intravenous injection via needle and syringe.

#### *Scanning Electron Microscopy (SEM)*

Cryofracturing of the injection molded bars was done using liquid nitrogen to observe the internal morphology of the sample. PEO and PVP were expected to be immiscible based on previously reported studies[34, 35]. Figure 4.8 A and D (navy arrows) shows the phase separated PVP and PEO. PVP is an amorphous material with a  $T_g$  of 160°C. The plasticization of PVP by TEC shifts the  $T_g$  down and enables it to be extruded at 120°C. The plasticized PVP is expected to remain amorphous within the matrix which provides beneficial impact modification to the tablets. The amorphous PVP regions are above their  $T_g$  at room temperature which means there is global molecular motion in the PVP

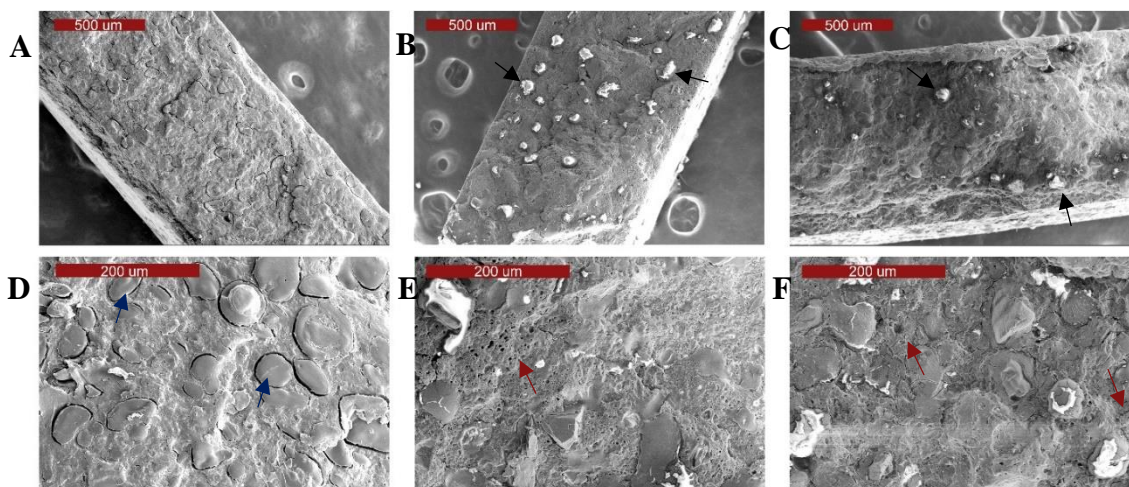


**Figure 4.8.** SEM of cross section of injection molded bars. F4 (A, D) formulation contains no effervescent granules, and the PVP/PEO phase separation is clearly visible as indicated by the navy blue arrow in D. F1-Moxi (B, E) contains moxidectin and effervescent granules. The effervescent granules are highlighted with black arrows. F1 (C, F) contains effervescent but no Moxi. The morphology of the Moxi and placebo formulation are identical. The porosity that develops as a result of bicarb decomposition is indicated with red arrows (E, F).



domains. These domains are able to absorb and dissipate impact stresses without cohesive failure of the tablet. Therefore, the tablets made with this formulation are able to withstand large compression forces without fracturing due in part to the PVP domains. This material property is beneficial for making strong tablets that pass USP mechanical testing, but beyond that, these amorphous domains contribute to the high impact resistance that would make these formulations useful for abuse deterrence.

Since citric acid and bicarb do not melt below 120C, they are solid fillers in the matrix and appear as large granules in F1 and F1\_Moxi as seen in Figure 4.8 B and C indicated by the black arrows. These granules are absent in Figure 4.8 A because no effervescent was added to F4. As expected from geometry and dissolution data, the effervescent granules are evenly distributed throughout the injection molded bar.

As further confirmation of the bicarb decomposition, CO<sub>2</sub> release generated bubbles in the molten matrix during extrusion which solidified to form pores throughout the injection molded parts. These are indicated in Figure 4.8 E and F with red arrows. There are some small bubbles present in the F4 sample, but they are fewer and smaller compared to F1 and F1\_moxi. These bubbles are likely the result of steam liberation from the inherent moisture in the excipients during extrusion. The lower moisture content of the pre-extrusion powder and the lack of CO<sub>2</sub> generating effervescent are the reasons that F4 has minimal porosity compared to F1 and F1 Moxi. Porosity is very evident in the cross sections of F1 and F1\_moxi even at only 200x magnification (Figure 4.8 B and C). The porosity caused by the CO<sub>2</sub> generation likely increases the dissolution rate of the injection molded tablets, especially in the first few minutes of dissolution as the matrix is wetting. The pores enable water to more quickly reach the bicarb, which once wet can

react with citric acid to produce more CO<sub>2</sub> in a positive feedback loop. The gas liberation inside of the matrix acts as a disintegrant to physically force the tablet apart, which enables more water in to react with more bicarb and citric acid. The bubbling action also forces the interfacial gel layer to disrupt and exposes more matrix to the water, thus improving dissolution.

### *Polarized Optical Microscopy*

Based on SEM analysis, it was suspected that PVP was forming amorphous domains within the crystalline matrix of PEO. Since bicarb and citric acid do not melt or dissolve into the matrix, they obstructed POM imaging, so samples were extruded without effervescent components to image the phase separation of plasticized PVP and PEO (F4). Figure 4.9 A shows the molten PEO. The small, fumed silica particles are visible in the melt, but otherwise the melt is a homogenous phase. In Figure 4.9 B, PEO and PVP phase separation can be seen once again. Pure PEO tends to form large spherulites (Figure 4.9 C). When PVP and TEC are added to PEO, the spherulite growth is impeded by the PVP, so spherulites are smaller and more numerous. This phenomenon is responsible for the downshift and broadening of the PEO T<sub>m</sub> observed via DSC. The PVP does remain amorphous, as can be seen by the absence of spherulites in the regions of phase separation. POM videos were recorded of the PEO crystallization, and the spherulites can be seen running up against the PVP phases and stopping. In the video, spherulite growth can be seen through the amorphous PVP regions, which are isotropic and thus appears clear under POM.

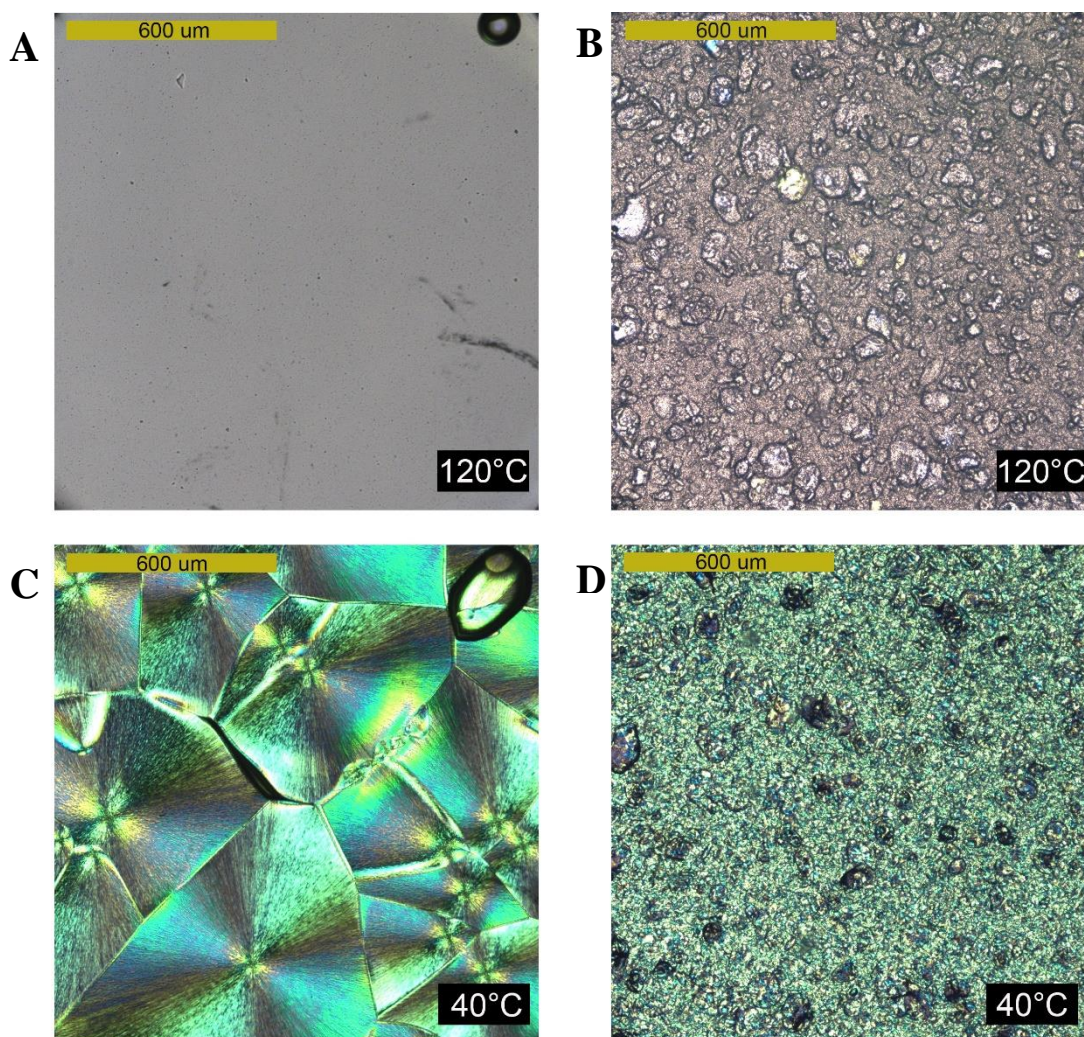


**Figure 4.9.** POM images of injection molded samples in the melt at 120°C to show the phase separation between PEO (A) and F4 (C). Additionally, 40°C highlighting the morphology differences between the spherulite structures in pure PEO (B) and F4 (D). The spherulites in D are smaller and more numerous compared to the spherulites of pure PEO.

### **Conclusion:**

Outside of the traditional benefits of ASD (i.e., increased solubility/bioavailability of an API), the chief benefit of this work is the increased efficiency and production capacity of ASD tablets by directly injection molding tablets. As a result of the formulation and injection processing, numerous secondary benefits arise. Firstly, the extrusion and

injection mold processing produces tablets with extremely consistent geometry and homogenous API loading. The injection molded tablets pass all USP uniformity testing. Secondly, the strength of the injection molded tablets and resilience to fragmentation facilitates ease of processing, including the ability to coat tablets, without chipping. Lastly, the injection molded tablets can be made into a variety of shapes that would be challenging to accomplish in powder compression without manufacturing complications, so new and highly recognizable tablet shapes could be generated. Not only does this increase market recognition of products, but it makes it easier for patients to distinguish between medications, reduces the risk of accidentally taking medications outside of their prescription regimen.

Some additional potential benefits that were not explored in this work include abuse deterrence and taste masking. The strength of the tablets lends itself to abuse deterrence applications for schedule 2 drugs while the melt processing of the API and encapsulation in a polymer matrix could mask the taste of bitter APIs. Masking the taste of bitter APIs improves patient experience and compliance.

It is worth noting that the material sparing approach of formulation development employed in previous work was also beneficial for the rapid and efficient development of injection molding tablet formulations in this study. By utilizing material sparing test methods, a formulation was developed that produced an immediate release amorphous solid dispersion that maintained the amorphous state of the API, using less than 10 g of API.

In future work, the degradation product identified via HPLC will be characterized to identify the excipient incompatibility or processing condition that is causing the

degradation so that modifications can be made to improve moxidectin stability. Another area of interest is utilizing extrusion temperatures and cycle time to control bicarb decomposition to influence the porosity of the injection molded tablets. Additionally, future studies could explore the dissolution rate of various injection molded tablet shapes to identify the surface area and density thresholds for achieving immediate release with these formulations. It is evident that injection molding of immediate release ASD tablets is an underexplored field with numerous benefits and room for growth.

## References

1. Wilson, V.R., et al., *Amorphous solid dispersions of enzalutamide and novel polysaccharide derivatives: investigation of relationships between polymer structure and performance*. Scientific Reports, 2020. **10**(1): p. 18535.
2. Baird, J.A., B. Van Eerdenbrugh, and L.S. Taylor, *A classification system to assess the crystallization tendency of organic molecules from undercooled melts*. J Pharm Sci, 2010. **99**(9): p. 3787-806.
3. Pandi, P., et al., *Amorphous solid dispersions: An update for preparation, characterization, mechanism on bioavailability, stability, regulatory considerations and marketed products*. Int J Pharm, 2020. **586**: p. 119560.
4. Agrawal, A., et al., *Development of Tablet Formulation of Amorphous Solid Dispersions Prepared by Hot Melt Extrusion Using Quality by Design Approach*. AAPS PharmSciTech, 2016. **17**(1): p. 214-232.
5. Lima, A.L., et al., *Hot-Melt Extrusion as an Advantageous Technology to Obtain Effervescent Drug Products*. Pharmaceutics, 2020. **12**(8).
6. Verreck, G., et al., *The effect of pressurized carbon dioxide as a temporary plasticizer and foaming agent on the hot stage extrusion process and extrudate properties of solid dispersions of itraconazole with PVP-VA 64*. European Journal of Pharmaceutical Sciences, 2005. **26**(3): p. 349-358.
7. Triboandas, H., et al., *Itraconazole Amorphous Solid Dispersion Tablets: Formulation and Compaction Process Optimization Using Quality by Design Principles and Tools*. Pharmaceutics, 2022. **14**(11).

8. Sarabu, S., et al., *Hypromellose acetate succinate based amorphous solid dispersions via hot melt extrusion: Effect of drug physicochemical properties*. Carbohydrate Polymers, 2020. **233**: p. 115828.
9. Xu, H., et al., *Hybrid Manufacturing of Oral Solid Dosage Forms via Overprinting of Injection-Molded Tablet Substrates*. Pharmaceutics, 2023. **15**(2).
10. Walsh, E., et al., *Manufacture of tablets with structurally-controlled drug release using rapid tooling injection moulding*. International Journal of Pharmaceutics, 2022. **624**: p. 121956.
11. Quinten, T., et al., *Evaluation of injection moulding as a pharmaceutical technology to produce matrix tablets*. European Journal of Pharmaceutics and Biopharmaceutics, 2009. **71**(1): p. 145-154.
12. Almeida, A., et al., *Ethylene vinyl acetate as matrix for oral sustained release dosage forms produced via hot-melt extrusion*. European Journal of Pharmaceutics and Biopharmaceutics, 2011. **77**(2): p. 297-305.
13. Quinten, T., et al., *Sustained-release and swelling characteristics of xanthan gum/ethylcellulose-based injection moulded matrix tablets: in vitro and in vivo evaluation*. J Pharm Sci, 2011. **100**(7): p. 2858-70.
14. Desai, P.M., et al., *Integrated hot-melt extrusion – injection molding continuous tablet manufacturing platform: Effects of critical process parameters and formulation attributes on product robustness and dimensional stability*. International Journal of Pharmaceutics, 2017. **531**(1): p. 332-342.

15. Melocchi, A., et al., *Evaluation of Hot-Melt Extrusion and Injection Molding for Continuous Manufacturing of Immediate-Release Tablets*. Journal of Pharmaceutical Sciences, 2015. **104**(6): p. 1971-1980.
16. Pharmacopeia, U.S., *General Chapter Dissolution <711>*. 2023.
17. Tan, B., et al., *Pharmacokinetics of oral moxidectin in individuals with Onchocerca volvulus infection*. PLoS Negl Trop Dis, 2022. **16**(3): p. e0010005.
18. Kush G. Patel, R.K.M., Lawrence S. Ferguson IV, Michael L. Broich II, Josh C. Bledsoe, Caitlin C. Wood, Grant H. Crane, Jessica A. Bramhall, Jonathan M. Rust, Amanda Williams-Rhaesa, and Jason J. Locklin, *Experimentally Determined Hansen Solubility Parameters of Biobased and Biodegradable Polyesters*. 2023: [Manuscript Submitted To]ACS Sustainable Chemistry and Engineering.
19. Hansen, C.M., *Hansen Solubility Parameters*. 2007.
20. Barbosa, J.L., G.B. Perin, and M.I. Felisberti, *Plasticization of Poly(3-hydroxybutyrate-co-3-hydroxyvalerate) with an Oligomeric Polyester: Miscibility and Effect of the Microstructure and Plasticizer Distribution on Thermal and Mechanical Properties*. ACS Omega, 2021. **6**(4): p. 3278-3290.
21. Immergut, E.H. and H.F. Mark. *Principles of Plasticization*. 1965.
22. El-Taweel, S.H., et al., *Glass transition and the rigid amorphous phase in semicrystalline blends of bacterial polyhydroxybutyrate PHB with low molecular mass atactic R, S-PHB-diol*. Polymer, 2004. **45**(3): p. 983-992.
23. Blaine, R.L. *THERMAL APPLICATIONS NOTE: Polymer Heats of Fusion*.



24. Yamashita, H. and C.C. Sun, *Material-Sparing and Expedited Development of a Tablet Formulation of Carbamazepine Glutaric Acid Cocrystal– a QbD Approach*. Pharmaceutical Research, 2020. **37**(8).
25. Wang, C. and C.C. Sun, *The efficient development of a sildenafil orally disintegrating tablet using a material sparing and expedited approach*. International Journal of Pharmaceutics, 2020. **589**: p. 119816.
26. Chatteraj, S., et al., *Sticking and Picking in Pharmaceutical Tablet Compression: An IQ Consortium Review*. Journal of Pharmaceutical Sciences, 2018. **107**.
27. Awasthi, A., et al., *Chapter Seven - Analytical Profile of Moxidectin*, in *Profiles of Drug Substances, Excipients and Related Methodology*, H.G. Brittain, Editor. 2013, Academic Press. p. 315-366.
28. Pharmacopeia, U.S., *Moxidectin Monograph*. 2020.
29. Larochelle, M.R., et al., *Rates of opioid dispensing and overdose after introduction of abuse-deterrent extended-release oxycodone and withdrawal of propoxyphene*. JAMA Intern Med, 2015. **175**(6): p. 978-87.
30. Wolff, C., et al., *The impact of the abuse-deterrent reformulation of extended-release OxyContin on prescription pain reliever misuse and heroin initiation*. Addict Behav, 2020. **105**: p. 106268.
31. Fletcher, J.M.B.B.M.P.H. and R.T.B.S.C.P.M.S.C. Tsuyuki, *Don't tamper with oxycodone: CPJRPC*. Canadian Pharmacists Journal, 2013. **146**(1): p. 6.
32. Townsend, T.N., et al., *Has Declining Opioid Dispensing to Cancer Patients Been Tailored to Risk of Opioid Harms?* J Pain Symptom Manage, 2022. **63**(2): p. 179-188.

33. Hoffman, K.A., J. Ponce Terashima, and D. McCarty, *Opioid use disorder and treatment: challenges and opportunities*. BMC Health Serv Res, 2019. **19**(1): p. 884.
34. Cesteros, L.C., et al., *Miscibility of poly(ethylene oxide) with poly(N-vinyl pyrrolidone): DMTA and DTA studies*. Journal of Polymer Science Part B: Polymer Physics, 1989. **27**(13): p. 2567-2576.
35. Caradant, L., et al., *Extrusion of Polymer Blend Electrolytes for Solid-State Lithium Batteries: A Study of Polar Functional Groups*. ACS Applied Polymer Materials, 2021. **3**(12): p. 6694-6704.

## CHAPTER 5

### CONCLUSION AND FUTURE WORK

#### **Conclusion and Future Work:**

##### *Material Sparing Granulation and Formulation Development*

The objective of this dissertation's first two research chapters was to use the material science principles to rapidly and efficiently develop formulations for APIs selected at random to demonstrate the universality of these principles for all APIs. The APIs were characterized using material sparing tests, and then formulations were designed based on each API's unique needs and characteristics. Powder blends were then tested against the FDA and USP standards to ensure the blends could be used to produce high-quality and functional tablets. Of the four APIs studied, two were suitable for direct compression and formulas were developed using less than 5 g of API in less than 2 weeks. The other two APIs were not suitable for direct compression, and assessment of that fact was done in one week using only 2 g of API. One of those two APIs had extremely poor intrinsic flowability as a result of its low true density, small particle size, and high compressibility. Additionally, both APIs had an average particle size of 10  $\mu\text{m}$  which led to blend segregation and content uniformity problems, as a result of these findings, a follow up study was done to explore material sparing granulation as a way to improve the content uniformity of the API that had only segregation issues. Building off the previous work, only 2 g of additional API were needed to dry granulate and develop formulations with improved content uniformity compared to the unmodified API. The tablets made from the granulated API had lower maximum tensile strength, but still passed all mechanical and disintegration testing within the limits of the USP standards. When compared to the 1 kg

or more of API needed for large scale formulation development, material sparing granulation reduced the API consumption to develop a formulation for clinical trial testing by almost three orders of magnitude. In future studies, the material sparing granulation approach will be applied to the other API to optimize the material sparing granulation method to improve particle size selection. To expand on this work further, material sparing methods can be applied to the development of other drug delivery systems such as controlled release tablets, amorphous solid dispersions made via spray drying, and sustained release microspheres made via spray congealing. All sectors of drug product development, and as a result patients, can benefit from material sparing and quality-by-design approaches to formulation development.

#### *Amorphous Solid Dispersion Injection Molded Tablets*

The last research chapter highlighted a new and more efficient method of producing ASD tablets via injection molding, which is a continuous manufacturing method unlike current batch production methods used to make ASD tablets. Less than 10 g of model API and material sparing test methods were used to demonstrate the feasibility of quality-by-design in all areas of formulation development, even with novel drug delivery methods. The goal of this work was to create an ASD injection molding formulation for the manufacture of immediate release tablets that conformed to all USP standards. While successful in that goal, the study also discovered some unexpected secondary benefits of injection molding tablets. As a result of the formulation and injection processing, numerous secondary benefits arise such as consistent geometry, homogenous API loading, tablets impervious to chipping or smashing, and unique/highly recognizable tablet geometries. The 2 mg dose ASD tablets made via injection molding did achieve

immediate release. However, as the dosage size of the tablet increased, the time to 80% release shifted from 45 minutes to 90 minutes. Future studies into the dosage size threshold for immediate release and how the extrusion conditions impact dissolution would be beneficial for exploring the capabilities of this innovative technology. Another future study will be the isolation and characterization of the moxidectin degradation product observed via HPLC. Identifying the molecular structure could aid in isolating the cause of the degradation so that formulation or processing parameters can be modified to improve moxidectin stability. It would also be beneficial to test injection molding of other APIs to see if and how API impacts the formulation performance. Finally, the ASD formulation developed in this work could work well as a compression molding formulation due to its higher viscosity at lower temperature. Compression molding is a continuous manufacturing technique often used in industrial candy making. During compression molding, a molten mass of material is mixed and then pressed into a mold. On modern industrial equipment, the mold is actually two rollers with indentations that line up on either roller, similar to how powder compression tooling forms tablets, so that as the molten material is pressed, a large sheet of the pressed shapes is generated. As the sheet cools, the material solidifies and the edges of each shape where the material has been pressed then becomes an engineered weak point for vibrating machinery to break the sheet into consistent shaped pieces. Compression molding has the capability to produce more tablets per unit time compared to injection molding, so testing the formula developed in this work as a compression molding formulation could have great benefits for increasing even further the efficiency of making ASD tablets.

**Final Remarks:**

The work presented here is representative of the shifting paradigm in pharmaceutical science toward more efficient and data driven formulation development. Not only does this approach save money and time, but it gets lifesaving medications to patients sooner by shortening the drug development timeline. Additionally, many new APIs that have the potential to treat debilitating illnesses such as cancer struggle to be developed into a final drug product due to the limited solubility and bioavailability of the API. Therefore, developing industrially relevant ways to improve the dissolution and absorption of such challenging APIs has the potential to revolutionize the pharmaceutical industry and significantly improve the lives of patients.